Fabrication and characterization of novel low-cost ternary titanium alloys

A thesis
submitted in fulfilment
of the requirements for the degree
of
Master of Engineering
at
The University of Waikato
by

Manpreet Paul

THE UNIVERSITY OF
WAIKATO
Te Whare Wānanga o Waikato

2021

Abstract

Titanium and titanium alloys are commonly used in applications such as aerospace and biomedical due to their excellent mechanical properties as well as biocompatibility. However, reduction of the cost in titanium alloys is still sought after aiming to expand the use of titanium to other consumer industries. By alloying β-stabilizer elements with titanium, superior mechanical properties can be obtained.

Novel ternary α + β Ti-xCu-xNb, Ti-xMn-xNb, Ti-xFe-xNb, Ti-xFe-xCu and Ti-xFe-xMn (x = 0.5, 1, 2, 3.5 and 5 in wt%) alloys were designed aiming to have enhanced mechanical properties compared to unalloyed titanium at lower cost. In this study, the alloys were fabricated via powder metallurgy (i.e. cold press and vacuum sintering) to lower the production costs. The microstructure and phase identification of the sintered alloys were performed using optical microscopy, scanning electron microscopy and X-ray diffraction. Mechanical properties were analysed through tensile testing and the Rockwell hardness test.

Experimental results showed that the mechanical properties (tensile and hardness) of all sintered ternary titanium alloys, proportionally increase with the amount of alloying elements added, nevertheless, ductility decreases.

High tensile properties were observed for the Ti-5Fe-5Cu alloy (due to the formation of the Ti_2Cu phase, the strong β-stabilizer effects of Fe as well as a refined microstructure), in comparison to all the sintered ternary titanium alloys. Ti-5Fe-5Mn showed the highest hardness compared to all the sintered ternary titanium alloys, owing to the strong β-stabilizer effects of Fe and Mn (strong solid-solution strengthening effect), and an equiaxed microstructure. Cu and Nb as alloying elements added to Ti show high ductility compared to Fe and Mn, because of that the Ti-xCu-xNb alloy system showed higher elongations than the other alloy systems at the same total amount of alloying elements. It is worth mentioning that Ti-5Fe-5Cu was the only alloy to show comparable UTS and YS with Ti-6Al-4V, and Ti-5Fe-5Mn showed higher hardness compared to Ti-6Al-4V.

Acknowledgements

Firstly, I would like to thank my supervisor Dr Leandro Bolzoni for his continuous support and guidance throughout my Master's degree. His guidance and assistance helped me in all the time of research and writing of this thesis. Once again, it was an honour to be under your supervision.

Secondly, I would like to thank the lab technicians Jonathan van Harselaar and Duncan Barnard for all the training and assistance for the use of equipment and machines. To Yousef Alshammari, thank you so much for your help and assistance throughout my study, it will always be appreciated of you. Also, I would like to thank Cheryl Ward for her help in formatting this thesis.

Last but not the least, I would like to thank my parents and family for all their support throughout my engineering degree. I could not have done it without you.

Table of Contents

List of Figures

List of Tables

Chapter 1

Introduction and Literature Review

1.1 Introduction

In 1791 William Gregor, British reverend, mineralogist and chemist was the first to discover titanium (Ti) [1]. He examined the magnetic sand from the local river, Helford, in the Menachan Valley in Cornwall, England, and isolated "black sand" known as "ilmenite" ($FeTiO_3$). The iron (Fe) was removed from the sand with a magnet, by treating the sand with hydrochloric acid he produced the impure oxide of a new element which he named "mechanite" after the location. Four years later, Martin Heinrich Klaproth, Berlin chemist isolated Ti oxide from a Hungarian mineral known as "rutile" (TiO_2) [1]. The story of the Greek mythological children of Uranos and Gia, the titans, provided Martin the inspiration for naming Ti.

It took more than 100 years to produce pure Ti. In 1932 Wilhelm Justin Kroll produced significant quantities of Ti by combining Ti tetrachloride ($TiCl_4$) with calcium [1]. Kroll demonstrated that Ti could be extracted commercially by reducing $TiCl_4$ by changing the reducing agent from calcium to magnesium. In today's world, this is still the most widely used method and it's known as the "Kroll process". After World War II, Ti and Ti-based alloys were considered key materials for aircraft engines [1]. Ti and Ti alloys have widespread use in applications such as aerospace, chemical and biomedical. Ti has been hard to process since the metal is never found in a pure state and is found rarely in high concentrations [1]. It is very expensive, approximately being four times that of stainless steel and comparable to that of superalloys [2].

Ti is the ninth most-abundant element on the planet and the fourth most-abundant structural metal, where mineral sources of Ti are rutile, ilmenite, and leucoxene, an alteration product of ilmenite [2]. Ti is classed as a light nonferrous metal. Ti alloys primarily stand out due to two properties: high specific strength and excellent corrosion resistance. The high specific strength of Ti is limited by its oxidation behaviour at elevated temperatures giving a disadvantage, consequently conventional Ti alloys are used only up to temperatures slightly above 500 °C well below the melting point of Ti (1668 °C) [1].

Commercially pure Ti (CP-Ti) or unalloyed Ti is alpha (α) in structure. Ti can crystallize in various crystal structures; however, each modification is only stable within particular temperature ranges [1]. The complete transformation from one into another crystal structure is called the allotropic transformation; the respective transformation temperature is called the beta (β) transus temperature [1]. Ti crystalizes at low temperatures in a modified hexagonal close packed (hcp) structure denoted as α Ti and the body-centered cubic (bcc) structure is stable at high temperatures and is denoted as β Ti [1]. The β transus temperature of Ti is 882 ± 2 °C and is defined as the lowest equilibrium temperature at which the material is 100% β [2]. The β transus temperature is very important because processing and heat treatments are often carried out with reference to some incremental temperature above or below the β transus [2]. The atomic unit cells of the hcp α Ti and bcc β Ti are shown in Figure 1-1. Elements alloyed to Ti produce a range of possible microstructures and alter the mechanical properties.

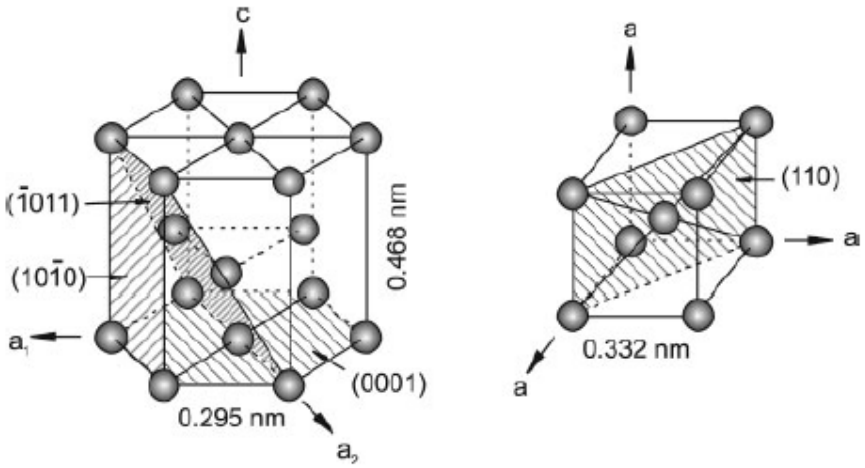

Figure 1-1 Crystal structure of hcp α Ti and bcc β Ti phases [1].

1.1.1 Ti alloys

The alloying elements added to Ti are classified as neutral, α-stabilizers or β-stabilizers (Figure 1-2). The α-stabilizing elements extend the α-phase field to higher temperatures, while the β-stabilizing elements shift the β-phase field to lower temperatures, and neural elements have minor influence on the β transus temperature [1].

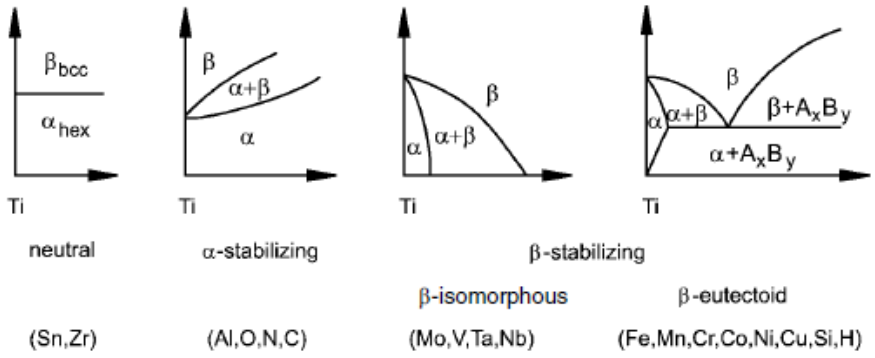

Figure 1-2 Influence of alloying elements on the phase diagrams of Ti alloys [1].

When extending the α-phase field to higher temperatures, the α-stabilizers develop a two-phase α + β field (Figure 1-3), and β-stabilizing elements are subdivided into β-isomorphous and β-eutectoid elements (Figure 1-2) [1].

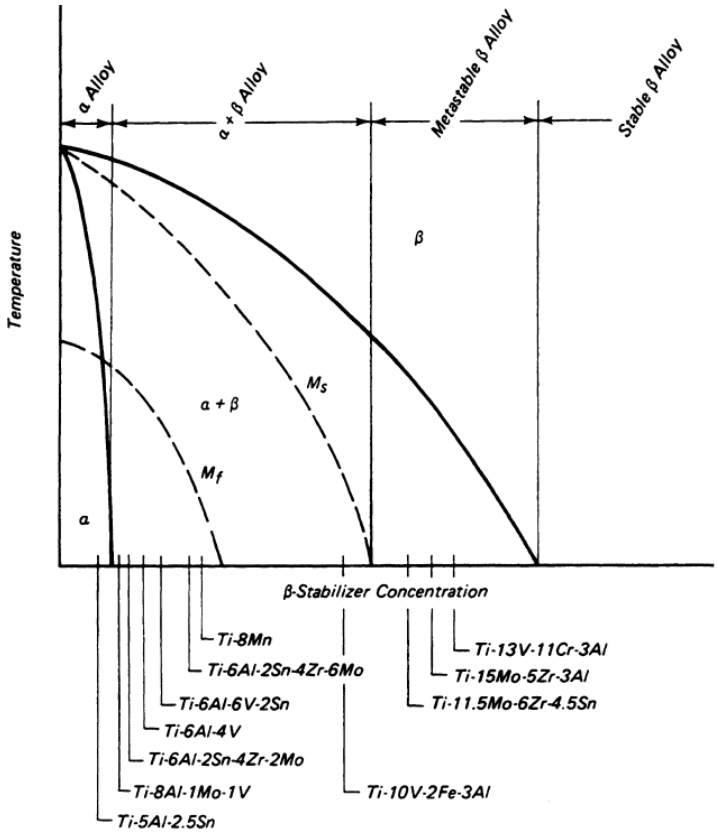

Figure 1-3 Pseudo-binary Ti phase diagram with different Ti alloys [2].

Effects of alloying elements

α-stabilizers such as aluminium (Al), oxygen (O) and nitrogen (N), raise the β transus temperature at which the α-phase is stable (favouring the α crystal structure) and β-stabilizers such as vanadium (V) and molybdenum (Mo), lower the

β transus temperature at which the β-phase is stable [2]. The interstitial elements O and N, are generally present as impurities, which contribute to interstitial hardening and different amounts of O are used to provide specific range of strength levels in numerous grades of CP-Ti [3]. β-isomorphous and β-eutectoid elements both stabilize the β crystal structure. The β-isomorphous group comprises of elements that are miscible in Ti, in contrast β-eutectoid elements have limited solubility in Ti and decrease the transformation temperature [2]. β-isomorphous elements do not form intermetallic compounds with Ti, whereas β-eutectoid elements do [2]. Intermetallic compounds are generally brittle with high melting point. β-eutectoid elements are typically added to alloys in combination with one or more β-isomorphous elements to stabilize the β-phase and impede formation of intermetallic compounds that can occur during service at elevated temperatures [2]. However β-eutectoid elements are used in β-rich α + β alloys or in β alloys because they are strong β-stabilizers and improve hardenability and response to heat treatment [2]. Neutral elements such as tin (Sn) and zirconium (Zr) are often alloyed to Ti. These elements have substantial solid solubility in α and β phases, they are useful as strengthening agents as they do not strongly promote phase stability, however the transformation rates are delayed.

Alloy design

Ti alloys can be designed using the Molybdenum Equivalent (MoE) approach, which is defined by the following equation:

$$\begin{aligned} \text{MoE} = {} & 1.0\,\text{Mo} + 0.67\,\text{V} + 0.44\,\text{W} + 0.28\,\text{Nb} + 0.22\,\text{Ta} + 2.9\,\text{Fe} + 1.6\,\text{Cr} \\ & + 1.25\,\text{Ni} + 1.70\,\text{Mn} + 1.70\,\text{Co} - 1.0\,\text{Al}\ (\text{wt\%}), \end{aligned}$$

and is generally used to indicate the β stability for a given Ti alloy composition [3-5]. The equation consists of β-stabilizing elements, α-stabilizing elements and neutral elements contained in a Ti alloy on the β-phase stability [5]. Mo is used as an arbitrarily chosen standard and normalises other elements to an equivalent Mo value [5]. Ti alloys with MoE value of $0 \leq \text{MoE} < 5$ are α + β, alloys with $5 \leq \text{MoE} < 10$ are near-β, and alloys with $\text{MoE} \geq 10$ are metastable β (a MoE value of 10 is essential to stabilize the β-phase during quenching) and will avoid the formation of martensite as these alloys contain enough β-stabilizing elements to avoid cooling

through the martensite start line (M_S) (Figure 1-3) [4; 5]. For example, a Ti alloy such as Ti-4.5Al-3V-2Mo-2Fe (near-β alloy) will have the following MoE value:

$$\text{MoE} = (1.0 \times 2)\,\text{Mo} + (0.67 \times 3)\,\text{V} + (2.9 \times 2)\,\text{Fe} - (1.0 \times 4.5)\,\text{Al}$$
$$\text{MoE} = 5.3$$

Types of Ti alloys

Ti alloys are classified as α, α + β and β alloys, with further subdivision into near-α and metastable β alloys (Figure 1-3) [1]. When small amounts of β-stabilizing elements are added to α alloys they are termed near-α alloys. The α + β alloys are the most widely used alloy group, at room temperature these alloys have a β volume fraction of about 5 to 40% [1]. If the β-stabilizing elements is increased to a level where β no longer transforms to martensite upon fast quenching, the alloys are still in the two-phase field and the class of metastable β alloys is reached [1].

α alloys are often alloyed with Al and Sn and are preferred for high temperature applications because of their superior creep characteristics [6]. The alloyed Al is in high volumes that contributes to oxidation resistance at high temperatures (α + β alloys also contain high amounts of Al as the principal element to stabilize the α-phase) [2]. α alloys have excellent corrosion resistance and good weldability. Strength and toughness are satisfactory, whereas forgeability is inferior to that of the other Ti alloy types [6]. α alloys are single phase alloys that cannot be heat treated to improve strength or mechanical properties [2; 6].

Near-α alloys comprises of both α and β phases, which contains small amounts of β-stabilizing elements (≤ 2 wt%) [3; 6]. Near-α alloys are ideal for high temperature applications (upper operating temperature is limited to about 500-550° C) since they combine the excellent creep behaviour of α alloys with the strength of α + β alloys [1]. The properties and fabrication characteristics are similar to those of the α alloys, apart from that a greater variety of microstructures and mechanical properties are feasible for near-α alloys [3].

α + β alloys consists of α-stabilizing and β-stabilizing elements. α + β alloys are widely used because of their good combinations of strength, toughness and formability. Ti-6Al-4V is the most popular α + β Ti alloy used around the world for

many applications; aerospace being the prime consumer. The alloy was developed in the early 1950s in the United States at the Illinois Institute of Technology and is one of the first alloys to be made [1]. The good balance of properties and intensively developed/tested Ti-6Al-4V alloy makes it very successful [1]. The strength of α + β alloys can be improved and controlled by heat treatments.

β alloys are defined as "those containing enough total alloying elements that enable the β-phase to be retained in either a metastable or stable condition after cooling to room temperature during heat treatment" [3]. β alloys are useful where very high tensile strengths are required and have good combinations of strength, toughness, and fatigue resistance. The main advantages of β alloys is their high hardenability, excellent forgeability and good cold formability in the solution-treated condition and can be hardened to adequately high strength levels [2]. The applications of β alloys are limited by their relatively high specific weight, modest weldability, high density, poor oxidation behaviour, and complex microstructure [1].

Microstructure development in Ti alloys

The common phases present in sintered Ti alloys are α, β, martensite phases (α' and α'') and ω. The ω and martensite phases are metastable phases and the β-phase is stable at room temperature provided that there is high enough β-stabilisers to decrease the β→α transformation temperature to below room temperature [7].

The morphology of the α-phase can exist as near equiaxed, lamellar (lath) or acicular depending on the alloy chemistry, processing pathway, and thermal chemistry. Therefore the α-phase can be formed from the ω phase (discussed later on) via ageing (Figure 1-4) [7].

As previously mentioned, the β-phase is generally stable at room temperature provided that there are adequate β-stabilizing elements. The two groups of β-stabilizers being β-isomorphous and β-eutectoid will have different phase arrangements owing to the different β-stabilizer groups.

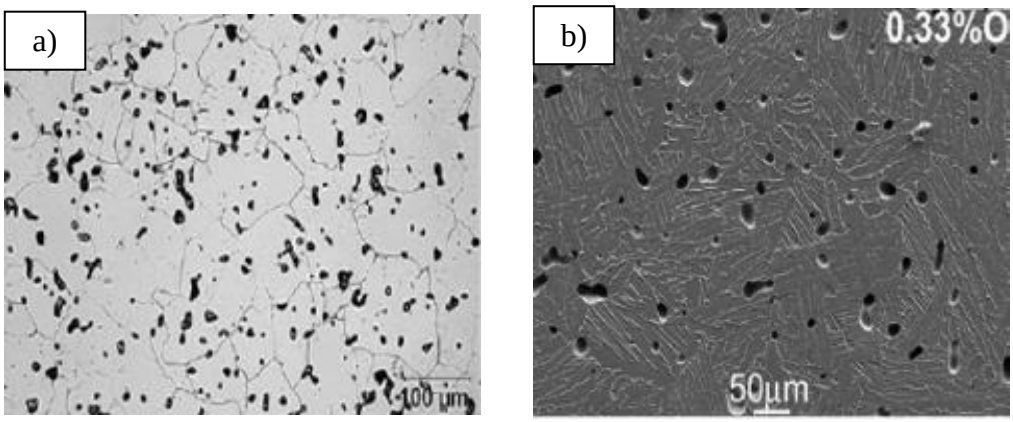

Figure 1-4 SEM micrograph of powder metallurgy Ti and Ti alloy consisting of the α-phase: a) CP-Ti, and b) Ti-6Al-4V [7].

α' and α" are two common phases of martensite in Ti alloys, α' has an hcp crystal structure while α" has an orthorhombic structured phase [7]. The α' phase is present in alloys with a lower β concentration in contrast to α" which is present in alloys with higher β concentration. In terms of morphology the α' phase can exist as an acicular or lath/lamellar morphology (Figure 1-5) while α" generally tends to show an acicular morphology [7].

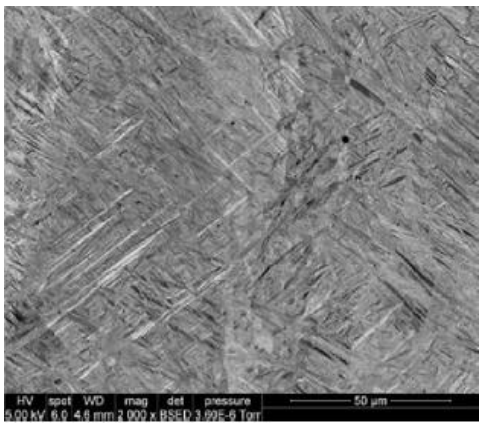

Figure 1-5 SEM micrograph of Ti-6Al-4V alloy consisting of the martensite phase (α') [7].

The ω phase has an hcp crystal structure and is categorized into athermal ω (formed during quenching) and isothermal ω (formed during aging/heat treatment) [7]. Athermal ω is "believed to be a product of martensite transformation, or due to a displacement/shear mechanism from a crystallographic point of view" and isothermal ω can be observed in sintered powder metallurgy (PM) Ti alloys [7]. Ageing at relatively lower temperatures with slow cooling rates satisfies sintering

(i.e. to provide an ageing like affect) hence forming isothermal ω in PM Ti alloys [7]. The ω phase is relatively present as fine particles in Ti alloys.

1.1.2 Processing of Ti alloys via PM

PM defined by Froes is "the production, processing, and consolidation of fine particles to make a solid metal" [8]. Advantages of PM over other processing methods such as casting are its compatibility of producing near net shape parts, complex geometry, and reduced processing steps. The main goal of PM Ti has been reducing manufacturing costs and materials savings as well as producing mechanical properties equivalent to cast and wrought ingot metallurgy. There are two PM approaches being the prealloyed (PA) and the blended elemental (BE) methods. The PA approach involves the use of prealloyed powder which has been produced by melting, either by the plasma rotating electrode process or by gas atomization, followed by hot consolidation (i.e. hot isostatic pressing (HIP)) [9; 10]. The PA powder generally is spherical in shape. In the BE approach CP-Ti (or Ti hydride powder) and alloying elements (or master alloys) are blended together followed by pressing and sintering. A density very close to 100% can be achieved if Ti hydride powder is used. The BE approach is cost effective compared to PA especially if any secondary pressing step i.e. HIP is avoided [9]. The processing steps for PM are powder production, mixing, pressing and sintering.

Mixing

Prepared metal powders consisting of CP-Ti and alloying elements are mixed together to obtain a homogenous mixture. Additives such as lubricants or binders are added if required.

Pressing

Mixed metal powder blends are pressed in a precision die (i.e. shape of the product) at a pressure in the range of 100 to 1000 MPa depending on the powder morphology. Pressing the metal powder may be done at room temperature or by cold isostatic press (CIP). The density of the pressed sample at room temperature is relatively low and can be increased by HIP. Once the metal powder is pressed into the desired shape it is now in the green state, the strength of the sample is only sufficient for handling purposes and must be sintered. Generally, CP-Ti and Ti

alloys are pressed around 600 MPa and will achieve a green density greater than 80%.

Sintering

During sintering parts are heated (in a protective atmosphere furnace) below the melting point of the metal to metallurgically bond the individual particles together, which further densifies the part and increases individual strength. The sintered part is cooled down in the furnace, this prevents oxidation, thermal shock and controls carbon content. Typical atmosphere gases used for sintering are hydrogen, inert or vacuum. The structure and porosity obtained in the sintered sample depends on the sintering conditions such as temperature, time and processing [11]. The porosity cannot be eliminated completely because voids are present from pressing (pores cannot be closed by pressing) and gases evolve during sintering [11]. Density values greater than 99% can be achieved by sintering provided that pressing was done under appropriate conditions (i.e. correct pressure and temperature ranges). Sintering CP-Ti and BE powder of a typical Ti alloy, is normally done at a temperature of 1200°C or higher to both facilitate densification and allow for sufficient homogenisation of the alloying elements [12].

1.2 Literature Review

CP-Ti has been used in many applications, however it possess disadvantages such as bacterial infections after implantation, and is considered to be more difficult to process because of its high melting temperature and increased chemical reactivity at high temperature [13; 14]. Ti-6Al-4V, the most widely used alloy, also possess disadvantages when implanted, studies have shown that the release of Al and V ions from the alloy may cause long term health problems, such as peripheral neuropathy, osteomalacia and alzheimer diseases [15; 16]. It has been reported that CP-Ti and Ti-6Al-4V alloys both have a low wear resistance and high Young's modulus (which is 4 to 10 times higher than that of the human bone (10~35 GPa)), long term studies suggest that insufficient load transfer from the artificial implant to adjacent remodelling bone may result in bone resorption and at last cause loosening of the prosthetic device [15]. This is known as the stress shielding effect, which is "a direct result of the stiffness mismatch between implant material and surrounding natural bone" [15]. To overcome these problems it is best to design α + β or β-type Ti-based alloys, as alloying Ti with other β-stabilizing elements will reduce the fusion temperature, provide superior mechanical properties and excellent biocompatibility [13].

Binary Ti-Cu, Ti-Nb, Ti-Mn and Ti-Fe alloys have been studied to an extent, however literature reports where two elements (Cu and Nb, Mn and Nb, Fe and Nb, Fe and Cu, Fe and Mn) added to Ti have not been reported (very limited). In this literature review, ternary Ti-Cu-Nb, Ti-Mn-Nb, Ti-Fe-Nb, Ti-Fe-Cu and Ti-Fe-Mn alloys are studied, alongside their binary alloy systems.

1.2.1 Ternary Ti-Cu-Nb alloys

In this section binary Ti-Cu and Ti-Nb alloys are first discussed followed by the ternary Ti-Cu-Nb alloys.

1.2.1.1 Ti-Cu alloys

Ti-Cu alloys have vastly been used in biomedical devices such as dental implants, hip replacements, and bone substitutes [13; 14; 17-24]. Copper (Cu) as a β–stabilizing element, alloyed to Ti produces strong antibacterial properties,

excellent biocompatibility, improved corrosion resistance as well as mechanical properties, along with a low friction coefficient and high wear resistance [14; 17; 19-21; 23]. The addition of Cu to Ti lowers the melting point of the alloy, thus increases thermal conductivity which improves the burn resistance and the machinability of the alloy [18]. Cu being a eutectoid element forms a eutectoid alloy (αTi + Ti_2Cu) at a Cu concentration of 7 wt% [13]. In a study by Alshammari *et al.* [14] reported that a Ti-Cu alloy with 5 wt% Cu was sufficient enough to form the intermetallic (Ti_2Cu) phase as shown in Figure 1-6 (confirmed in X-ray diffraction (XRD) results).

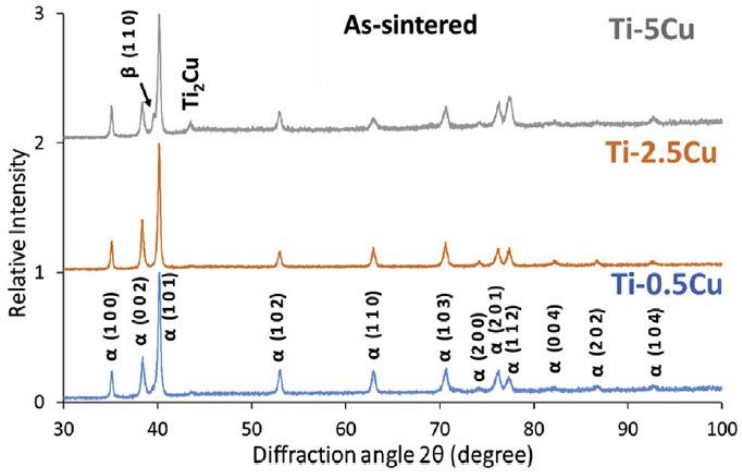

Figure 1-6 XRD patterns of sintered Ti-Cu alloys [14].

It has been reported in many studies that a Cu concentration of 5 wt% in Ti-Cu alloys has strong antibacterial activity against bacterial infections such as *Staphylococcus aureus* (S. *aureus*) and *Escherichia coli* (E. *coli*) [14; 21-24]. The Ti_2Cu phase is responsible for providing high antibacterial rates greater than 90% (in comparison with CP-Ti), as the antibacterial property is ascribed to the release of Cu^{+2} ions from the Ti_2Cu compounds formed in Ti-Cu alloys [19]. A small amount of Cu can improve the grindability of Ti-Cu alloys [23].

The effects of increasing Cu concentration in Ti-Cu alloys

The addition of Cu to Ti leads to a lower corrosion resistance compared to CP-Ti, because of the higher repassivation ability [14]. The mechanical and antibacterial properties of Ti-Cu alloys improve with the addition of Cu, because Cu provides a solid-solution strengthening effect even at lower concentrations such as 0.5 wt%. The Ti_2Cu phase is also responsible for improving the mechanical

properties of Ti-Cu alloys (similar to the antibacterial properties). The addition of Cu increases the volume fraction of the Ti_2Cu phase, thus a higher amount of Ti_2Cu phase will increase the resistance to plastic deformation, which improves the mechanical properties such as strength (ultimate tensile strength (UTS), yield strength (YS)), and hardness of Ti-Cu alloys [14; 18]. Ductility tends to deteriorate as the Cu concentration increases due to the fine Ti_2Cu particles present [14; 20; 22].

Since Cu is a β-stabilizer in Ti, its addition to Ti (if fabricated via PM) leads to the formation of the typical α + β lamellar structure, this is because the β-phase remains stable upon slow cooling from the sintering temperature [14]. As shown in Figure 1-7, the increase in Cu from 0.5 to 5 wt% causes the β-phase to increase while the thickness of the β lamellae decreases. The fine α + β lamellar microstructure of the Ti-5Cu alloy gives better mechanical properties compared to the Ti-0.5Cu alloy (discussed later on). From Figure 1-6 (XRD results) it can be seen that the β-phase (β-phase peak) increases with the addition of Cu in Ti. Generally PM Ti alloys with β-stabilizing elements will consist of α + β lamellar microstructures.

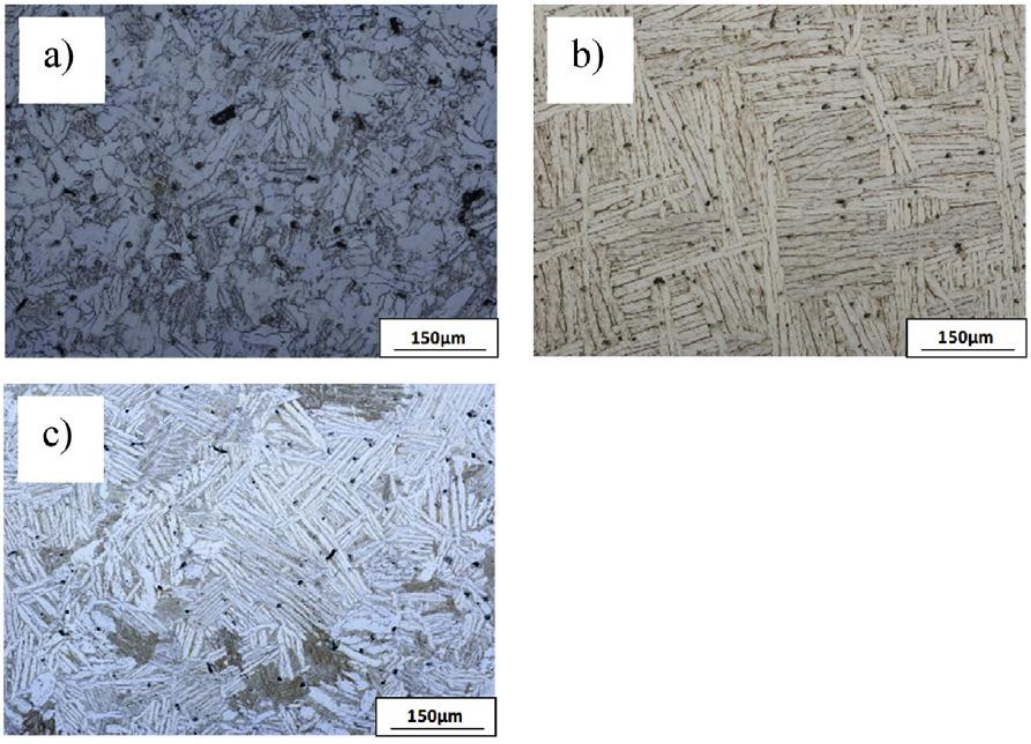

Figure 1-7 OM of sintered Ti-xCu alloys: a) Ti-0.5Cu, b) Ti-2.5Cu, and c) Ti-5Cu [14].

Processing of Ti-Cu alloys

Alshammari *et al.* [14] fabricated Ti-xCu (x = 0.5, 2.5 and 5% all in wt% unless specified) alloys (Ti and Cu powders with 99.4% and 99.7% purity respectively) by PM (cold press and vacuum sintering), followed by a subsequent conventional β forging step (to further seal the residual porosity left and improve the mechanical properties). Zhang *et al.* [23] prepared Ti-xCu (x = 5 and 10%) alloys (with high purity Ti and Cu powder (99.99%)), which were ball milled for 3-6 hours followed by hot pressure sintering (samples with a diameter of 40 mm) under vacuum condition (at 30 MPa and 850 – 1050 °C for 120 minutes and left to cool inside the furnace), samples labelled as Ti-5Cu(S) and Ti-10Cu(S) (where S represents sintering). After sintering the samples were subjected to extrusion at a rate of 10 mm/s at 800 °C into cylindrical bars (samples with a diameter of 16 mm), samples labelled as Ti-5Cu(E) and Ti-10Cu(E) (where E represents extrusion). In another study by Zhang *et al.* [21], Ti-5Cu(S) and Ti-10Cu(S) alloys similar to the ones described above, were prepared via ball milling for 0.5 hour, then hot pressure sintered under vacuum condition (in argon at 0.093 MPa and 800 °C for 60 minutes). Liu *et al.* [24] also hot pressure sintered Ti-xCu (x = 2, 5, 10 and 25%) alloys (with high purity Ti and Cu powder (99.99%)) under vacuum condition similar to Zhang *et al.* [23] method.

Zhang *et al.* [21] also looked at producing Ti-Cu alloys by an ingot casting method. In this method CP-Ti and Cu (with high purity CP-Ti and Cu powder (99.99%)) were used to prepare Ti-5Cu(I) and Ti-10Cu(I) alloys in a vacuum non-consumable furnace, the samples were remelted at least six times to obtain homogenous compositions. The alloys were vacuum sealed in a crystal tube and heat treated at different temperatures, labelled as Ti-5Cu(T4) and Ti-5Cu(T6), Ti-10Cu(T4) and Ti-10Cu(T6) (in the T4 treatment the alloys were heat treated at 900 °C for 2 hours and quenched in water, in the T6 treatment the alloys were treated the same as T4 with a further step of heating the alloy after quenching to 400 °C for 12 hours). Kikuchi *et al.* [13] produced Ti-xCu (x = 0.5, 1, 2, 5 and 10%) alloys, which were fabricated in an argon-arc melting furnace. Each alloy was produced by melting Ti sponge (99.8% purity) and oxygen-free Cu (Cu: 99.99%, 0: 0.0005%) into 30 g buttons, the samples were remelted and cast into a magnesia mold at 200 °C in a centrifugal casting machine. A similar method was observed in another study by Zhang *et al.* [22], where Ti-xCu (x = 2, 3 and 4%) alloys were fabricated using high

purity (99.99%) Ti and Cu powders. After casting, the alloys were subjected to a solid-solution heat treatment (T4) at 900 °C for 3 hours, followed by an ageing treatment (T6) at 400 °C for 12 hours. Yi *et al.* [17] also had a similar method where Ti-xCu (x = 2, 5, 7 and 10%) alloys were fabricated. After casting the samples were heat treated at 950 °C for 3 hours in vacuum furnace, followed by cooling inside the furnace to room temperature. Wang *et al.* [20] annealed heat treated Ti-xCu (x = 3, 5 and 7%) alloys prepared by arc-melting high purity (99.9%) Ti and Cu powders. The alloys were annealed at 740 °C, 830 °C and 910 °C for 1 hour, followed by air cooling.

Properties of Ti-Cu alloys

Ti-Cu alloys have superior properties compared to CP-Ti. The density of sintered Ti-Cu alloys tends to be higher than CP-Ti, however due to pores present in the material it is unlikely that a density of 100% is achievable, a density greater than 99% has been achieved using hot working [14; 23]. The elongation of sintered Ti-Cu alloys tends to decrease as the Cu concentration increases, as shown in Figure 1-8. As previously mentioned the Ti_2Cu phase is responsible for the decrease in ductility, since Ti_2Cu is a hard metal interphase it tends to show brittle behaviour [18].

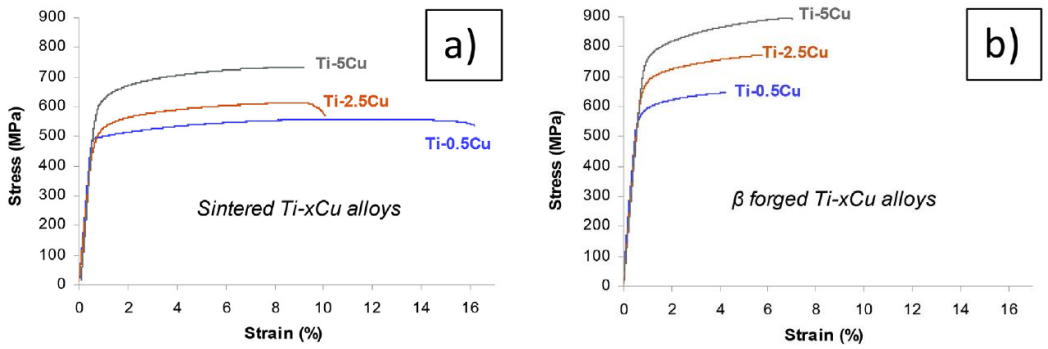

Figure 1-8 Stress vs stain curves of Ti-xCu alloys: a) sintered and b) β forged [14].

Ti-Cu alloys have higher UTS and YS properties than CP-Ti. A Ti-Cu alloy with just 0.5 wt% Cu (fabricated by PM [14]) has an UTS of 555 ± 8 MPa and YS of 467 ± 16 MPa (as shown in Figure 1-8a), which is higher than the UTS (235 MPa) and YS (140 MPa) of CP-Ti (with high purity Ti powder (99.98%)) [1]. The tensile properties of Ti-Cu alloys can be improved by hot working. The study by Alshammari *et al.* [14] looked at β forging sintered Ti-Cu alloys where UTS and

YS for the β forged Ti-0.5Cu alloy was 650 ± 26 MPa and 602 ± 26 MPa respectively, showing an increase of 95 MPa in UTS and 135 MPa in YS from the sintered Ti-0.5Cu alloy (as shown in Figure 1-8) [14]. Similar results were observed in a study by Zhang *et al.* [23], where extruded Ti-Cu alloys had higher UTS and YS properties than sintered Ti-Cu alloys (as referenced in [23]). In two other studies by Zhang *et al.* [21; 22], heat treatment options (T4) and (T6) further improved the UTS and YS properties of sintered Ti-Cu alloys.

The hardness of Ti-Cu alloys is higher than CP-Ti (100 Vickers Hardness (HV)), generally hardness of Ti-Cu alloys are in the range of 150-400 HV depending on the Cu concentration [1]. The hardness of Ti-Cu alloys can be improved by hot working treatments similar to the ones mentioned above for UTS and YS.

1.2.1.2 Ti-Nb alloys

Ti-Nb alloys have attracted great attention in biomedical devices such as dental implants [15; 16; 25-27]. The alloys stand out due to their low Young's modulus, superior biocompatibility, corrosion resistance as well as mechanical properties. Niobium (Nb) as a (isomorphous) β-stabilizing element, alloyed to Ti is beneficial in lowering the Young's modulus of the alloy and is less cytotoxic/non-toxic compared to other elements [16; 27]. A lower Nb concentration in Ti-Nb alloys is reported to exhibit the shape memory phenomenon, which is employed in dentistry for orthodontic wires [25; 27]. Nb is a rare expensive metal with a very high melting point, thus it is best to design Ti-Nb alloys with a low Nb concentration to benefit cost savings and reduce manufacturing steps (i.e. to avoid operating at very high temperatures) [16]. Ti-Nb alloys with a concentration up to 4 wt%, consist of an α-phase at 400 °C and from 4 – 56 wt%, they consist of an α + β microstructure as per the Ti-Nb binary equilibrium phase diagram [16; 25].

The effects of increasing Nb concentration in Ti-Nb alloys

The addition of Nb to Ti improves the corrosion resistance, biocompatibility and mechanical properties of Ti-Nb alloys. With increasing Nb concentration in Ti-Nb alloys, the β transus temperature decreases [27]. Small additions of Nb improve the tensile properties of Ti-Nb alloys, as Nb provides a solid-solution strengthening effect. The hardness of Ti-Nb alloys increases with increasing Nb concentration,

however the ductility decreases (ductility of Ti alloys with β-stabilizers decreases with increasing β-stabilizer content).

Processing of Ti-Nb alloys

Lee *et al.* [15] fabricated Ti-xNb (x = 5, 10, 15, 17.5, 20, 22.5, 25, 27.5, 30 and 35%) alloys (with high purity Ti and Nb powder (99.9%)), by using a commercial arc-melting vacuum-pressure type casting system. The casting process consists of an "upper melting chamber and lower casting chamber, connected by a central hole. A casting ring is set at the top of it and a Cu crucible lies on top of it. The alloy ingot is placed at the centre of the crucible" as mentioned in [15]. The alloys were melted three times to obtain homogenous compositions. The same method was used by Xu *et al.* [26], where Ti-xNb (x = 5, 10, 15 and 20%) alloys (with high purity Ti: 99.4% and Nb: 99.9% powder) were prepared. A similar method was used by Kikuchi *et al.* [25], where Ti-xNb (x = 2, 5, 10, 15, 20, 25 and 30%) alloys (Ti powder: >99.8% grade S-90 and Nb powder: >99.9%) were prepared in an argon-arc melting furnace. The alloys were remelted and cast into a magnesia-based mold using a dental casting machine. Han *et al.* [27] also used a similar technique, where Ti-xNb (x = 5, 10, 15 and 20%) alloys were prepared by arc-melting the alloys using high purity argon gas. After the remelting process, the samples were heat treated using a tube furnace under argon atmosphere (99.9999%) for 4 hours at 150 °C. The samples were then cooled to 600 °C at 10 °C/min and air cooled to room temperature.

Other manufacturing methods have been used to produce Ti-Nb alloys, however the alloys studied are β-type Ti-Nb alloys with Nb concentrations greater than 10 wt%. Zhao *et al.* [28] produced Ti-xNb (x = 10, 16 and 22%) alloys (Ti powder particle size: <45 μm and Nb powder particle size: <110 μm), by metal injection molding (MIM) process. In a study by Yilmaz *et al.* [29], Ti-xNb (x = 16, 28, 40%) alloys (Ti powder particle size: 32.95 μm and Nb powder particle size: 30.15 μm) were prepared by powder injection molding (PIM) process. Kalita *et al.* [30] fabricated Ti-xNb (x = 14, 20 and 26%) alloys (with high purity Ti: 99.9% and Nb: 99.8% powder), by spark plasma sintering. After the sintering process, the alloys were subjected to annealing heat treatment at 1250 °C for 24 hours.

Properties of Ti-Nb alloys

The elongation of Ti-Nb alloys generally decreases (same as Ti-Cu alloys) as the Nb concentration increases, due to the volume fraction of the β-phase increasing (as shown in Figure 1-9). Sintered Ti-Nb alloys have porosity present in the material, this porosity results in the alloys having a density less than 100%, and with increasing Nb concentration the density of the alloy decreases further [28; 29]. The sintered density of Ti-Nb alloys is higher than the sintered density of CP-Ti. Similar to Ti-Cu alloys, the ductility of Ti-Nb alloys can be improved with the addition of hot working treatments.

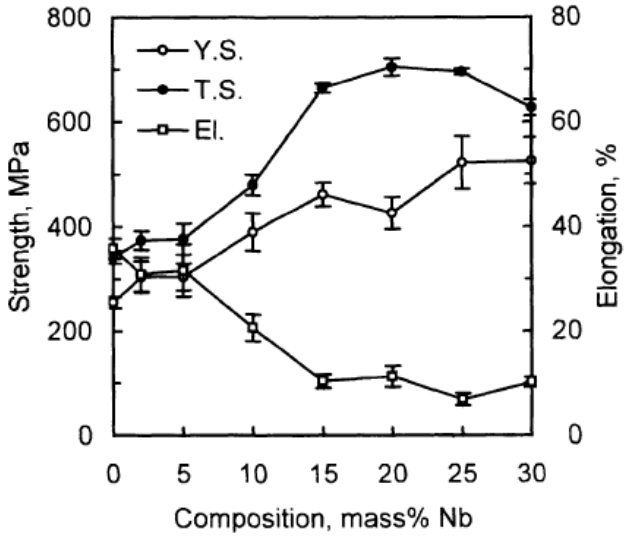

Figure 1-9 Tensile strengths, YS and elongations of Ti-Nb alloys [25].

Tensile properties of Ti-Nb alloys are superior than CP-Ti. A Ti-Nb alloy with just 2 wt% Nb has an UTS of 380 MPa and YS of 300 MPa (as shown in Figure 1-9) [25]. With 5 wt% Nb added to Ti, the alloy has an UTS of 536 MPa and YS of 407 MPa [16].

The hardness of Ti-Nb alloys is significantly greater than CP-Ti. With 2 and 5 wt% Nb added to Ti, it gives a hardness of 135 HV [25] and 319 HV [26] respectively. Hot working treatments can further improve the tensile and hardness properties of Ti-Nb alloys (similar to Ti-Cu alloys).

1.2.1.3 Ternary Ti-Cu-Nb alloys

Literature is very limited on Ti-Cu-Nb alloys, where there is no reported ternary Ti-Cu-Nb equilibrium phase diagram suggesting that work should be done in this field.

The addition of Nb to Ti-Cu alloys

In a study by Takahashi *et al.* [31], Ti-6Nb-4Cu, Ti-18Nb-2Cu and Ti-24Nb-1Cu alloys (Ti sponge: >99.8% grade S-90, Nb: >99.9% and Cu: >99.99%) were produced via casting, the alloy ingots were cast into testing specimens in a magnesia mold using a dental casting machine. The motivation of this study was based on previously studied binary Ti-5Cu and Ti-30Nb alloys, which demonstrated superior strengths (twice than that of CP-Ti) due to the formation of Ti_2Cu and ω phases in Ti-5Cu and Ti-30Nb alloys, respectively. The grindability of Ti improves with the addition of alloying elements, including a third element may exhibit good grindability over a wide range of grinding speeds, thus making machinability easier [31]. It has been reported that the Cu-Nb system is an immiscible system, due to the solid-solubility limit of Nb in Cu (α solid-solution) is about 0.15% and the limit of Cu in Nb (β solid-solution) is about 0.8% [31]. The elongation for all Ti-Nb-Cu alloys was around 4%, which was lower than both binary Ti-5Cu (6%) and Ti-30Nb (10%) alloys (as shown in Figure 1-10).

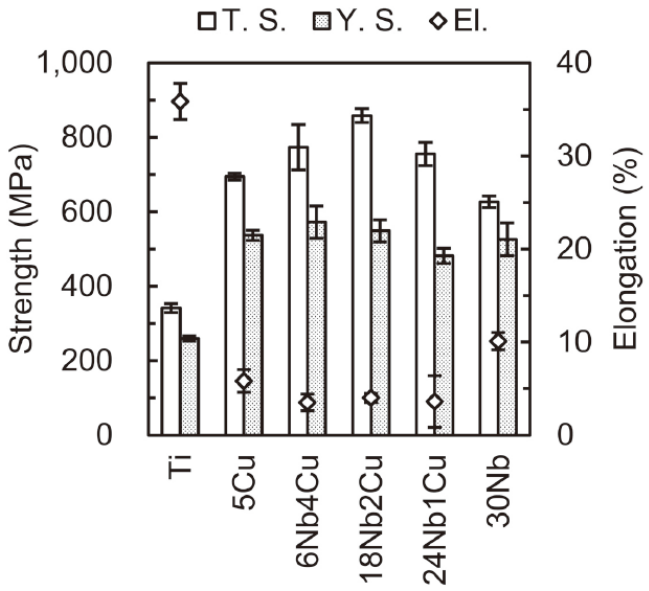

Figure 1-10 Tensile strengths, YS and elongations of the Ti-Nb-Cu alloys [31].

Experimental results showed that all Ti-Nb-Cu alloys exhibited higher tensile strengths (>750 MPa) than Ti-5Cu (~695 MPa) and Ti-30Nb (~640 MPa) alloys (as shown in Figure 1-10). The ternary solid-solution strengthening was very effective in improving strength, compared to binary solid-solution strengthening [31]. No significant differences were observed in YS of the ternary and binary alloys, the highest YS was reported for the Ti-6Nb-4Cu alloy (572 MPa). The hardness of the Ti-24Nb-1Cu (340 HV) alloy was the highest among the ternary alloys, however it was lower than binary Ti-30Nb (~380 MPa) and higher than Ti-5Cu (~280 MPa) alloys. The Ti-6Nb-4Cu alloy exhibited the lowest hardness (~260 HV) among the alloys.

Other ternary Ti alloys with Cu

New ternary Ti-xMn-yCu alloys (purity of Ti, Cu and Mn powder is 99.4%, 99.7% and 99.0% respectively) were designed by Alqattan *et al.* [32] and manufactured via PM (i.e. cold uniaxial pressing plus vacuum sintering). Two sets of samples were designed the first being Cu-dominant i.e. one with Mn/Cu ratio of 1:3, which consisted of the following compositions of Ti-xMn-yCu (x = 0.2, 0.4, 0.8 and 1.6% & y = 0.6, 1.2, 2.4 and 4.8%) and the second being Mn-dominant (discussed later in section 1.2.2.2). With the addition of Cu to the Ti-xMn-yCu alloy, the tensile properties and hardness of the alloys increased significantly. The highest reported UTS and YS (was for the Ti-0.8Mn-4.8Cu alloy) was 692 MPa and 567 MPa respectively. Meanwhile the elongation of all the Cu-dominant Ti-xMn-yCu alloys was fairly constant (16.4 ± 2.3%). Hardness of the Ti-0.8Mn-4.8Cu alloy was the highest (60 Rockwell Hardness (HRA)). The presence of the Ti_2Cu phase was detected by XRD (as shown in Figure 1-11) at 2.4 wt% Cu (Ti-0.8Mn-2.4Cu), this lead to precipitation strengthening, hence increasing the strength of the Cu-dominant ternary Ti-xMn-yCu alloys [32]. The microstructure of Ti-xMn-yCu alloys consisted of α + β lamellar structure, with increasing Cu concentration the thickness of the β lamellae decreased resulting in a finer microstructure for Ti-1.6Mn-4.8Cu alloy.

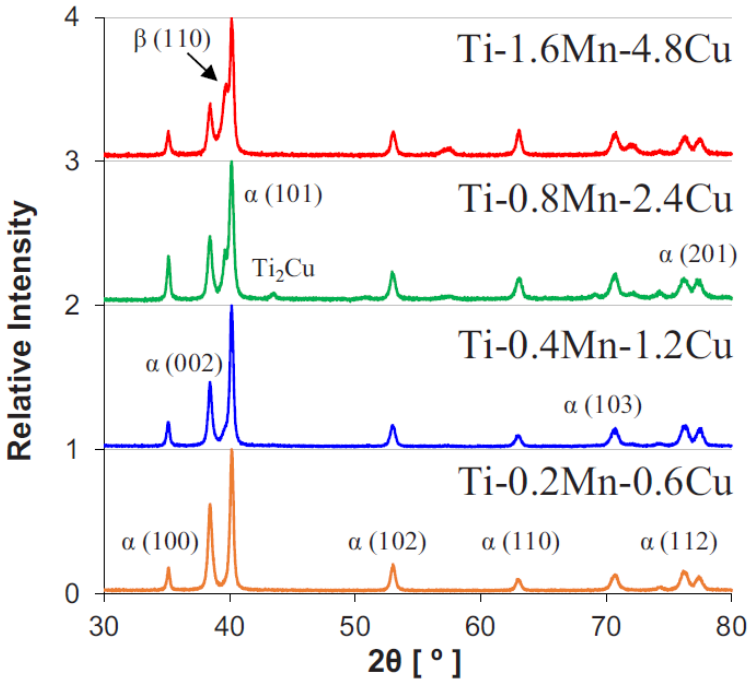

Figure 1-11 XRD patterns of Cu-dominant ternary Ti-xMn-yCu alloys [32].

Sato *et al.* [33] looked at constructing a Ti-Nb-Cu phase diagram that could potentially be used to develop new Ti alloys with superior machinability and mechanical properties. The study comprised of fifteen experimental Ti-Nb-Cu alloys with compositions of Ti-(5-30)Nb-(2-20)Cu (Ti sponge: >99.8% grade S-90, Nb: >99.9% and Cu: >99.99%), which were designed and fabricated via casting. The alloy ingots were each cast into testing specimens in a magnesia mold using an argon gas-pressure dental casting machine. The phase diagrams constructed in this study were under conditions applicable for dental casting. XRD results were used to construct the Ti-Nb-Ti_2Cu pseudo-ternary phase diagram.

Other Ti-Cu-Nb alloys

Other ternary Ti-Cu-Nb alloys have been manufactured, however these alloys have concentrations greater than 10 wt% which primarily are β-type alloys. Mutlu [34] produced precipitation hardenable metastable β-type Ti-30Nb-10Cu alloy specimens via PM. The specimens were sintered, quenched and aged in a single-step process to enhance the mechanical properties. In previous studies by the same author, the corrosion behaviour/potential of β-type Ti-Nb-Cu alloys manufactured via PM was analysed. Two of the studies [35; 36] produced metal foams, while the other didn't [37]. The use of metal foams exhibits a structure similar to cancellous bone, the main advantage is their ability to provide anchorage

for the surrounding tissue via ingrowth of tissue into their pores (as previously mentioned biomedical implants suffer from mismatch of their Young's Modulus with the human bone) [35; 36].

1.2.2 Ternary Ti-Mn-Nb alloys

In this section binary Ti-Mn alloys are first discussed followed by the ternary Ti-Mn-Nb alloys. Binary Ti-Nb alloys have already been discussed in section 1.2.1.2.

1.2.2.1 Ti-Mn alloys

Ti-Mn alloys are highly employed in biomedical devices, Manganese (Mn) is a strong β-stabilizing element, when alloyed to Ti it increases the mechanical properties as well as the biocompatibility. Mn is widely chosen because of its lower cost/cytotoxicity, strong solid-solution strengthening effects and higher availability compared to other alloying elements [38-42]. The melting point of Mn (1246 °C) is lower than that of Ti, thus alloying with Ti will lower the fusion temperature of the alloy [42].

The effects of increasing Mn concentration in Ti-Mn alloys

The addition of Mn to Ti significantly increases the mechanical properties and hardness of Ti-Mn alloys [38]. The strong solid-solution strengthening effect of Mn is responsible for the superior mechanical properties of Ti-Mn alloys, compared to other alloying elements. However, with increasing Mn concentration in Ti-Mn alloys, ductility decreases dramatically (as shown in Figure 1-12).

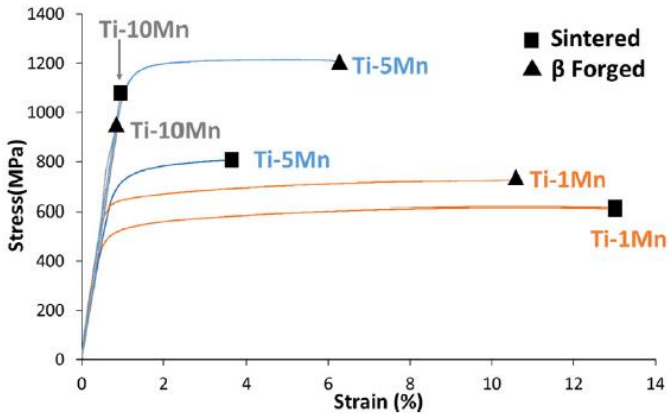

Figure 1-12 Stress vs strain curves of sintered and β forged Ti-Mn alloys [38].

An alternative method to improve the ductility of Ti-Mn alloys is by adding a third alloying element. Mo is considered to be an effective alloying element as Santos *et al.* [39; 41], have concluded that adding Mo increases the ductility of Ti-Mn-Mo alloys by promoting mechanical twinning. It is reported that a Mn concentration higher than 18 wt% should be avoided in biomedical applications, due to the risk of Mn intoxication [38].

Processing of Ti-Mn alloys

Alshammari *et al.* [38] produced two sets of Ti-xMn (x = 1, 5 and 10%) alloys (pure Ti and Mn powder with 99.4% and 99.0% purity respectively) via PM, one set was as-sintered (cold press and vacuum sintered), while the other was subject to β forging. The study by Gouda *et al.* [40], looked at producing Ti-xMn (x = 4.75, 10.3, 13.1 and 15.3%) alloys by MIM, the samples were in the as-sintered condition. The samples were subjected to solution treatment under vacuum (1000 °C) for 1 hour followed by quenching in iced water, the solution treated samples were further subjected to aging at 400, 500 and 560 °C for 0.5 and 3 hours under vacuum. Santos *et al.* [39] also looked at MIM Ti-Mn alloys with Mo as a third element, four sintered samples of Ti-(5-6)Mn-(3-4)Mo were fabricated.

Kim *et al.* [42] fabricated Ti-xMn (x = 5, 10, 15 and 20%) alloys (Ti sponge: 99.9% and Mn ingot: 99.95%) by casting. The samples were remelted seven times and heat treated using the tube furnace under argon atmosphere for 4 hours, at a temperature lower than the respective solidus temperatures (150 °C). They were cooled in the furnace at 10 °C/min down to 600 °C and later air cooled.

In another study by Santos *et al.* [41] the same four Ti-(5-6)Mn-(3-4)Mo alloys were prepared via cold crucible levitation melted (CCLM) method. In this method CP-Ti (grade 1) chips, Mn flakes and Mo wires (with high purity powder: >99.9%) were used. The CCLM process was experimentally performed in a high purity argon atmosphere, the alloy ingots were remelted followed by ice-water quenching. After the CCLM process the alloys were subjected to hot rolling and hot forging, both at 900 ºC and later air-cooled.

Properties of Ti-Mn alloys

The density of sintered Ti-Mn alloys decreases with increasing Mn concentration. A Ti-Mn alloy with 1 wt% Mn has a relative density of 94.4%, and with 10 wt% Mn has a relative density of 90.9% [38]. The density of sintered Ti-Mn alloys can be improved by hot working treatments. Ti-Mn alloys have shown very low ductility, which can be improved by adding a third element such as Mo to Ti-Mn [39; 41]. As previously mentioned adding Mo to Ti-Mn promotes mechanical twinning which is responsible for the increased ductility, hence it increases the mechanical properties. The Ti-5Mn-3Mo alloy fabricated by CCLM [41] had the highest elongation of 18% compared to 2% and 3%, for the Ti-5Mn-3Mo (fabricated by MIM [39]) and Ti-5Mn (fabricated by PM [38]) alloys respectively. The low elongation in the Ti-5Mn-3Mo alloy (fabricated by MIM [39]) is attributed to the high O content, and the presence of pores and carbides, thus they tend to decrease the ductility of the alloy.

Ti-Mn-Mo alloys (fabricated by MIM [39] and CCLM [41]) have shown superior mechanical properties compared to sintered Ti-Mn alloys. The Ti-5Mn-3Mo alloy (prepared by MIM [39]) had an UTS of 1036 MPa and YS of 980 MPa, which reportedly was higher than the sintered Ti-5Mn alloy [38], which had an UTS of 800 MPa and YS of 716 MPa (as shown in Figure 1-12). The highest UTS and YS was reported for the Ti-5Mn-3Mo produced by MIM, compared to the Ti-5Mn-3Mo alloy fabricated by CCLM (UTS: 920 MPa and YS: 855 MPa [41]). The hardness of sintered Ti-Mn alloys is higher than CP-Ti (100 HV), with just 1 wt% of Mn added to Ti, it poses a hardness of 180 HV and increases to 245 HV (Ti-5Mn) [38]. By adding Mo to Ti-Mn alloys, it increases the hardness of the alloy. The Ti-5Mn-3Mo alloy had a hardness of 372 HV (fabricated via CCLM [41]) which reportedly was the highest compared to the sintered Ti-5Mn alloy and Ti-5Mn-3Mo alloy fabricated via MIM (331 HV [39]).

1.2.2.2 Ternary Ti-Mn-Nb alloys

The addition of Mn to Ti-Nb alloys

Chen *et al.* [43] prepared Ti-16Nb-xMn (x = 0, 1, 3, 5, 7 and 9%) alloys (from 99.9% pure Ti, Nb and Mn metals) via CCLM. The alloys were cold rolled into a plate with a thickness reduction of ~60%, later the ingots were sealed in

quartz capsules evacuated to a pressure of $1x10^{-5}$ Pa and solution treated at 900 °C for 30 minutes. After solution treatment, the alloys were quenched in water by breaking the capsules. The purpose of this study was to look at how the addition of Mn to Ti-16Nb would affect the microstructure and mechanical properties of the alloy. The Ti-16Nb alloy was chosen on the basis of previous studies indicating that the alloy comprised of α" and β phases, and with the addition of Mn to Ti-16Nb it would suppress the α" phase and form a single β-phase (as shown in Figure 1-13).

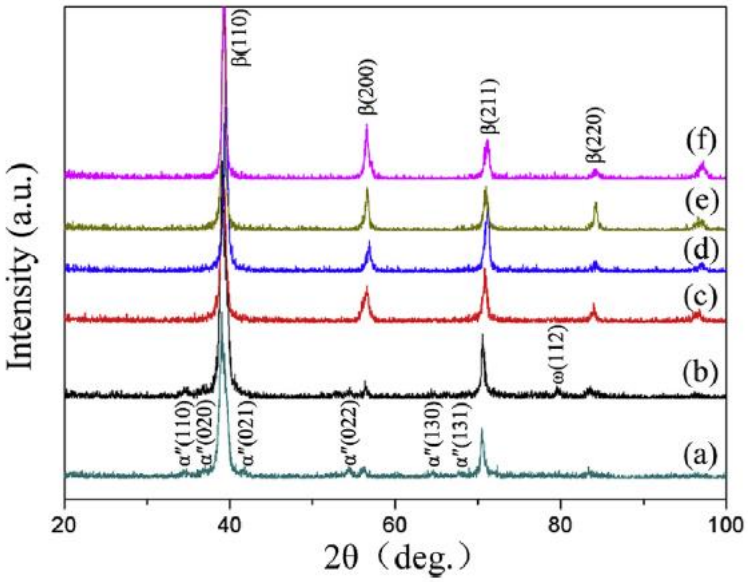

Figure 1-13 XRD patterns of a) Ti-16Nb, b) 1Mn, c) 3Mn, d) 5Mn, e) 7Mn and f) 9Mn alloys [43].

The MoE of Ti-16Nb-xMn alloys is higher than 10 indicating that the alloys will consist of β-phase, and with increasing Mn concentration the MoE increases significantly. The microstructure of the alloys consisted of an equiaxed β matrix. The experimental results showed that the Ti-16Nb-5Mn alloy exhibited the highest UTS of 716 MPa and YS of 657 MPa which was 26% and 77% respectively higher, than that of the Ti-16Nb alloy. The presence of the athermal ω phase, β-phase and solid-solution strengthening effects of Mn affected the tensile properties of the Ti-16Nb-xMn alloys. The tensile strengths of Ti-16Nb-(1-5)Mn alloys increased (from 644-716 MPa) and then decreased (from 695-660 MPa) for the Ti-16Nb-(7-9)Mn alloys. In this study no hardness measurements were reported.

The addition of Nb to Ti-Mn alloys

A study by Ethemam *et al.* [44] looked at a new group of ternary Ti-7Mn-xNb (x = 0, 3, 7 and 10%) alloys fabricated via PM (conventional press and sinter) from BE powder. The average powder particle size for Ti, Mn and Nb powders were <50 μm, ≤10 μm and <50 μm, respectively. The microstructure, phase composition and mechanical properties were investigated on the effects of increasing the Nb concentration in Ti-7Mn-xNb alloys. The study primarily focused on producing β-type ternary Ti-7Mn-xNb alloys, with the addition of Nb to Ti-7Mn, the intensity of the β-phase increased and in contrast the intensity of the α-phase decreased. α + β lamellar microstructures consisted for all the alloys as shown in Figure 1-14.

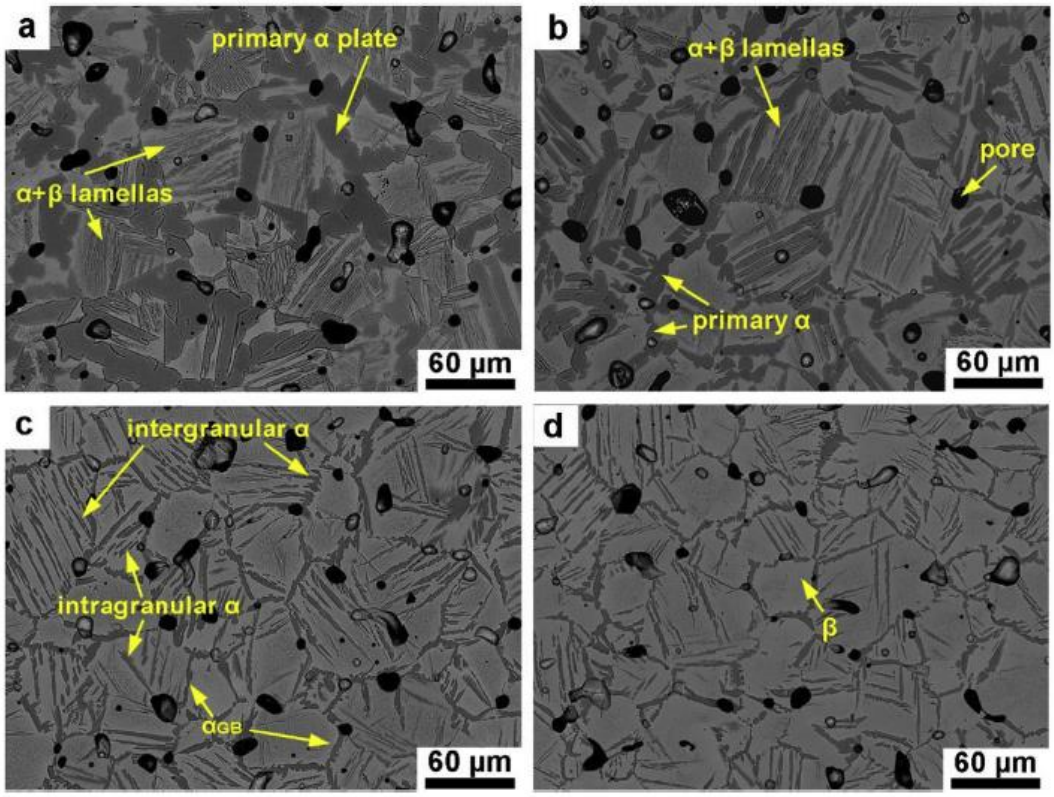

Figure 1-14 SEM micrographs of the sintered Ti-7Mn-xNb alloys: a) Ti-7Mn, b) Ti-7Mn-3Nb, c) Ti-7Mn-7Nb, and d) Ti-7Mn-10Nb [44].

With the addition of 3 wt% Nb (Figure 1-14b), the α-phase becomes finer and its amount decreases. Increasing the Nb concentration to 7 wt% (Figure 1-14c) enhances the β-phase while the α-phase reduces even further. Lastly, with the addition of 10 wt% Nb (Figure 1-14d), the β-phase is more stabilized and the α-phase is further reduced (refined microstructure). Experimental results showed that

with increasing Nb concentration, the ultimate compressive strength (UCS) and YS of the Ti-7Mn-xNb alloys gradually decreased. Compressive strength was chosen instead of tensile strength, as it is a key factor in determining the suitability of implant materials since bone tissues are mainly exposed to compressive stresses [44]. The compressive strain of the Ti-7Mn-xNb alloys increased gradually as the Nb concentration increased. The highest UCS (2127 MPa) and YS (1005 MPa) was observed for the Ti-7Mn alloy, whereas the lowest was observed for the Ti-7Mn-10Nb alloy (UCS: 1842 MPa & YS: 842 MPa). The hardness was again the highest for the Ti-7Mn alloy (375 HV), and gradually decreased as the Nb concentration increased (similar to the trends of UCS and YS). The high mechanical properties of the Ti-7Mn alloy is due to the strong solid-solution strengthening effect of Mn. Overall the properties of the Ti-7Mn-xNb alloys was significantly greater than the sintered CP-Ti alloy.

Chicardi *et al.* [45] fabricated ternary Ti-Nb-xMn (x = 0, 3, 6, 9 and 12%) alloys (with high purity metal powders Ti: 99.6%, Nb: 99.9% and Mn: 99.9%) via mechanical alloying (MA) in a planetary ball mill with different milling times between 1 hour and 120 hours at spinning rate of 300 rpm [45]. The aim of the study was to manufacture β-type ternary Ti-Nb-xMn alloys, with the addition of Mn, and a Nb concentration in the range of 30-35 wt% was used. It has been reported in previous studies that, the Ti-30Nb alloy is sufficient to stabilize the β-phase [25; 45].

Other ternary Ti alloys with Mn

As mentioned in section 1.2.1.3, the second set of samples were Mn-dominant ternary Ti-xCu-yMn alloys designed by Alqattan *et al.* [32]. The Mn-dominant samples were in a ratio of 3:1 i.e. one with Mn/Cu, which consisted of the following compositions of Ti-xMn-yCu (x = 0.6, 1.2, 2.4, and 4.8% & y = 0.2, 0.4, 0.8 and 1.6%). The experimental results showed that with the addition of Mn to the Ti-xMn-yCu alloy, the tensile properties of the alloy increased remarkably, the highest reported UTS and YS (was for the Ti-4.8Mn-1.6Cu alloy) was 817 MPa and 729 MPa respectively. However, as the Mn concentration increased the elongation of the Ti-xMn-yCu alloys decreased gradually (from to 20% to 5%). The hardness of the Ti-xMn-yCu alloys increased considerably (from 56 – 63.5 HRA) with increasing Mn concentration. With the addition of two alloying elements (Mn

and Cu) they both contributed to the increased properties of Mn-dominant ternary Ti-xMn-yCu alloys. It is worth mentioning that Mn has a stronger stabilizing effect on the β-Ti phase than Cu at the same concentration, hence Mn-dominant alloys are predominantly stronger and have higher UTS, YS and hardness in comparison to Cu-dominant alloys (as mentioned in section 1.2.1.3) [32]. As shown in Figure 1-15, it is evident that at same Mn-dominant and Cu-dominant concentrations, the Mn-dominant alloy has a much finer microstructure compared to the Cu-dominant alloy, thus it is responsible for the increased mechanical properties.

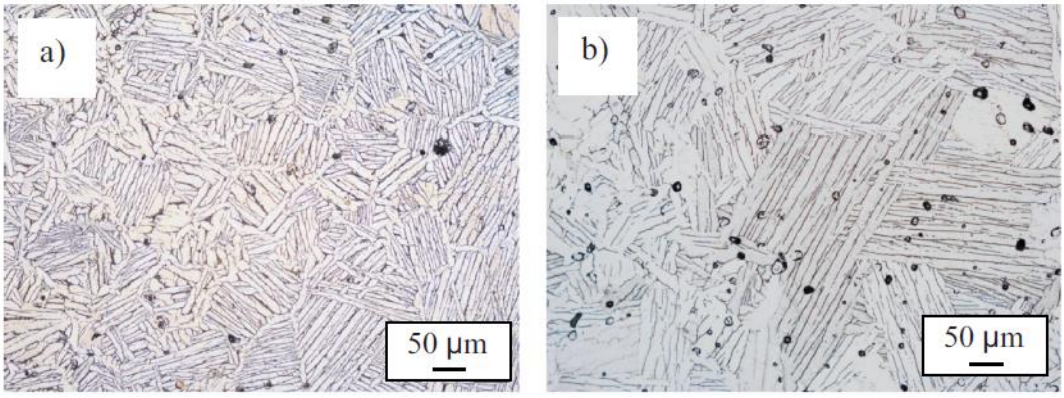

Figure 1-15 OM of a) Mn-dominant alloy (Ti-1.2Mn-0.4Cu) and b) Cu-dominant alloy (Ti-0.4Mn-1.2Cu) [32].

1.2.3 Ternary Ti-Fe-Nb alloys

In this section binary Ti-Fe alloys are first discussed followed by the ternary Ti-Fe-Nb alloys. Binary Ti-Nb alloys have already been discussed in section 1.2.1.2.

1.2.3.1 Ti-Fe alloys

Fe is the cheapest metallic element being readily available across the word. Fe is a strong β-stabilizing element (providing strong solid-solution strengthening effect) when alloyed to Ti, permitting to achieve similar properties to other binary Ti alloys (i.e. binary Ti-(Cu or Nb or Mn) alloys); however, Fe has a high diffusivity in Ti, making it favourable for the sinterability of the material (Fe is an ideal element to develop PM Ti alloys) [46-53]. The addition of Fe to Ti lowers the cost of the alloy, thus cost effective PM Ti-Fe alloys can be manufactured [50; 52]. Fe is a β-eutectoid element and will form TiFe intermetallic compounds at 1085 °C at a Fe concentration of 32.5 wt% according to the binary Ti-Fe equilibrium phase

diagram [54]. Ti-Fe alloys have been studied by many researches and have been fabricated by PM approach which is beneficial in making comparisons in this study.

The effects of increasing Fe concentration in Ti-Fe alloys

The addition of Fe to Ti increases the mechanical properties of Ti-Fe alloys similar to other binary Ti alloys. With increasing Fe concentration, the elongation decreases as well as the relative density of Ti-Fe alloys. Tensile properties such as UTS and YS increase with increasing Fe concentration as well as the hardness of Ti-Fe alloys. The increase in the mechanical properties of Ti-Fe alloys is due to the strong solid-solution strengthening effect of Fe.

Processing Ti-Fe alloys

In a study by Chen *et al.* [46], Ti-xFe (x = 3, 5 and 7%) alloys (gas atomized Ti powder and carbonyl Fe powder with particle size of 25.2 and 3.4 μm respectively) alloys were fabricated via PM route (i.e. press and vacuum sintering at 1250 °C), followed by cooling at different cooling schedules. The objective of the study was to analyse the effects of post-sintering heat treatment parameters, mainly at different holding temperatures in the α + β region and cooling rates on the mechanical properties of Ti-xFe alloys. Bolzoni *et al.* [47] used PM in their work to fabricate Ti-xFe (x = 5 and 7%) alloys (elemental Ti and Fe powder: 99.6% and 85Fe/15Ni respectively). In a study by Raynova *et al.* [48], binary Ti-5Fe alloy (HDH Ti powder and elemental 5 wt% Fe powder) was fabricated by a combination of sintering plus thermomechanical treatment. Two stage sintering was used for consolidation of the powder compacts, to guarantee chemical homogeneity of the materials. The thermomechanical treatment involved open die forging/extrusion, further some of the samples were subjected to annealing heat treatment [48]. In another study by the same author [49], induction sintering method was used to produce binary Ti-5Fe alloy (HDH Ti powder and Fe carbonyl powder). In this method high-frequency induction heating was used as the heating source to induction sinter BE Ti-5Fe alloy (warm pressing at 250 °C at a uniaxial pressure of 700 MPa) [49]. Romero *et al.* [50] also fabricated PM Ti-5Fe alloy (HDH Ti powder and Fe carbonyl powder) by the BE route (warm pressing at 230 °C at a compacting pressure of 400 MPa), followed by thermomechanical processing. In the thermomechanical processing the alloy was extruded at different temperatures and heat treatment such as solution treatment and aging were investigated [50]. The

same method was used by Alshammari *et al.* [51] to fabricate binary Ti-5Fe_c and Ti-5Fe_m alloys (HDH Ti powder, c = carbonyl powder and m = milled powder), via PM route (i.e. warm compaction at 250 °C applying a uniaxial pressure of 600 MPa and vacuum sintering). Thermomechanical processing of the alloys was done by forging in the β region to enhance the mechanical properties as well as refine the microstructure of the alloy [51].

Niu *et al.* [55] manufactured a series of binary Ti-xFe (x = 0.2, 0.5, 1, 2,3 and 4%) alloys (high purity grade 0 Ti sponge: >99.8% and Fe powder: 99.9%) via casting. The alloys were fabricated by vacuum CCLM method.

Properties of Ti-Fe alloys

Many researchers have studied binary Ti-Fe alloys, with Fe concentrations between 5 to 7 wt%, due to the excellent mechanical properties obtained with the β-Ti phase being retained [46-53; 55]. Literature is very limited on Ti-Fe alloys with less than 5 wt% Fe additions. The relative density of Ti-Fe alloys is higher than CP-Ti, and with the addition of Fe to Ti, the ductility of Ti-Fe alloys decreases (similar affects to other binary Ti alloys). The highest elongation reported for a Ti-Fe alloy is 26 ± 8.90% (Ti-0.2Fe), fabricated via casting (CCLM) [55].

Tensile properties of Ti-Fe alloys are significantly higher than CP-Ti. The sintered Ti-5Fe alloy [48] has an UTS and YS value of 930 MPa and 850 MPa respectively (with a low ductility of 2.6% at a relative density of 98.73%) as shown in Figure 1-16.

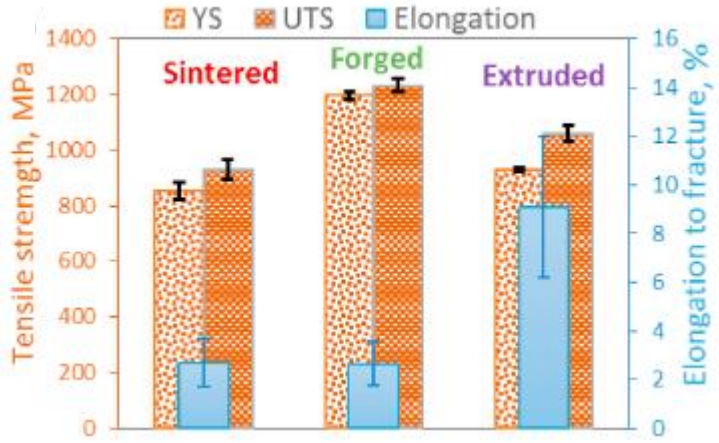

Figure 1-16 Characterization of the sintered, forged and extruded Ti-5Fe alloy [48].

Similar tensile properties have been reported for other binary Ti-5Fe alloys fabricated by the PM approach [46; 49-51]. Hardness of Ti-Fe alloys increases with Fe additions, the highest reported hardness for Ti-5Fe is 345 HV (fabricated via PM method [52]). Similar hardness values have also been reported for other Ti-5Fe alloys (fabricated by PM method) [46; 47; 51].

Subsequent treatments such as extrusion, forging and solution treatment have been reported to further increase the ductility (remove most of the porosity left behind from sintering), mechanical properties (as shown in Figure 1-16) as well as the hardness of PM Ti-5Fe alloys [46; 48; 50-52].

1.2.3.2 Ternary Ti-Fe-Nb alloys

The addition of Fe to Ti-Nb alloys

Ternary Ti-5Nb-xFe (x = 0, 1, 2, 3, 4 and 5%) alloys were studied by Hsu *et al.* [56]. The alloys were fabricated using a commercial arc-melting vacuum-pressure casting system using Ti (ASTM grade 2), Nb and Fe powders with 99.95% purity. With increasing Fe concentrations retention of the metastable β-phase started to begin, small amounts were obtained with 1 to 2 wt% Fe and large amounts were retained at higher Fe concentrations (≥ 3 wt% Fe) as shown in Figure 1-17.

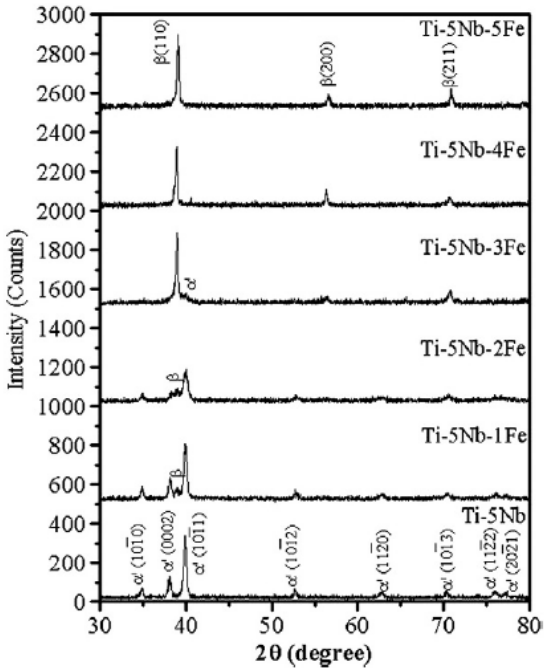

Figure 1-17 XRD patterns of Ti-5Nb-xFe alloys [56].

It was reported that the binary Ti-5Nb alloy mainly consisted of the α' phase, and is shown in the XRD spectra (Figure 1-17). A three-point bending test was performed to evaluate the mechanical properties of the ternary alloys. All ternary alloys showed higher bending strengths (from 1466 – 2460 MPa) than CP-Ti (844 MPa), the alloys Ti-5Nb-2Fe and Ti-5Nb-5Fe both showed the highest bending strengths compared to the other alloys [56].

The addition of Fe (0.5, 3.5, 6 and 9%) to binary Ti-11Nb alloys were designed by Ehtemam-Haghighi *et al.* [57], and fabricated via CCLM. Raw Ti, Fe and Nb powders with 99.9% purity were used. With increasing Fe concentration, the volume fraction of the β-phase increased, with the resultant microstructure comprised mainly with β and very small amount of α". The addition of Fe (from 0.5 – 6 wt% Fe) to Ti-11Nb increased the compressive YS (from 796 – 1137 MPa) as well as the hardness (from 278 – 357 HV5) of the alloys.

The addition of Nb to Ti-Fe alloys

Ehtemam-Haghighi *et al.* [58] also fabricated a series of ternary Ti-xNb-7Fe (x = 0, 1, 4, 6 and 11%) alloys via CCLM under an argon atmosphere. The alloys were made using raw Ti, Nb and Fe powders from 99.9% purity. With the addition of Nb to Ti-7Fe, the volume fraction of the β-phase increased while the volume fraction of the α" phase decreased (as shown in Figure 1-18).

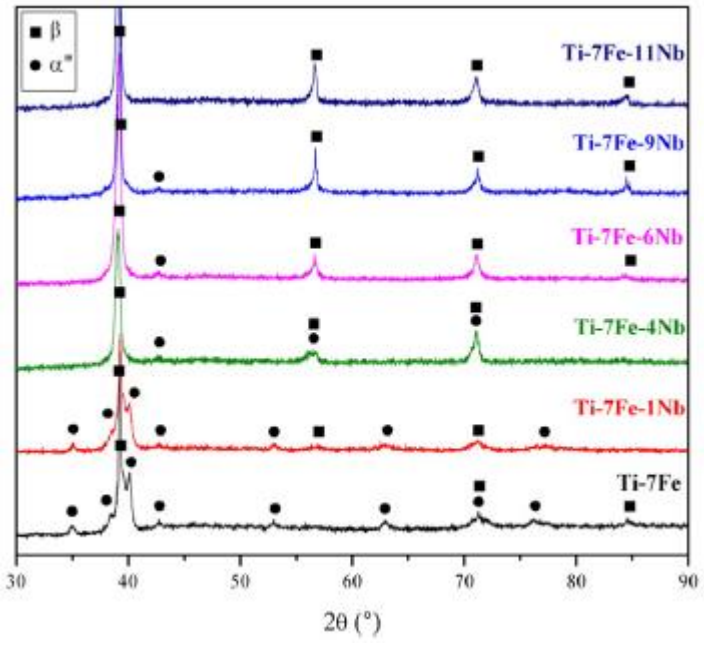

Figure 1-18 XRD patterns of the as-cast Ti-7Fe-xNb alloys [58].

The experimental results showed that the compressive stresses for the ternary alloys (except Ti-7Fe-1Nb) did not fail when the maximum load capacity of the machine reached 100 kN. However, the alloys Ti-7Fe and Ti-7Fe-1Nb failed due to the high-volume fraction of the α" phase. The Ti-7Fe alloy showed the highest compressive YS (1874 MPa) and hardness (560 HV), and the lowest plastic strain (2%) compared to the ternary alloys [58]. With the addition of Nb to Ti-7Fe, the compressive strength (from 2093 – 1990 MPa), compressive YS (from 1847 – 985 MPa) and hardness (from 520 – 325 HV) decreased as the concentration of Nb increased (from 1 – 11 wt% Nb). In another study by the same author [59], the same ternary Ti-xNb-7Fe alloys were fabricated by the same manufacturing methods (CCLM). In this study the mechanical and wear properties of the ternary alloys were evaluated. With the addition of Nb to Ti-7Fe, the wear resistance reduced with increasing Nb concentration (from 0 – 11 wt% Nb), thus showing better wear resistance than CP-Ti and Ti-6Al-4V.

In a study by Afonso *et al.* [60], ternary Ti-3Fe-xNb (x = 10, 15, 20, 25, 30 and 35%) alloys were prepared by arc melting and then copper mold cast into cylinder and plate shapes. Two sets of samples were produced, the first being 30 g as-cast (slowly cooled (SC)), and the other being rapidly solidified (RS). From the initial ingots (30 g), samples of 10 g were cut, melt and rapidly solidified in another arc furnace melting system (RS – samples). Pure elements of Ti sponge (99.5%), Nb (99.8%) and electrolytic Fe (99.7%) were used as raw materials. The aim of the study was to produce β-type ternary Ti-3Fe-xNb alloys applicable for biomedical applications, with low Young's modulus (i.e. close to the human bone). Experimental results showed that increasing the Nb concentration from 10 – 25 wt%, stabilized the β-phase (as shown in Table 1-1), while the volume fraction of the α-phase decreased (as confirmed by XRD results). The Ti-25Nb-3Fe alloy consisted of only the β-phase, since the addition of 3 wt% Fe, a strong β-stabilizing element, favoured the stabilization of the β-phase (instead of a minimum of 35 wt% Nb to obtain the stable β-phase in binary Ti-Nb system [60]). No martensite α' and α" phases were identified by XRD, and it is believed that with the addition of 3 wt% Fe, there should be no formation of these phases [60]. The RS samples obtained β-Ti structures with volume fractions of the ω phase at lower Nb concentrations (10 and 15 wt%). For the SC samples, α + β structures were obtained up to 20 wt% Nb addition (the ω phase was only detected for the Ti-20Nb-3Fe alloy), and for higher

additions of Nb (from 25 – 35 wt%), β-Ti structure was obtained. Microstructure of alloys showed refinement, with the addition of Nb. The RS Ti-10Nb-3Fe and Ti-15Nb-3Fe alloys showed higher hardness values (due to the formation of the ω phase, as confirmed by XRD analysis), compared to SC samples as shown in Table 1-1. The SC Ti-20Nb-3Fe alloy, showed the highest hardness among the other SC alloys, due to the formation of the ω phase (as confirmed by XRD analysis) as shown in Table 1-1.

Table 1-1 Vickers hardness values for arc melting as-cast (SC) sample and RS copper mold samples for cylinder with 6 mm diameter of Ti-xNb-3Fe alloys [60].

Alloy [wt%]		Vickers hardness [$HV_{0.2}$]	Phases [XRD]
Ti–10Nb–3Fe	SC	278 ± 18	$\alpha + \beta$
	6 mm	463 ± 34	$\beta + \omega$
Ti–15Nb–3Fe	SC	271 ± 17	$\alpha + \beta$
	6 mm	600 ± 46	$\beta + \omega$
Ti–20Nb–3Fe	SC	417 ± 19	$\alpha + \beta + \omega$
	6 mm	347 ± 22	$\beta + \omega$
Ti–25Nb–3Fe	SC	278 ± 9	β
	6 mm	272 ± 6	β
Ti–30Nb–3Fe	SC	253 ± 12	β
	6 mm	256 ± 4	β
Ti–35Nb–3Fe	SC	259 ± 7	β
	6 mm	244 ± 8	β

Li *et al.* [61] fabricated a series of ternary Ti-xNb-2Fe (x = 14, 16, 18, 20, 22 and 24%) alloys via casting. After casting the ingots were solution treated at 850 °C for 1 hour and then quenched in water. The alloys were cold-rolled (room temperature) under a reduction ratio of 88% to a sheet with a thickness of 1.4 mm. Lastly the alloys were subjected to solution treatment at 800 °C for 1 hour followed by water quenching. The aim of the study was to design β-type ternary alloys with excellent mechanical properties and biocompatibility for biomedical applications. The results showed that the Ti-14Nb-2Fe (comprised of both α" and ω phases) alloy displayed the highest UTS (830 MPa) and YS (685 MPa), compared to the other alloys (comprised of just single β-phases), this was due to the ω phase (detected by XRD) which showed the precipitation strengthening effect [61]. Increasing the Nb concentration (from 14 – 24 wt% Nb) caused a decrease in the mechanical properties of the ternary alloys as shown in Figure 1-19.

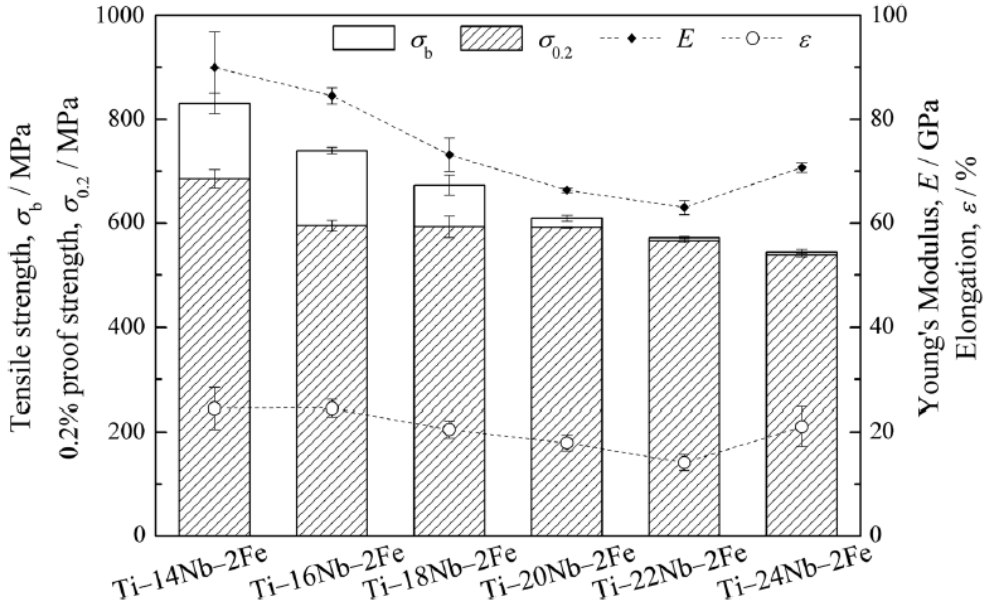

Figure 1-19 Tensile strength (σ_b), YS ($\sigma_{0.2}$), elongation (ϵ) and Young's modulus (E) of Ti-xNb-2Fe alloys [61].

Other Ti-Fe-Nb alloys

In a study by Chirico *et al.* [62], binary Ti-xFe (x = 5 and 7%) and Ti-xNb (x = 12, 25 and 40%), and ternary Ti-xFe-yNb (x = 5 and 7%, and y = 25 and 40%) alloys were fabricated via PM. The study primarily focused on producing β-type Ti alloys by using TiH_2, elemental Nb and Fe powders with average particle sizes of 27, 18 and 4 μm, respectively. No mechanical properties were reported in the study.

1.2.4 Ternary Ti-Fe-Cu alloys

Both Fe and Cu are cheap alloying elements (Fe being cheaper than Cu), when both elements are alloyed to Ti, the overall cost of the material is low compared to other alloying elements (such as Nb, Mo, V and Ta). By adding both Fe and Cu to Ti, the melting temperature of the alloy is relatively low (lower than Ti), thus making it favourable for the sinterability of the material (Fe has a high diffusivity in Ti) [48]. Studies on ternary Ti-Fe-Cu alloys have not been reported extensively, suggesting more work should be done on this alloy system.

In a study by Cho *et al.* [63], six ternary Ti-xFe-yCu (x = 18, 22, 30, 27, 30 and 30% & y = 4, 5, 2, 6, 4 and 6.6%) alloys were studied (designed using a *d*-electrons alloy method) and fabricated by casting, followed by heat treatment under high-purity argon atmosphere at 900 ºC for 6 hours followed by air cooling. All alloys except

Ti-18Fe-4Cu and Ti-22Fe-5Cu were further subjected to heat treatment under a high-purity argon atmosphere at 900 ºC for 24 hours followed by air cooling. Ti sponge (99.7%), Fe wire (99%) and high purity Cu (99.99%) were used in this work. The aim of the study was to develop new ternary Ti-Fe-Cu alloys with high ductility, Young's modulus, hardness as well as compressive strength compared to existing Ti alloys. Experimental results show that the as-cast Ti-Fe-Cu alloys, consist of the β-Ti phase and dendritic TiFe phase (confirmed by XRD analysis and optical microscopy (OM)) as shown in Figure 1-20, and no Ti_2Cu phase was reported in the study.

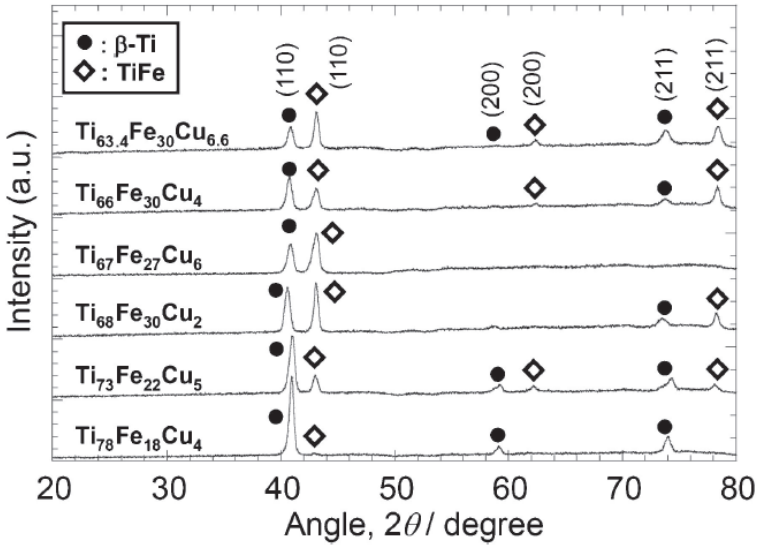

Figure 1-20 XRD patterns of studied Ti-Fe-Cu alloys before heat treatment (as-cast) [63].

The hardness of as-cast Ti-Fe-Cu alloys increased from 490 HV (Ti-18Fe-4Cu) to 550 HV (Ti-30Fe-6.6Cu), with increasing Fe concentration. The hardness of these as-cast alloys is relatively higher than the heat treated alloys (hardness decreased by 6% after the heat treatment for all alloys), CP-Ti (145 HV) and Ti-64 (extra low interstitial (ELI)) (320HV) [63]. The high hardness of as-cast Ti-Fe-Cu alloys is due to the formation of the TiFe phase (volume fraction of TiFe phase increases with the addition of Fe). From compressive testing, the heat treated Ti-Fe-Cu alloys displayed high compressive strengths and strains compared to as-cast Ti-Fe-Cu alloys. With the highest reported compressive strength and strain being 2121 MPa and 24.5% respectively, which was reported for the heat-treated alloy (Ti-27Fe-6Cu at 24 hours). This is because the fracture of as-cast alloys does not occur in the plastic region but occurs in the elastic region, and for the heat treated alloys it is

vice versa since the hardness decreases and the fracture occurs in the plastic region ("this is a well-known phenomenon for brittle alloys with intermetallic phase" [63]).

1.2.5 Ternary Ti-Fe-Mn alloys

Ternary Ti-Fe-Mn alloys have not been studied in depth in literature, suggesting more work should be done on this alloy system.

Ikeda *et al.* [64] studied the influence of Fe additions to Ti-Mn-Fe (Ti-10Mn (0Fe), Ti-8.7Mn-1Fe (1Fe), Ti-6.1Mn-3Fe (3Fe) and Ti-3.5Mn-5Fe (5Fe)) alloys via casting. The alloys were designed based on an average ratio of valence electrons to atoms (i.e. e/a) of 4.26. Ti sponge, flake-like Mn and Fe wire were used in this study. The alloy ingots were hot forged and rolled at 847 ºC. Furthermore, the specimens were encapsulated in a silica tube and solution treated at 900 ºC for 1 hour, and then quenched by breaking the capsules in ice water. Lastly the specimens were isothermally aged at 300, 400 and 500 ºC. From the experimental results all alloys showed equiaxed grain structures (Figure 1-21a) and only the β-phase (Figure 1-21b), expect for the Ti-10Mn alloy (athermal ω and β-phase were observed as shown in Figure 1-21b). The hardness of the Ti-Mn alloys was relatively uniform, with the 5Fe alloy having a significantly higher hardness, followed by the 3Fe alloy.

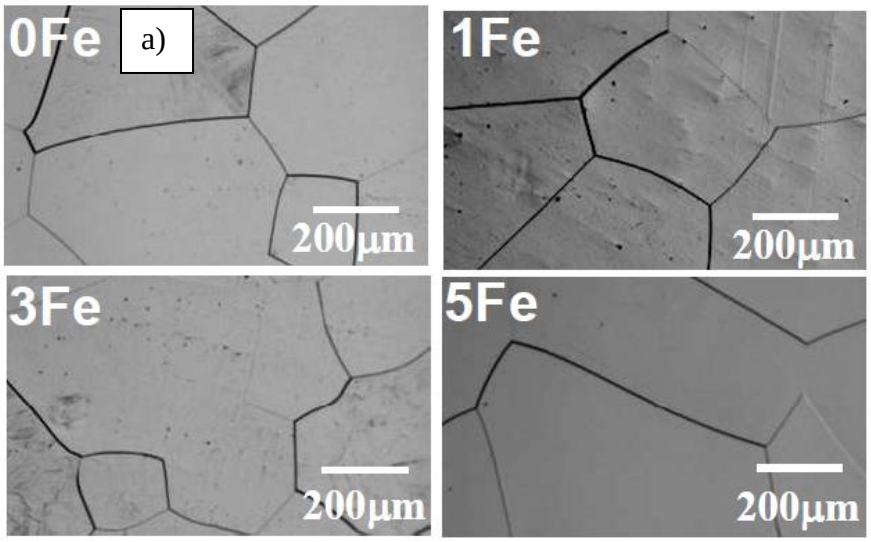

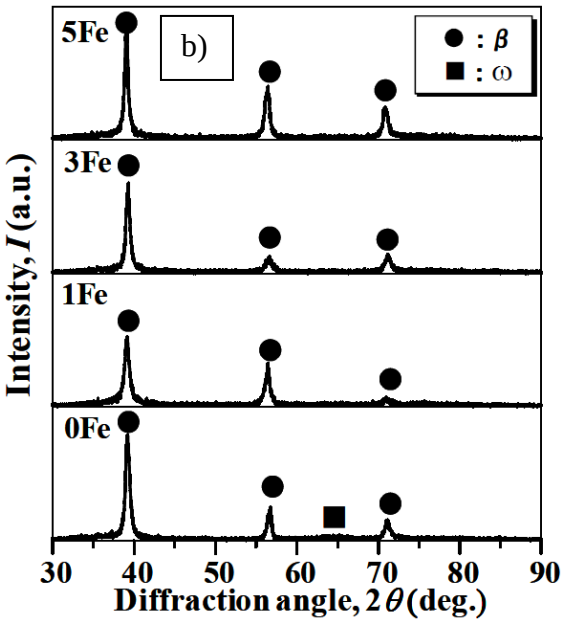

Figure 1-21 a) OM and b) XRD of Ti-Mn-Fe alloys [64].

1.3 Conclusions

Binary Ti-Cu, Ti-Nb, Ti-Mn and Ti-Fe alloys have been studied to a great extent, compared to ternary Ti-Cu-Nb, Ti-Mn-Nb, Ti-Fe-Nb, Ti-Fe-Cu and Ti-Fe-Mn alloys. The additions of Cu, Nb, Mn and Fe to Ti have shown to significantly increase the mechanical properties (compared to CP-Ti), as well as refine the microstructure of the alloy (especially Mn and Fe, as they are strong β-stabilizers providing strong solid-solution strengthening effect). Fabrication of binary Ti alloys has been considered via casting and PM, PM being cost effective. However, literature studies reported for the binary Ti-Nb alloy system, have only fabricated the alloys via casting, suggesting the alloy should be fabricated by PM (in order to make comparisons of the alloy by both processes). Reported literature studies for the ternary alloy systems, aiming to produce β-type ternary Ti alloys, with high β-stabilizer concentrations, thus increasing the cost of the alloy are lacking. Both ternary Ti-Fe-Cu and Ti-Fe-Mn alloy systems, reported only one literature study, showing that the alloy systems are not studied extensively. Reported studies indicate that, adding two elements to Ti, could lower the overall cost, melting temperature of the alloy as well as enhancing the mechanical properties of the alloy.

Chapter 2

Motivation and Objectives

2.1 Motivation of This Work

Based on the conclusions from the literature review, to a great extent, binary Ti-Cu, Ti-Nb, Ti-Mn and Ti-Fe alloys have been studied, compared to ternary Ti-Cu-Nb, Ti-Mn-Nb, Ti-Fe-Nb, Ti-Fe-Cu and Ti-Fe-Mn alloys. With only one relevant literature study reported for the Ti-Fe-Cu and Ti-Fe-Mn alloy systems, the work proposed in this thesis fills a big gap in literature. For the studies reported in literature, they mainly focused on fabricating the ternary alloy systems via casting, whereas fabrication by PM has not been considered. With the limited amount of literature, it is in best interest to fabricate novel ternary Ti-Cu-Nb, Ti-Mn-Nb, Ti-Fe-Nb, Ti-Fe-Cu and Ti-Fe-Mn alloys via PM route (PM being more economical than casting). The alloying elements Cu, Nb, Mn and Fe are chosen because of their low cost (except for Nb), strong β-stabilizing effect (especially Fe and Mn) when alloyed to Ti (providing different strengthening effects), and their ability to provide superior mechanical properties as well as biocompatibility when alloyed to Ti. By adding two different elements to Ti, the overall cost is reduced, the melting temperature is lowered, and better mechanical properties compared to CP-Ti are expected.

2.2 Aim and Objectives

2.2.1 Aim

This study aims to understand the effects of adding two different β-stabilizing elements (Cu, Nb, Mn and Fe) to Ti. The main goal of this thesis is to fabricate cost effective PM ternary Ti alloys, with small additions of alloying elements (from 0.5 – 5 wt%), aiming to have enhanced properties compared to CP-Ti. In order to achieve this, certain objectives need to be fulfilled.

2.2.2 Objectives

- Review current literature studies on binary Ti-Cu, Ti-Nb, Ti-Mn and Ti-Fe alloys, and ternary Ti-Cu-Nb, Ti-Mn-Nb, Ti-Fe-Nb, Ti-Fe-Cu and Ti-Fe-Mn alloys.
- Design novel ternary Ti alloy compositions using the MoE approach.
- Fabricate the novel ternary Ti alloy compositions via PM (i.e. cold press and vacuum sintering).
- Evaluate the properties of the sintered novel ternary Ti alloys through density measurements (theoretical, green, and sintered), microstructure analysis (OM, SEM, and XRD), and mechanical testing (tensile test and hardness).
- Compare the performance of the novel ternary Ti alloys with relevant counterpart Ti alloys used in engineering applications.

Chapter 3

Experimental Method

3.1 Alloy Design and Materials

In this thesis new ternary Ti alloy compositions are designed using the MoE. In a study by Tang *et al.* [65], two MoE models were used, one proposed by Bania (Equation (1)) [66]:

$$\text{MoE} = 1.0\,\text{Mo} + 0.67\,\text{V} + 0.44\,\text{W} + 0.28\,\text{Nb} + 0.22\,\text{Ta} + 2.9\,\text{Fe} + 1.6\,\text{Cr} + 0.77\,\text{Cu} + 1.11\,\text{Ni} + 1.43\,\text{Co} + 1.54\,\text{Mn} - 1.0\,\text{Al}\ (\text{wt\%})$$

$$\text{Simplified MoE} = 0.28\,\text{Nb} + 2.9\,\text{Fe} + 0.77\,\text{Cu} + 1.54\,\text{Mn}\ (\text{wt\%}) \qquad \text{Eq. 1}$$

and the other proposed by Wang *et al*. (Equation (2)) [67]:

$$\text{MoE} = 1.0\,\text{Mo} + 1.25\,\text{V} + 0.59\,\text{W} + 0.28\,\text{Nb} + 0.22\,\text{Ta} + 1.93\,\text{Fe} + 1.84\,\text{Cr} + 1.50\,\text{Cu} + 2.46\,\text{Ni} + 2.67\,\text{Co} + 2.26\,\text{Mn} + 0.30\,\text{Sn} + 0.47\,\text{Zr} + 3.01\,\text{Si} - 1.47\,\text{Al}\ (\text{wt\%})$$

$$\text{Simplified MoE} = 0.28\,\text{Nb} + 1.93\,\text{Fe} + 1.50\,\text{Cu} + 2.26\,\text{Mn}\ (\text{wt\%}) \qquad \text{Eq. 2}$$

which were used to classify the three metastable β Ti alloys, Ti-5553 (Ti-5Al-5Mo-5V-3Cr), Ti-55531 (Ti-5Al-5Mo-5V-3Cr-1Zr) and Ti-7333 (Ti-7Mo-3Cr-3Nb-3Al). The aim of the study involved, using the MoE, to discuss the effect of chemical composition on the starting temperature of the ω phase transformation (during isothermal ageing and continuous heating process) for the metastable β Ti alloys [65]. Results showed that the metastable β Ti alloys with lower MoE had lower starting temperature of the ω phase transformation and wider transformation, it was concluded that Eq. 2 was more accurate than Eq. 1 for discussing the starting temperature of the ω phase transformation. However, both MoE models will be used to design the ternary Ti alloy compositions in this thesis, as they have the alloying elements Cu, Nb, Mn and Fe, to prove which model better predicts the equilibrium microstructure of vacuum sintered Ti alloys.

Raw Ti, Cu, Nb, Mn and Fe powders were used in this study (details of the raw powders are shown in Figure 3-1 and Table 3-1). The raw Ti, Cu, Nb, Fe and Mn powders are characterized by an irregular, dendritic, irregular, spherical, and irregular morphology, respectively, as shown in Figure 3-1.

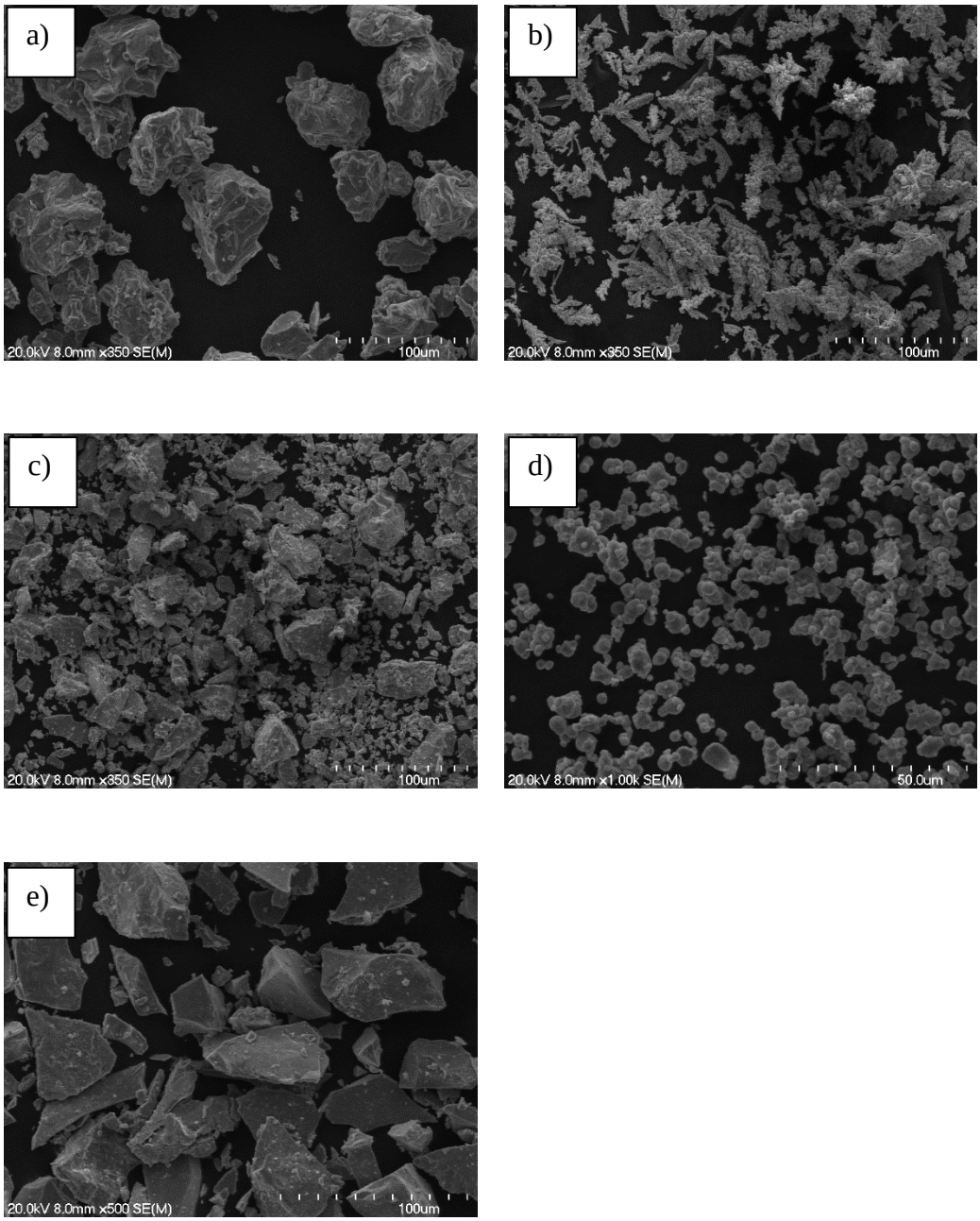

Figure 3-1 Morphology of the raw materials: a) Ti, b) Cu, c) Nb, d) Fe, and e) Mn.

Table 3-1 Details of the raw powders.

Materials	Purity	Particle size	Supplier
Ti	99.4%	200 mesh (<75 µm)	Goodfellow Cambridge Ltd (UK)
Cu	99.7%	230 mesh (63µm)	Merck KGaA (Germany)
Nb	99.8%	325 mesh (<45 µm)	Alfa Aesar (USA)
Mn	99.0%	325 mesh (63 µm)	Sigma-Aldrich (USA)
Fe	99.0%	1200 mesh (<10 µm)	Goodfellow Cambridge Ltd (UK)

The designed alloy compositions of Ti-xCu-xNb, Ti-xMn-xNb, Ti-xFe-xNb, Ti-xFe-xCu and Ti-xFe-xMn (x = 0.5, 1, 2, 3.5 and 5 in wt%), are displayed on Table 3-2, Table 3-3, Table 3-4, Table 3-5 and Table 3-6, respectively, with their theoretical density (calculated using the rule of mixtures equation as shown in section 3.3.1 [68]), MoE and the predicted alloy type. The designed ternary Ti alloy compositions were prepared using the correct ratio of powders weighed on an analytical scale (2-decimal digits).

Table 3-2 Designed ternary Ti-xCu-xNb alloys.

Compositions	Theoretical density	MoE		Alloy type	
Ti-xCu-xNb	**(g/cm^3)**	**Eq. 2**	**Eq. 1**	**Eq. 2**	**Eq. 1**
Ti-0.5Cu-0.5Nb	4.55	0.9	0.5	α + β	α + β
Ti-1Cu-1Nb	4.60	1.8	1.1		
Ti-2Cu-2Nb	4.68	3.6	2.1		
Ti-3.5Cu-3.5Nb	4.81	6.2	3.7	Near-β	
Ti-5Cu-5Nb	4.94	8.9	5.3		Near-β

Table 3-3 Designed ternary Ti-xMn-xNb alloys.

Compositions	Theoretical density	MoE		Alloy type	
Ti-xMn-xNb	**(g/cm^3)**	**Eq. 2**	**Eq. 1**	**Eq. 2**	**Eq. 1**
Ti-0.5Mn-0.5Nb	4.54	1.3	0.9	α + β	
Ti-1Mn-1Nb	4.58	2.5	1.8		
Ti-2Mn-2Nb	4.65	5.1	3.6		

Ti-3.5Mn-3.5Nb	4.75	8.9	6.4	Near-β	Near-β
Ti-5Mn-5Nb	4.85	12.7	9.1	Metastable β	

Table 3-4 Designed ternary Ti-xFe-xNb alloys.

Compositions	**Theoretical density**	**MoE**		**Alloy type**	
Ti-xFe-xNb	**(g/cm^3)**	**Eq. 2**	**Eq. 1**	**Eq. 2**	**Eq. 1**
Ti-0.5Fe-0.5Nb	4.55	1.1	1.6	α + β	α + β
Ti-1Fe-1Nb	4.58	2.2	3.2		
Ti-2Fe-2Nb	4.66	4.4	6.4		Near-β
Ti-3.5Fe-3.5Nb	4.77	7.7	11.1	Near-β	Metastable β
Ti-5Fe-5Nb	4.88	11.1	15.9	Metastable β	

Table 3-5 Designed ternary Ti-xFe-xCu alloys.

Compositions	**Theoretical density**	**MoE**		**Alloy type**	
Ti-xFe-xCu	**(g/cm^3)**	**Eq. 2**	**Eq. 1**	**Eq. 2**	**Eq. 1**
Ti-0.5Fe-0.5Cu	4.55	1.7	1.8	α + β	
Ti-1Fe-1Cu	4.59	3.4	3.7		
Ti-2Fe-2Cu	4.67	6.9	7.3	Near-β	
Ti-3.5Fe-3.5Cu	4.78	12.0	12.8	Metastable β	
Ti-5Fe-5Cu	4.90	17.2	18.4		

Table 3-6 Designed ternary Ti-xFe-xMn alloys.

Compositions	**Theoretical density**	**MoE**		**Alloy type**	
Ti-xFe-xMn	**(g/cm^3)**	**Eq. 2**	**Eq. 1**	**Eq. 2**	**Eq. 1**
Ti-0.5Fe-0.5Mn	4.54	2.1	2.2	α + β	
Ti-1Fe-1Mn	4.57	4.2	4.4		
Ti-2Fe-2Mn	4.63	8.4	8.9	Near-β	
Ti-3.5Fe-3.5Mn	4.73	14.7	15.5	Metastable β	
Ti-5Fe-5Mn	4.82	21.0	22.2		

3.2 Alloy Fabrication

3.2.1 Mixing

The metal powder blends of the designed ternary Ti alloy compositions were mixed in the V-blender (Figure 3-2) at speed of 45 Hz for 30 minutes, to obtain homogeneous compositions.

Figure 3-2 V-blender used for mixing the designed ternary Ti alloy compositions.

3.2.2 Pressing

The mixed metal powders of the ternary Ti alloy compositions were pressed in a 40 mm diameter cylindrical die (Figure 3-3) using a hydraulic press with a compaction pressure of 600 MPa.

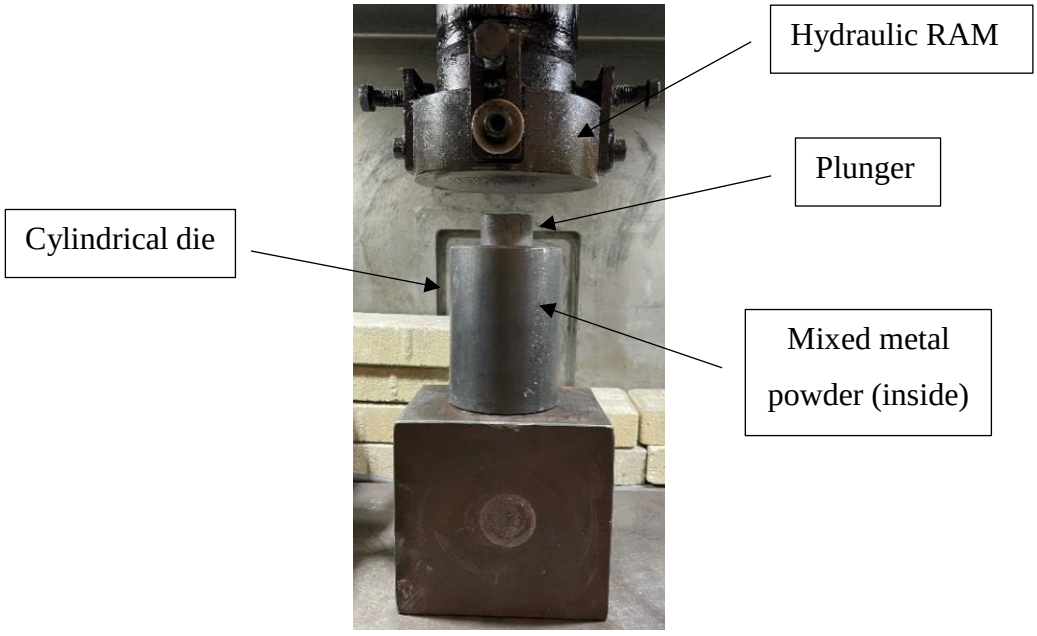

Figure 3-3 Picture of the set up used to press the ternary Ti alloy compositions.

3.2.3 Sintering

The pressed ternary Ti alloy samples were sintered in a vacuum sintering furnace (Figure 3-4). Sintering of the samples was carried out at a starting rate of 10 ºC/min up to 1300 ºC/min which were held for 2 hours, followed by cooling inside the furnace. This temperature was chosen in order to both facilitate densification and allow for sufficient homogenisation of the alloying elements.

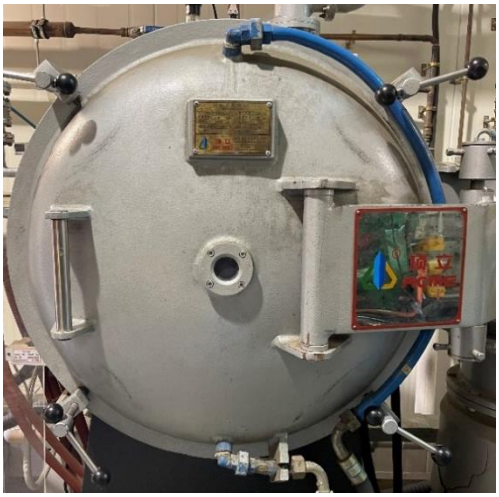

Figure 3-4 Vacuum sintering furnace.

3.3 Characterization

Characterization of the ternary Ti alloy samples involved density measurements (theoretical, green, and sintered), microstructure analysis (OM, SEM, and XRD), and mechanical behaviour (tensile and hardness).

3.3.1 Density

The theoretical density (as shown in Table 3-2 – 3-6) of each designed ternary Ti alloy composition was calculated using the rule of mixtures Equation (3);

$$\rho_{theorectical} = \%X_{e1}\rho_{e1} + \%X_{e2}\rho_{e2} + \%X_{e3}\rho_{e3} \qquad \text{Eq. 3}$$

where $\rho_{theoretical}$ is the theoretical density (g/cm^3), $\%X_e$ is the percentage of the element in the alloy, and ρ_e is the density of the element (g/cm^3).

Secondly, the green density of each pressed ternary Ti alloy was measured using a digital Vernier caliper (2-decimal digits) to measure the dimensions of the green sample (i.e. diameter (d) and thickness (t)) and an analytical scale (4-decimal digits) to measure the weight of the green sample. The green density of the samples was calculated using Equation (4), with average values taken for each sample (5 measurements of the thickness, and 3 for the diameter).

$$\rho_g = \frac{M}{V} \qquad \text{Eq. 4}$$

Where ρ_g is the green density (g/cm^3), M is the mass (g), and V is the volume of the green sample (cm^3) (i.e. $V = \pi d^2 t/4$).

Lastly, the sintered density of the ternary Ti alloys was measured using the Archimedes principle. The density values were calculated using Equation (5) with 5 values taken from each sample and averaged.

$$\rho_s = \frac{W_{air}}{W_{air} - W_{water}} \times \rho_w \qquad \text{Eq. 5}$$

Where ρ_s is the sintered density (g/cm^3), W_{air} is the weight of the sample in air (g), W_{water} is the weight of the sample in water (g), and ρ_w is the density of water at room temperature (0.977 g/cm^3).

3.3.2 Microstructure analysis

OM

Microstructural characteristics of all the sintered ternary Ti alloys were captured by a Nikon digital camera attached to an Olympus BX53 microscope. To observe each sample, a small metal piece with dimensions of 4x4x20 mm^3 was cut from the sintered 40 mm diameter cylindrical sample using an EDM (electric discharge machine) wire cutter. All cut samples went through a grinding process which involved removing the oxide surface on the metal alloy using Struers RotoPol-21 grinding machine with Struers #320, #600, #1000 and #2000 grit silicon carbide (SiC) grinding papers. The samples were then polished with colloidal silica suspension (OP-S NonDry, Struers), to obtain mirror-like surface finish using

Struers Tegramin-25 automatic polisher. Lastly, before microstructure observation, all samples were etched with Kroll's solution, consisting of HF, HNO_3 and distilled water.

SEM

Further microstructure analysis of the sintered ternary Ti alloys was done using a Hitachi S4700 microscope. SEM was done using the OM samples, with an additional step involving coating the OM samples with a thin layer of carbon.

XRD

Phase analysis of the ternary Ti alloys was done by XRD. Before the analysis, a small metal piece with dimensions of 2x20x10 mm^3 was cut from the sintered 40 mm diameter cylindrical sample using the wire cutter. Each sample went through the same grinding processes as done for the OM samples ensuring the oxide surface on the metal alloy was removed. A Philips X'Pert diffractometer (45 kV and 40 mA) with Cu Kα radiation (1.54056 Å) was used to collect the diffraction patterns. The scanning angle range was 5º to 100º, and the step size was 0.013º.

3.3.3 Mechanical behaviour

Tensile testing

Mechanical properties such as UTS, YS and elongation of the ternary Ti alloys were measured on an Instron 33R4204 universal tester using a crosshead speed of 0.1 mm/min with a mechanical extensometer used to record the deformation. Before testing, 5 dog-bone tensile testing samples (with dimensions shown in Figure 3-5) were cut from each sintered 40 mm diameter cylindrical samples using the wire cutter.

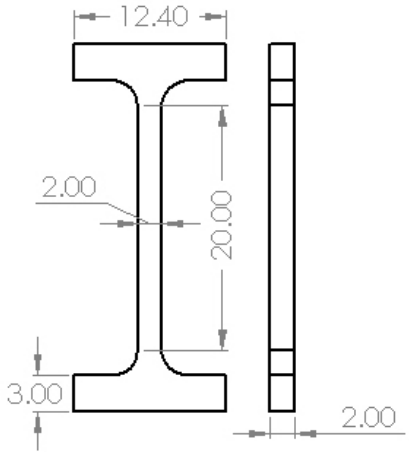

Figure 3-5 Dog-bone tensile testing sample with dimensions (in mm).

The side surfaces of the dog-bone tensile testing samples were ground using a Dremel 3000 electric hand grinder with a SiC grinding wheel. Both surfaces of the dog-bone samples went through the same grinding processes as done for the OM samples.

Hardness

Hardness measurements of the ternary Ti alloys were done on the Rockwell A tester. Testing was performed on the cross section of the tested tensile dog-bone samples, with 5 measurements taken for each sample giving an overall average value.

Chapter 4

Results and Discussion

In this chapter the results of the characterized sintered ternary Ti-Cu-Nb, Ti-Mn-Nb, Ti-Fe-Nb, Ti-Fe-Cu and Ti-Fe-Mn alloys, are discussed individually followed by an overall discussion. Density measurements are first discussed, followed by the microstructure analysis (OM, SEM, and XRD), and lastly the mechanical behaviour (tensile testing and hardness).

4.1 Sintered Ternary Ti-Cu-Nb Alloys

4.1.1 Density

The physical properties of the ternary Ti-Cu-Nb alloys, including relative green and sintered density, are shown in Figure 4-1.

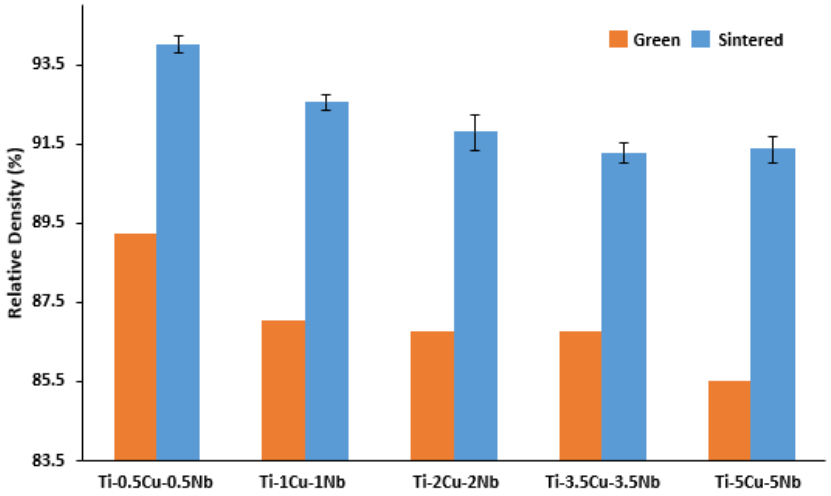

Figure 4-1 Relative densities of the Ti-Cu-Nb alloys.

The relative green and sintered density decreased from 89.2% to 86.7% and 94% to 91.3% respectively, with increasing Cu-Nb concentration. The density of all the samples increased during sintering. The relative green density of the samples decreases due to the interaction between the three types of powder during pressing [14; 38]. Ti, Cu and Nb have different particle size (Table 3-1), hardness, deformability and morphology (Figure 3-1), thus the relative green density decreases with the amount of Cu and Nb added to Ti [14; 38]. Similar relative

sintered density was observed for the Ti-3.5Cu-3.5Nb (91.3%) and Ti-5Cu-5Nb (91.4%) alloys. Similar relative densities have been reported in the literature, for Ti-Cu [14] and ternary Cu-dominant [32] alloys processed via PM with low Cu content (i.e. less than 5 wt%). The relative green and sintered density of CP-Ti was 86.4% and 92.6% respectively. The porosity left by the compaction of the powder blends, increased from 11% to 15% (i.e. relative green density decreases) as the amount of Cu-Nb increased. After sintering, the amount of porosity present in the samples increased from 6% to 9% (i.e. relative sintered density decreases) as the amount of Cu-Nb increased. Porosity is partially eliminated via sintering, and increases with the addition of alloying elements.

4.1.2 Microstructure analysis

Microstructure analysis of the ternary Ti-Cu-Nb alloys is shown in Figure 4-2. The sintered samples show the presence of some residual porosity, where the pores are characterized by a spherical or elongated morphology. The size of the spherical pores is approximately within the range of 5 – 55 μm, and there is a small amount of irregular/elongated pores present.

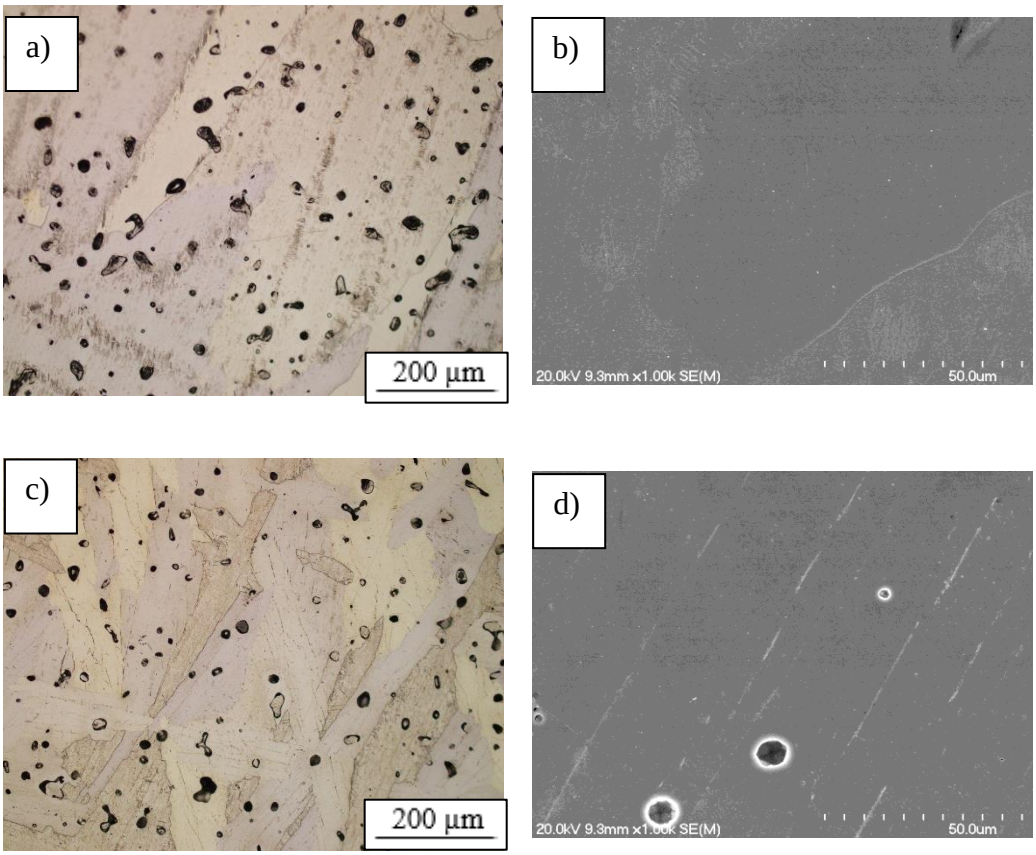

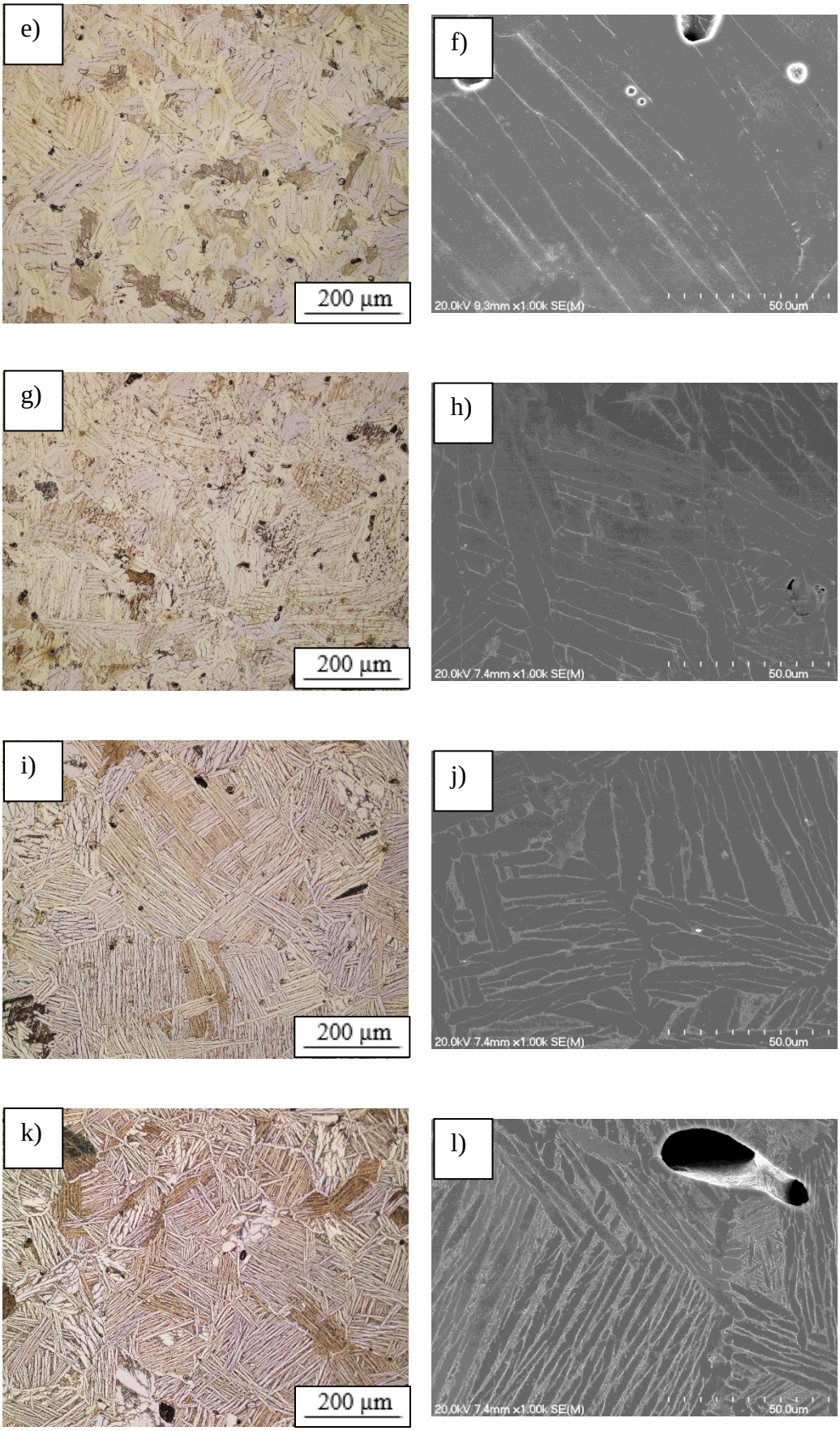

Figure 4-2 Optical and SEM micrographs, respectively, for: (a) and (b) CP-Ti, (c) and (d) Ti-0.5Cu-0.5Nb, (e) and (f) Ti-1Cu-1Nb, (g) and (h) Ti-2Cu-2Nb, (i) and (j) Ti-3.5Cu-3.5Nb, and (k) and (l) Ti-5Cu-5Nb.

The sintered Ti-Cu-Nb alloys are characterized by an α + β lamellar microstructure because of the slow cooling from above the β transus temperature regardless of the Cu-Nb content [14]. CP-Ti is composed of only equiaxed α-Ti grains (Figure 4-2 a) and b)). The lamellar microstructure for the Ti-0.5Cu-0.5Nb alloy is coarse due to the low amount of β-stabilizer (Figure 4-2 c) and d)). By increasing the amount of Cu-Nb (from 0.5 to 5 wt%), the thickness of the β lamellae decreases resulting in a finer microstructure for the Ti-5Cu-5Nb alloy (Figure 4-2 k) and l)) [14]. A Ti alloy characterized by an α + β lamellar microstructure generally has better mechanical properties compared to CP-Ti, since the β-Ti phase is stronger than the α-Ti phase [69]. Moreover, a finer lamellar microstructure tends to give higher mechanical properties, compared to an alloy with a coarse lamellar microstructure (the effects are seen later on). Similar α + β lamellar microstructures have been reported in literature for sintered Ti-Cu [14] as well as ternary Cu-dominant [32] alloys, and cast Ti-Cu [13] as well as Ti-Nb [16] alloys, with less than 5 wt% Cu and Nb additions.

The microstructure of the sintered Ti-Cu-Nb alloys are compared with their predicted MoE and alloy type in Table 3-2. It shows that alloys Ti-0.5Cu-0.5Nb, Ti-1Cu-1Nb and Ti-2Cu-2Nb, and Ti-0.5Cu-0.5Nb, Ti-1Cu-1Nb, Ti-2Cu-2Nb and Ti-3.5Cu-3.5Nb predicted by Eq. 2 and Eq. 1, respectively, agree with the sintered Ti-Cu-Nb alloys, as their microstructure is composed of α + β lamellae. However, the Ti-3.5Cu-3.5Nb and Ti-5Cu-5Nb alloys, and Ti-5Cu-5Nb predicted by Eq. 2 and Eq. 1, respectively, are not in agreement with the sintered Ti-Cu-Nb alloys, due to the high MoE (i.e. greater than 5 wt%), and alloy type being near-β. From Table 3-2, Eq. 1 is more accurate than Eq. 2, for predicting the alloy type for sintered Ti-Cu-Nb alloys, since the MoE values are lower than the ones predicted by Eq. 2.

XRD patterns of the ternary Ti-Cu-Nb alloys are shown in Figure 4-3. The results show that only the α-phase was detected in all alloys, while the β-phase was only detected in the Ti-5Cu-5Nb alloy. The β-phase is generally retained at small β-stabilizer (Cu-Nb) additions (as shown in Figure 4-2), however it is not visible in the XRD spectra for Cu-Nb concentrations of 0.5, 1, 2 and 3.5 wt% (since the amount of β-phase is below the detection limit of the equipment [14; 32]). The Ti_2Cu phase was also detected in the Ti-3.5Cu-3.5Nb and Ti-5Cu-5Nb alloys, and its intensity increases with the addition of Cu. It has been reported in literature [14;

32] that the Ti_2Cu phase is found at low Cu concentrations (i.e. less than 5 wt%), and is in agreement with the current results. It is worth mentioning that the Ti_2Cu phase was not clearly visible in the microstructural analysis for the Ti-3.5Cu-3.5Mn and Ti-5Cu-5Nb alloys via SEM. In literature [18; 20-22], studies have detected the Ti_2Cu phase via TEM (transmission electron microscope), since it is hard to find in SEM.

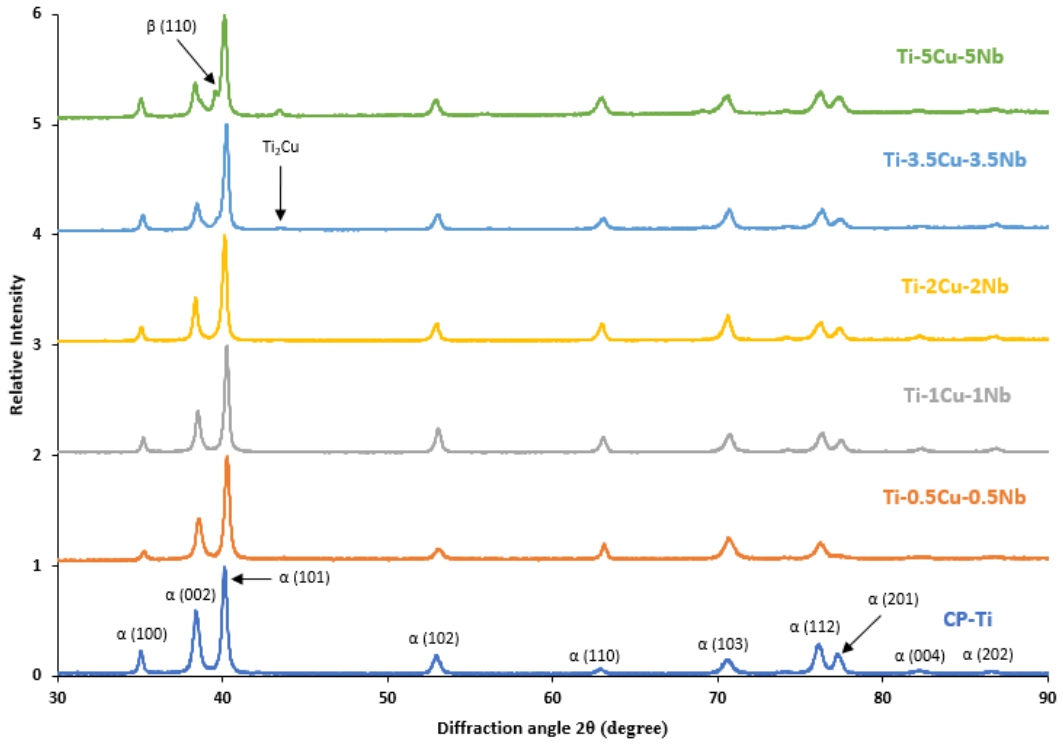

Figure 4-3 XRD patterns of the sintered Ti-Cu-Nb alloys.

4.1.3 Mechanical behaviour

Figure 4-4 shows representative stress-strain curves of the ternary Ti-Cu-Nb alloys in comparison to CP-Ti, and Table 4-1 shows the average mechanical properties. The tensile stress of the alloys increases as the amount of alloying elements (Cu-Nb) increase, and is higher in comparison to CP-Ti. The elongation initially increases, reaching the highest value for the Ti-1Cu-1Nb alloy (23%), and then decreases. Due to the strain limit of the testing machine (maximum strain was 23%), the Ti-1Cu-1Nb alloy did not break, suggesting that the alloy displayed good ductility. Strength and ductility are mutually exclusive. The Ti-Cu-Nb alloys are characterized by a ductile behaviour, showing both an elastic and plastic deformation region in their stress-strain curves. The YS and UTS of the Ti-Cu-Nb

alloys increases from 404 MPa to 553 MPa and 495 MPa to 655 MPa, respectively, as the amount of alloying elements increases, and is higher in comparison to CP-Ti (YS = 281 MPa and UTS = 374 MPa). The Ti-5Cu-5Nb alloy shows the highest YS and UTS, however the elongation was the lowest (9.1%), in comparison to the other Ti-Cu-Nb alloys, and higher than that of CP-Ti (5.7%).

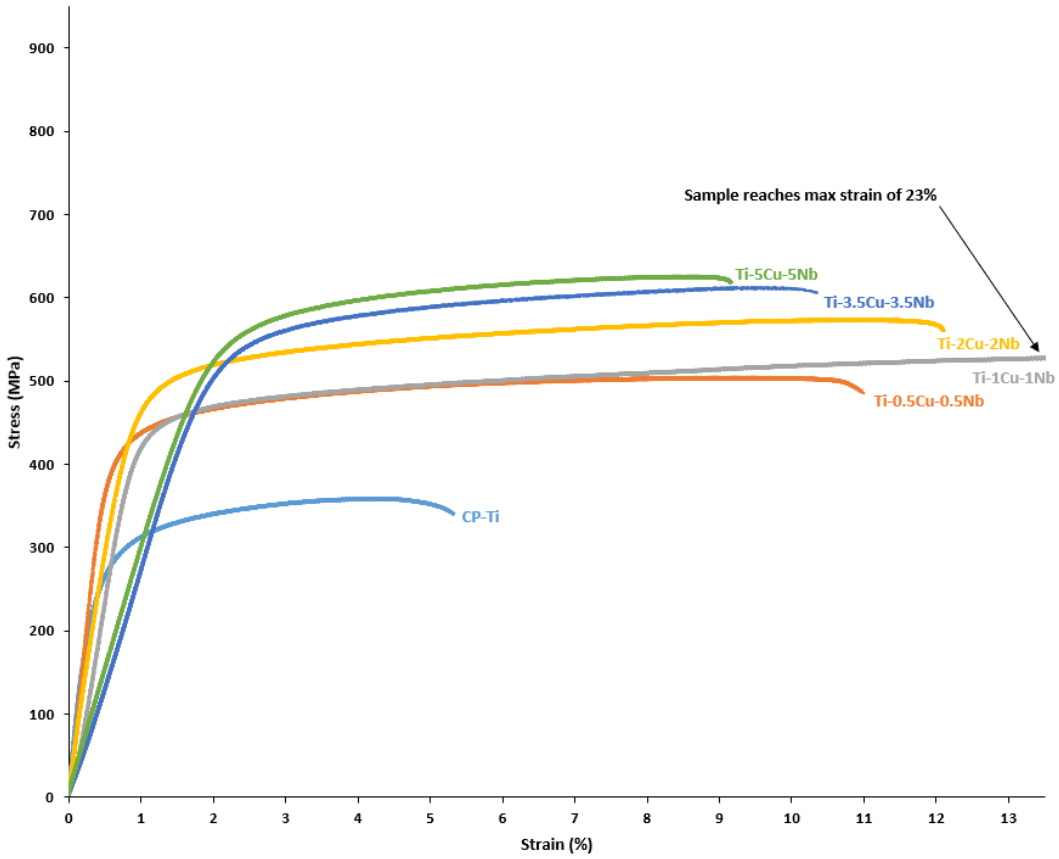

Figure 4-4 Representative stress-strain curves of the sintered Ti-Cu-Nb alloys.

Table 4-1 Average mechanical properties of the sintered Ti-Cu-Nb alloys.

Material	YS (MPa)	UTS (MPa)	Elongation (%)	Hardness (HRA)
Ti-0.5Cu-0.5Nb	404 ± 24	495 ± 21	10.3 ± 1.9	51 ± 0.9
Ti-1Cu-1Nb	432 ± 7	532 ± 9	23.0 ± 0.1	54 ± 1.0
Ti-2Cu-2Nb	485 ± 20	588 ± 17	12.0 ± 1.7	56 ± 1.7
Ti-3.5Cu-3.5Nb	544 ± 38	635 ± 22	10.9 ± 1.7	57 ± 0.9
Ti-5Cu-5Nb	553 ± 47	655 ± 38	9.1 ± 0.4	58 ± 1.0

The hardness of the Ti-Cu-Nb alloys increases linearly (Figure 4-5), from 51 HRA to 58 HRA as the amount of alloying elements increases, and is higher than that of CP-Ti (46 HRA). The addition of Cu and Nb to Ti improves the mechanical properties (tensile strength and hardness) due to the solid-solution strengthening

effect they have in Ti, and the increase volume fraction of the β-Ti phase (β-Ti phase has higher strength/hardness and lower ductility than the α-Ti phase). A finer α + β lamellar microstructure (Ti-5Cu-5Nb) tends to give higher mechanical properties, compared to an alloy with a coarse lamellar microstructure (Ti-0.5Cu-0.5Nb). The Ti_2Cu phase is also responsible for improving the mechanical properties, as present in the Ti-3.5Cu-3.5Nb and Ti-5Cu-5Nb alloys. The intermetallic phase increases the resistance to plastic deformation, thus improving the mechanical properties [14; 18]. Another factor affecting the mechanical properties of PM Ti and Ti-Cu-Nb alloys is the residual porosity. An alloy with a high relative density (i.e. greater than 98%) results in better mechanical properties, compared to an alloy with a low relative density. This is because of pores, as they act as stress concentration sites, which therefore decreases the strength, hardness and ductility of the alloys [44].

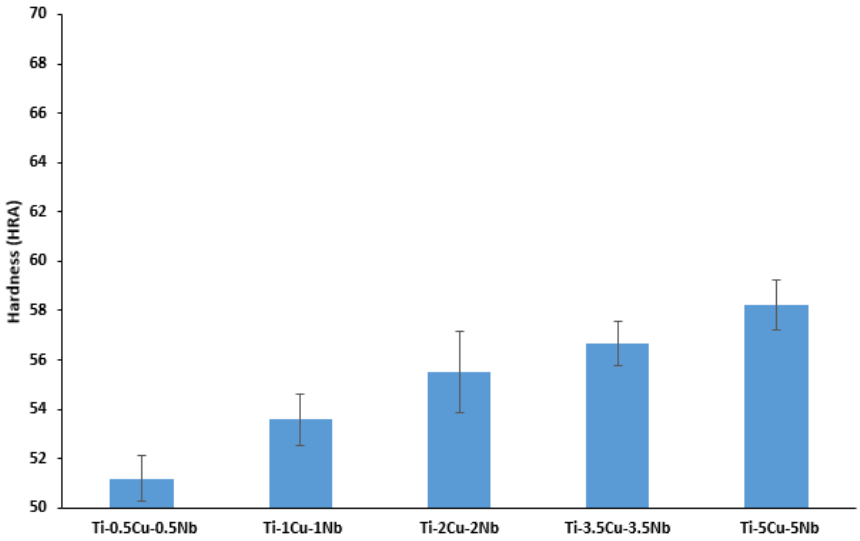

Figure 4-5 Rockwell hardness of the sintered Ti-Cu-Nb alloys.

The mechanical properties (Figure 4-6 (tensile) and Figure 4-7 (hardness)) of the sintered Ti-Cu-Nb alloys are compared with other Cu- and Nb- based Ti alloys, as well as Ti-6Al-4V. From Figure 4-6, the UTS and YS of the sintered Ti-5Cu-5Nb (UTS = 655 MPa and YS = 553 MPa) are higher compared to the cast Ti-5Cu (UTS = approximately 630 MPa and YS = approximately 570 MPa [13]) and cast Ti-5Nb (UTS = 536 MPa and YS = 407 MPa [16]) alloys, however lower than cast Ti-6Al-4V (UTS = 976 MPa and YS = 847 [70]), cast Ti-4Cu-6Nb (UTS = approximately 790 MPa and YS = approximately 572 MPa [31]) and sintered Ti-5Cu (UTS = 754 MPa and YS = 627 MPa [14]) alloys. Furthermore, the sintered Ti-5Cu-5Nb (9.1%)

alloy shows a higher elongation than cast Ti-6Al-4V (5.1%), cast Ti-4Cu-6Nb (approximately 4%) and cast Ti-5Cu (approximately 3.2%), however lower than that of cast Ti-5Nb (11%), and comparable with the sintered Ti-5Cu (9.5%) alloy. The high YS and UTS of the cast Ti-6Al-4V alloy is due to the fine lamellar microstructure consisting of both α-phase and β-phase, and the presence of no porosity in comparison to the sintered Ti-5Cu-5Nb alloy. Ti alloys fabricated via casting consist of no porosity and this effect tends to result in better mechanical properties in comparison to sintered Ti alloys with porosity. As mentioned before, the amount of porosity tends to lower the mechanical properties compared to a fully dense material. The cast Ti-4Cu-6Nb alloy showed acicular structures and consisted of only the α-phase which contributed to the high UTS in comparison to the sintered Ti-5Cu-5Nb alloy. The Ti_2Cu phase was present in both sintered Ti-5Cu and cast Ti-5Cu alloys, and the effect was noticeably higher for the sintered Ti-5Cu alloy in comparison to both sintered Ti-5Cu-5Nb and cast Ti-5Cu alloys. It is worth mentioning that high YS and UTS of the sintered Ti-5Cu alloy is also due to the fine lamellar microstructure. The low YS/UTS and high elongation of the cast Ti-5Nb alloy is due to the α and/or metastable α' phase found in the alloy (confirmed in XRD results) [16; 25]. Both the sintered Ti-5Cu-5Nb and Ti-5Cu alloys were processed in the same manner, achieving similar elongations, relative sintered density and microstructure (α + β lamellar microstructure).

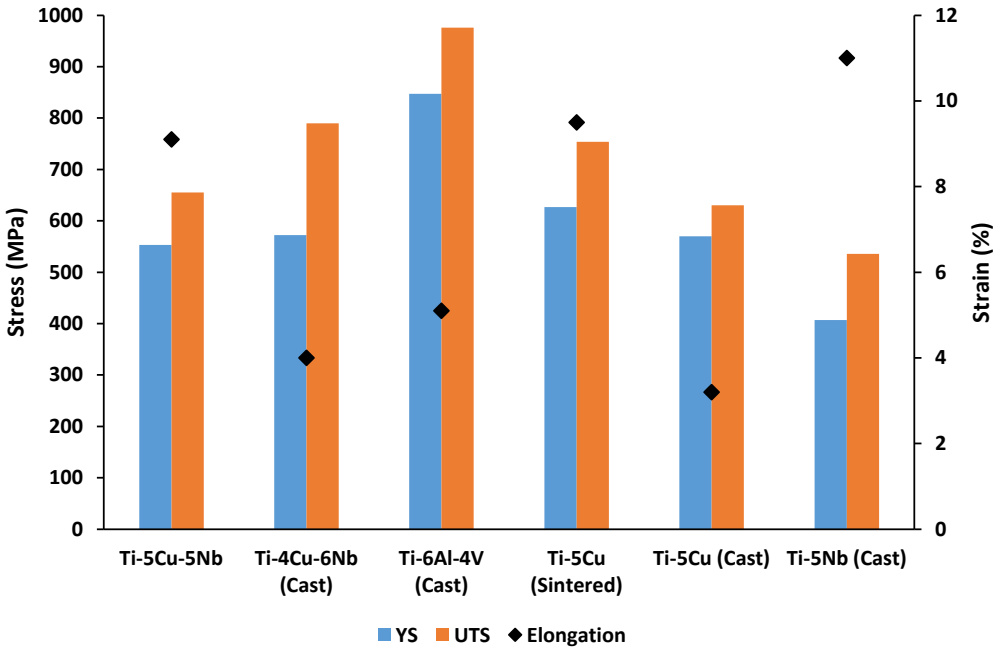

Figure 4-6 Comparison of the tensile properties of the sintered Ti-5Cu-5Nb alloy to other Cu- and Nb- based Ti alloys, as well as Ti-6Al-4V.

In terms of hardness (Figure 4-7), the sintered Ti-5Cu-5Nb (222 HV) alloy shows a higher hardness than cast Ti-5Nb (177 HV), however lower than that of cast Ti-6Al-4V (approximately 340 HV) and cast Ti-4Cu-6Nb (approximately 260 HV) alloys, and is comparable with the cast Ti-5Cu (approximately 230 HV) and sintered Ti-5Cu (227 HV) alloys. The trends of hardness (Figure 4-7) are similar to the trends of the tensile properties (Figure 4-6).

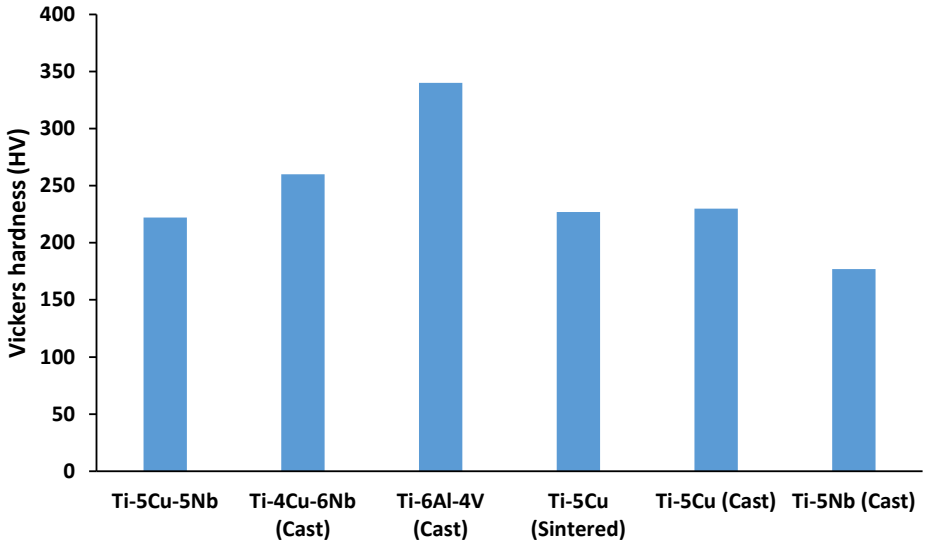

Figure 4-7 Comparison of the hardness of the sintered Ti-5Cu-5Nb alloy to other Cu- and Nb- based Ti alloys, as well as Ti-6Al-4V.

4.2 Sintered Ternary Ti-Mn-Nb Alloys

4.2.1 Density

The physical properties of the ternary Ti-Mn-Nb alloys, including relative green and sintered density, are shown in Figure 4-8.

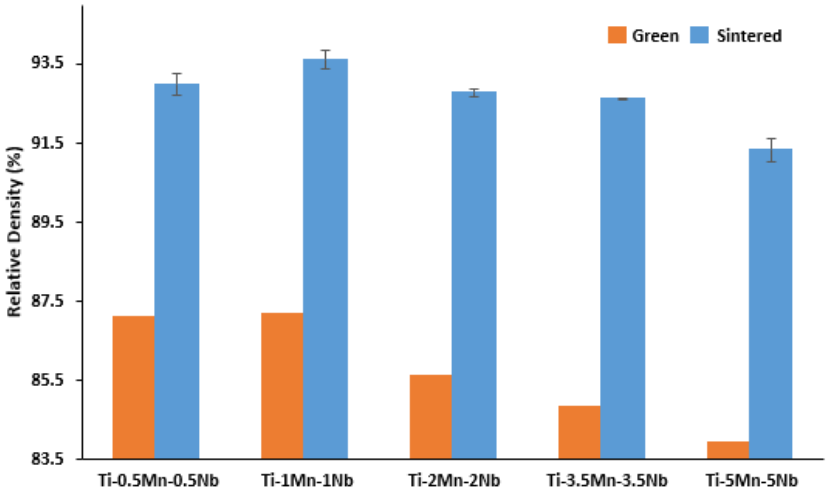

Figure 4-8 Relative densities of the Ti-Mn-Nb alloys.

The relative green and sintered density decreases from 87.2% to 83.9% and 93.6% to 91.3%, respectively, with increasing Mn-Nb concentration (from 1 to 5 wt%). The relative sintered density of the Ti-0.5Mn-0.5Nb (93%) alloy was the second highest, compared to the other ternary Ti-Mn-Nb compositions. The relative green density of the samples decreases due to the interaction between the Ti, Mn and Nb powders during pressing, as they have different particle sizes (Table 3-1), hardness, deformability and morphology (Ti and Mn have the same morphology (Figure 3-1)) [14; 38]. Similar relative densities have been reported in literature, for Ti-Mn [38] and ternary Mn-dominant [32] alloys processed via PM with low Mn content (i.e. less than 5 wt%). The porosity left by the compaction of the powder blends, increases from 13% to 16% as the amount of Mn-Nb increases. After sintering the amount of porosity present in the samples increases from 7% to 9% as the amount of Mn-Nb increases.

4.2.2 Microstructure analysis

Figure 4-9 shows the microstructure analysis of the ternary Ti-Mn-Nb alloys. The sintered samples show pores, where they are characterized by a spherical or irregular morphology. The size of the spherical pores is approximately within the range of 5 – 55 μm, and a small amount of irregular/elongated pores are present. The sintered Ti-Mn-Nb alloys are characterized by an α + β lamellar microstructure (Figure 4-9). With the addition of 0.5 wt% of Mn and Nb to Ti the lamellar microstructure is coarse (Figure 4-9 a) and b)). By increasing the amount of Mn-Nb (from 0.5 to 5 wt%) the lamellar microstructure is refined, which is clearly visible in the OM/SEM micrographs (Figure 4-9). Similar α + β lamellar microstructures have been reported in literature, for sintered Ti-Mn [38; 40], Ti-Mn-Nb [44] as well as ternary Mn-dominant [32] alloys, and cast Ti-Nb [16] alloys, with less than 5 wt% Mn and Nb additions.

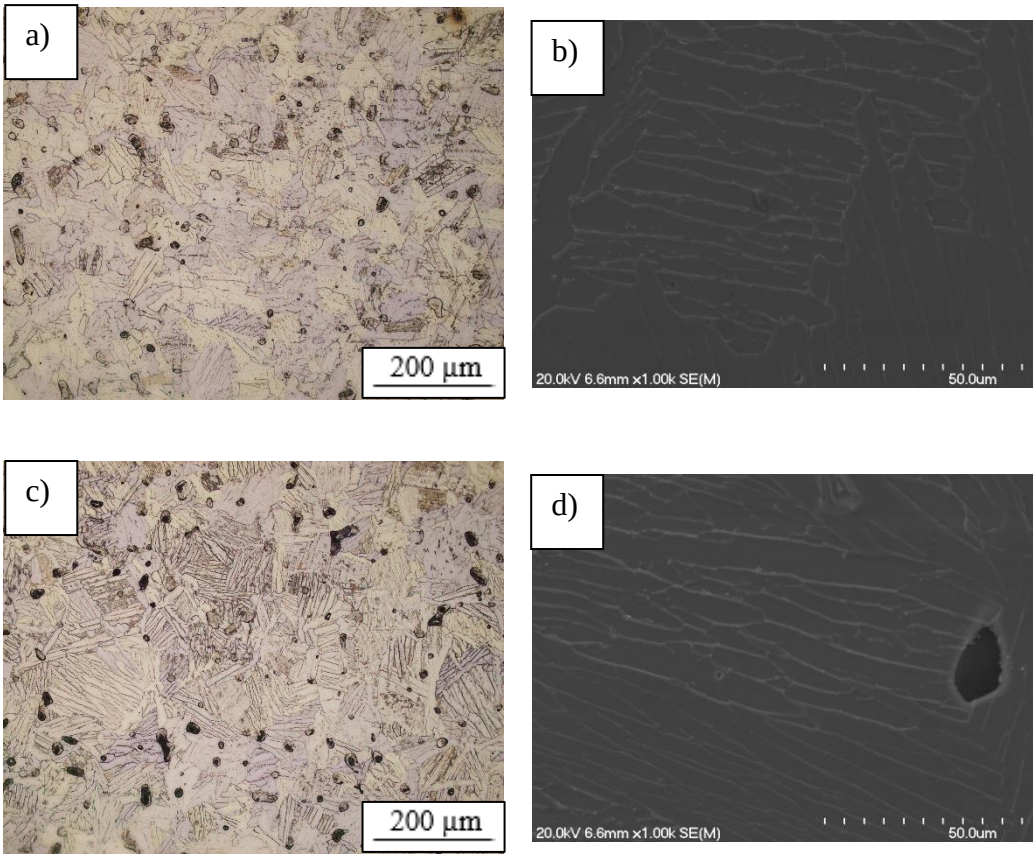

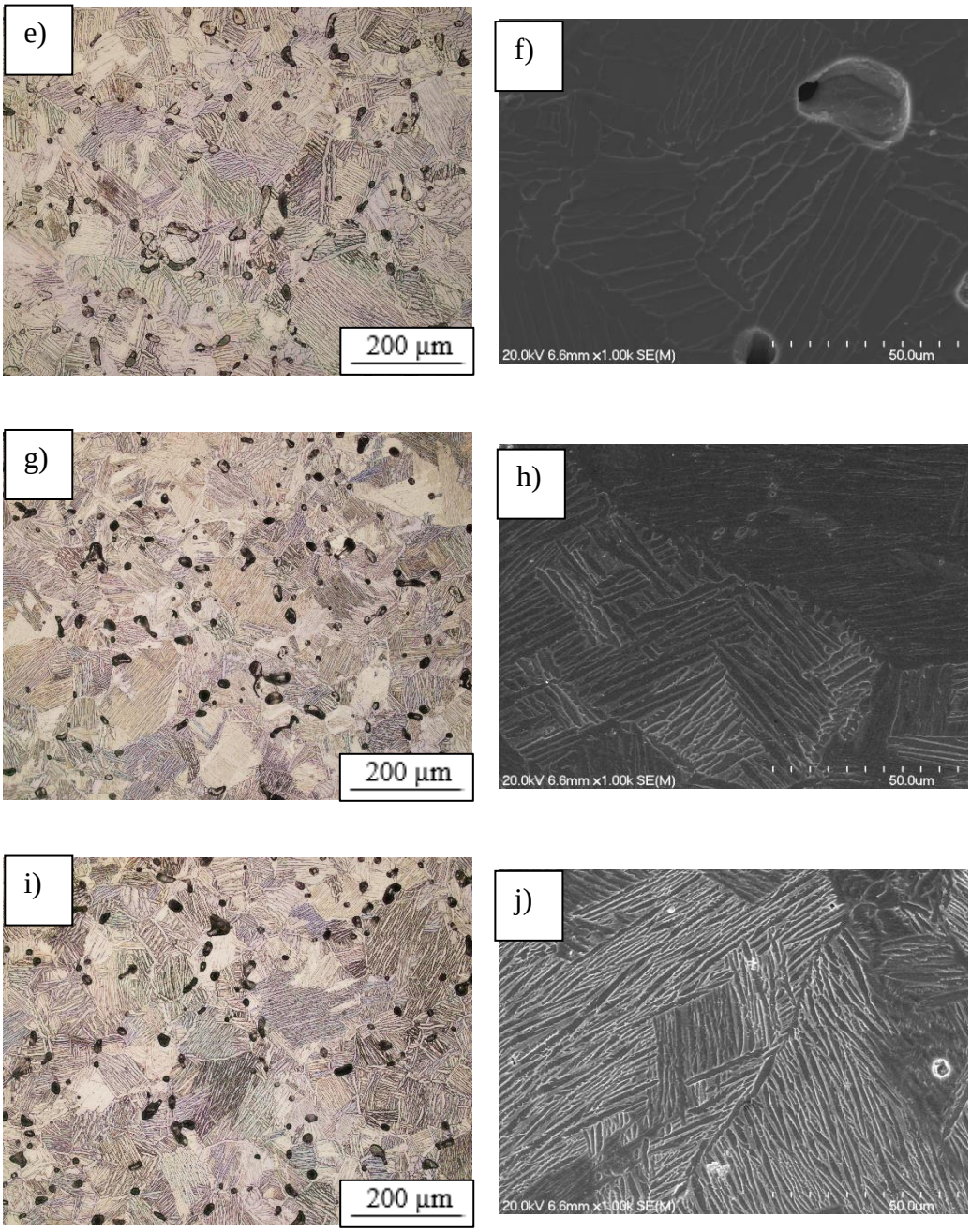

Figure 4-9 Optical and SEM micrographs, respectively, for: (a) and (b) Ti-0.5Mn-0.5Nb, (c) and (d) Ti-1Mn-1Nb, (e) and (f) Ti-2Mn-2Nb, (g) and (h) Ti-3.5Mn-3.5Nb, and (i) and (j) Ti-5Mn-5Nb.

The predicted MoE and alloy type of ternary Ti-Mn-Nb alloys in Table 3-3, are compared with the microstructure (Figure 4-9) of sintered Ti-Mn-Nb alloys. Table 3-3 shows that alloys Ti-0.5Mn-0.5Nb, Ti-1Mn-1Nb and Ti-2Mn-2Nb, predicted by both Eq. 2 and 1 agree with the sintered Ti-Mn-Nb alloys, as their microstructure is composed of α + β lamellae. However, alloys Ti-3.5Mn-3.5Nb and Ti-5Mn-5Nb are not in agreement with the sintered Ti-Mn-Nb alloys, since their microstructure does not consist of near-β and metastable β. Overall Eq. 2 appears to be more

accurate than Eq. 1 for predicting the alloy type of sintered Ti-Mn-Nb alloys, since the MoE values are lower than the ones predicted by Eq. 1 (Table 3-3).

Figure 4-10 shows the XRD patterns of the ternary Ti-Mn-Nb alloys. The results show that the α-phase was detected in all alloys, whereas the β-phase was only detected in the Ti-2Mn-2Nb, Ti-3.5Mn-3.5Nb and Ti-5Mn-5Nb alloys. The relative intensity of the main β peak (β (110)) increases as the amount of β-stabilizer (Mn-Nb) increases.

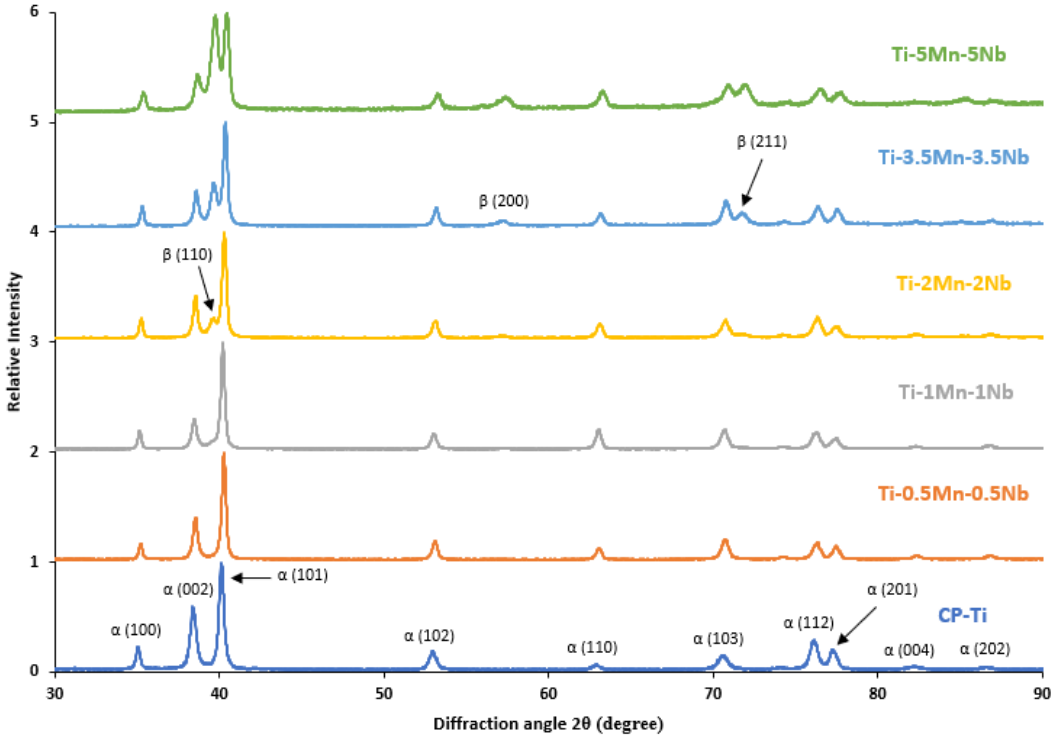

Figure 4-10 XRD patterns of the sintered Ti-Mn-Nb alloys.

4.2.3 Mechanical behaviour

Table 4-2 shows the average mechanical properties of the ternary Ti-Mn-Nb alloys, and Figure 4-11 shows representative stress-strain curves in comparison to CP-Ti. The tensile stress of the alloys increases as the amount of alloying elements (Mn-Nb) increase. The elongation initially increases, reaching the highest value for the Ti-1Mn-1Nb alloy (13.2%), and then decreases.

Table 4-2 Average mechanical properties of the sintered Ti-Mn-Nb alloys.

Material	YS (MPa)	UTS (MPa)	Elongation (%)	Hardness (HRA)
Ti-0.5Mn-0.5Nb	431 ± 10	514 ± 19	9.2 ± 2.6	53 ± 1.7
Ti-1Mn-1Nb	470 ± 15	560 ± 15	13.2 ± 0.9	55 ± 1.2
Ti-2Mn-2Nb	538 ± 8	626 ± 2	8.2 ± 0.3	56 ± 1.3
Ti-3.5Mn-3.5Nb	622 ± 9	704 ± 2	6.0 ± 0.1	59 ± 0.9
Ti-5Mn-5Nb	670 ± 11	726 ± 13	2.6 ± 0.7	61 ± 2.2

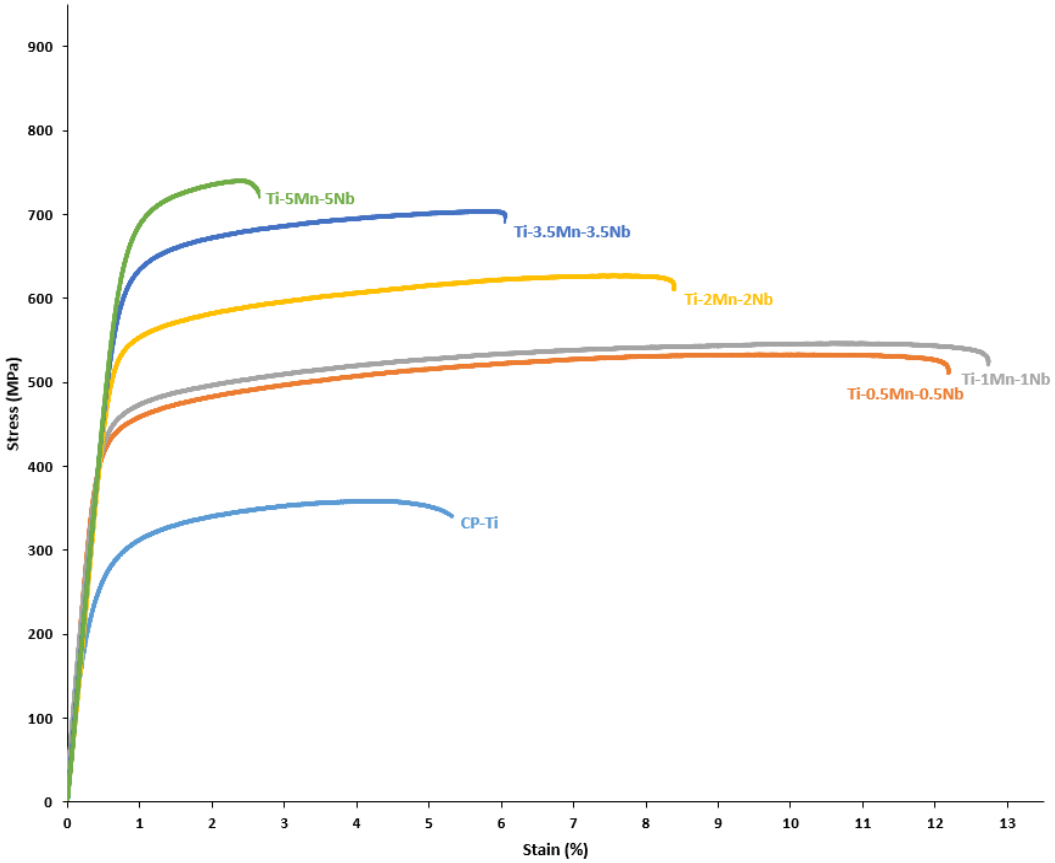

Figure 4-11 Representative stress-strain curves of the sintered Ti-Mn-Nb alloys.

The Ti-Mn-Nb alloys are characterized by a ductile behaviour, showing both an elastic and plastic deformation in their stress-strain curves. The YS and UTS of the alloys increases from 431 MPa to 670 MPa and 514 MPa to 726 MPa, respectively, as the amount of alloying elements increases. The Ti-5Mn-5Nb alloy shows the highest YS and UTS, however the elongation was the lowest (2.6%) in comparison to the other tested samples as shown in Figure 4-11. The hardness of the Ti-Mn-Nb alloys increases linearly (Figure 4-12), from 53 HRA to 61 HRA as the amount of alloying elements increases, and is higher than that of CP-Ti (46 HRA). With the addition of Mn and Nb to Ti the mechanical properties are improved due to the solid-solution strengthening effect both alloying elements have in Ti, and the

increased volume fraction of the β-Ti phase (as shown in Figure 4-10 (XRD)). It is worth mentioning that the addition of Mn and Nb to Ti refines the coarse α + β lamellar microstructure of Ti-0.5Mn-0.5Nb, thus higher mechanical properties are attained for the Ti-5Mn-5Nb alloy (fine α + β lamellar microstructure as shown in Figure 4-9 i) and j)).

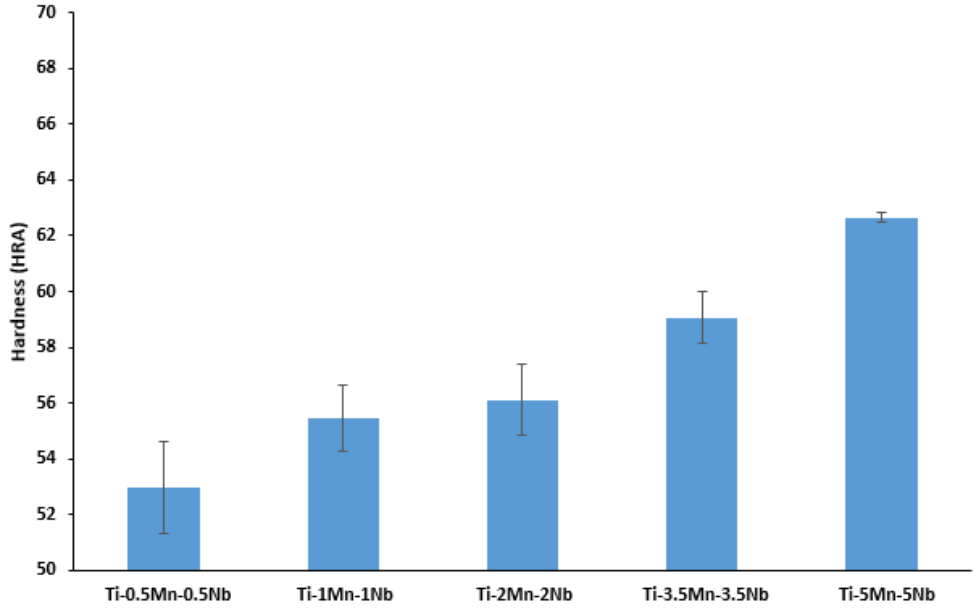

Figure 4-12 Rockwell hardness of the sintered Ti-Mn-Nb alloys.

The mechanical properties (Figure 4-13 (tensile) and Figure 4-14 (hardness)) of the sintered Ti-Mn-Nb alloys are compared with other Mn- and Nb- based Ti alloys, as well as Ti-6Al-4V. From Figure 4-13, the UTS and YS of the sintered Ti-5Mn-5Nb (UTS = 726 MPa and YS = 670 MPa) are higher compared to the cast Ti-5Nb (UTS = 536 MPa and YS = 407 MPa [16]) alloy, however lower than cast Ti-6Al-4V (UTS = 976 MPa and YS = 847 MPa [70]) and sintered Ti-5Mn (UTS = 800 MPa and YS = 716 MPa [38]) alloys, and is comparable with the cast Ti-5Mn-16Nb (UTS = 716 MPa and YS = 657 MPa [43]) alloy. Furthermore, the sintered Ti-5Mn-5Nb (2.6%) alloy shows a lower elongation than cast Ti-5Mn-16Nb (26%) and cast Ti-5Nb (11%), and is comparable to cast Ti-6Al-4V (5.1%) and sintered Ti-5Mn (3%) alloys. The high strength of the sintered Ti-5Mn alloy is due to the fine α + β lamellar microstructure in comparison to the sintered Ti-5Mn-5Nb alloy. Although both alloys have an α + β lamellar microstructure, the solid-solution strengthening effect of Mn is stronger in Ti-5Mn compared to Ti-5Mn-5Nb. Both Ti-5Mn and Ti-5Mn-5Nb alloys show comparable elongations as they were fabricated using the

same process, and have a similar relative sintered density. The cast Ti-5Mn-16Nb alloy consists of only a single β-phase and shows lower/comparable strengths in comparison to the sintered Ti-5Mn-5Nb alloy.

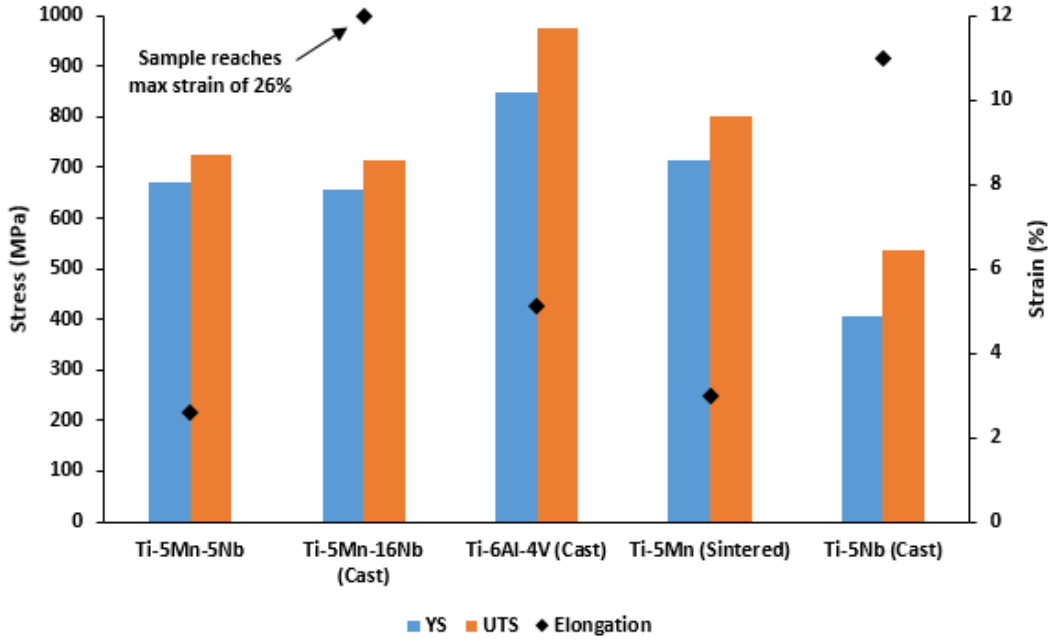

Figure 4-13 Comparison of the tensile properties of the sintered Ti-5Mn-5Nb alloy to other Mn- and Nb- based Ti alloys, as well as Ti-6Al-4V.

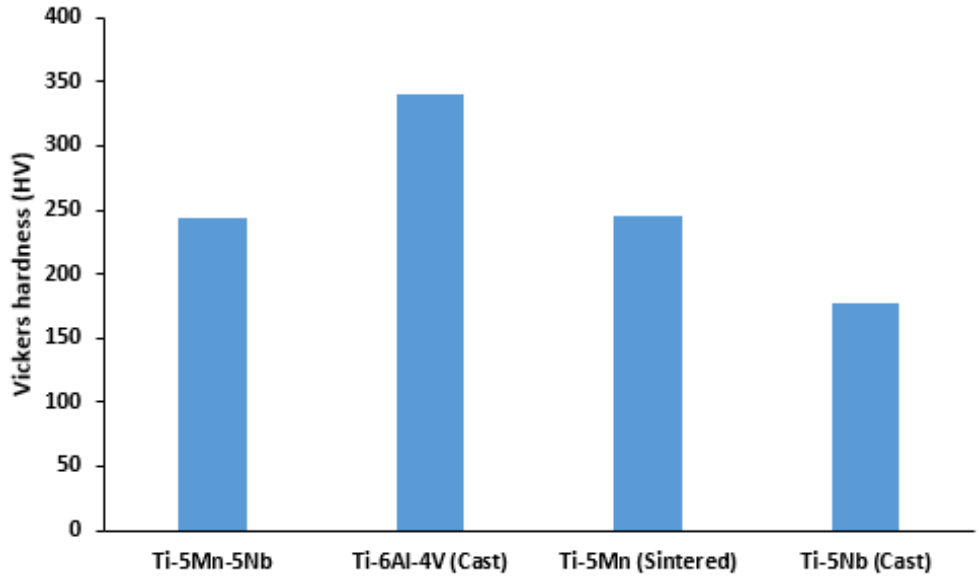

Figure 4-14 Comparison of the hardness of the sintered Ti-5Mn-5Nb alloy to other Mn- and Nb- based Ti alloys, as well as Ti-6Al-4V.

In terms of hardness (Figure 4-14), the sintered Ti-5Mn-5Nb (243 HV) alloy shows a higher hardness than cast Ti-5Nb (177 HV), however lower than that of cast Ti-6Al-4V (approximately 340 HV), and is comparable with the sintered Ti-5Mn (245

HV) alloy. No hardness was reported for the cast Ti-5Mn-16Nb alloy. As mentioned before, both sintered Ti-5Mn and Ti-5Mn-5Nb alloys have a fine $\alpha + \beta$ lamellar microstructure and relative sintered density, thus having a similar hardness.

4.3 Sintered Ternary Ti-Fe-Nb Alloys

4.3.1 Density

Figure 4-15 shows the physical properties of the ternary Ti-Fe-Nb alloys, including relative green and sintered density. The relative green and sintered density decreases from 87.1% to 84.4% and 93.9% to 91.8%, respectively, with increasing Fe-Nb concentration (from 0.5 to 3.5 wt%). The relative green density decreases due to the interaction between the Ti, Fe and Nb powders which have different particle sizes (Table 3-1), morphology (Ti and Nb have the same morphology (Figure 3-1)), hardness and deformability [14; 38]. The relative sintered density of the Ti-5Fe-5Nb (92.3%) alloy is the second lowest, compared to the other ternary Ti-Fe-Nb compositions. Similar relative densities have been reported in literature for Ti-Fe [46-49; 51] alloys processed via PM. The porosity left by the compaction of the powder blends increases from 13% to 16% as the amount of Fe-Nb increases. After sintering the amount of porosity present in the sample increases from 6% to 8% as the amount of Fe-Nb increases.

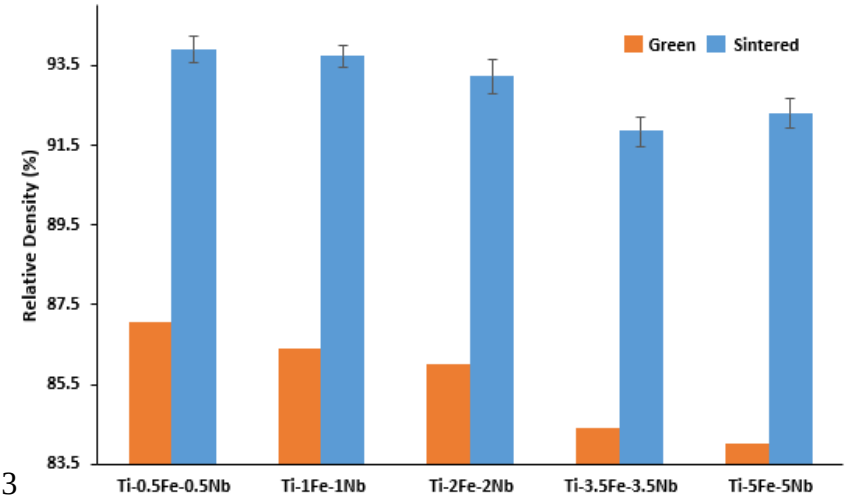

3

Figure 4-15 Relative densities of the Ti-Fe-Nb alloys.

4.3.2 Microstructure analysis

Figure 4-16 shows the optical and SEM micrographs of the ternary Ti-Fe-Nb alloys. The sintered samples show the presence of some residual porosity, where the pores are characterized by a spherical or elongated morphology. The size of the spherical pores is approximately within the range of 5 – 60 μm, and a small amount of irregular/elongated pores are also present. The sintered Ti-Fe-Nb alloys are

characterized by an α + β lamellar microstructure. By increasing the amount of Fe-Nb (from 0.5 to 5 wt%) the lamellar microstructure is refined as shown in Figure 4-16. Similar α + β lamellar microstructures have been reported in literature, for sintered Ti-Fe [46-51], and cast Ti-Nb-Fe [57] as well as Ti-Nb [16] alloys.

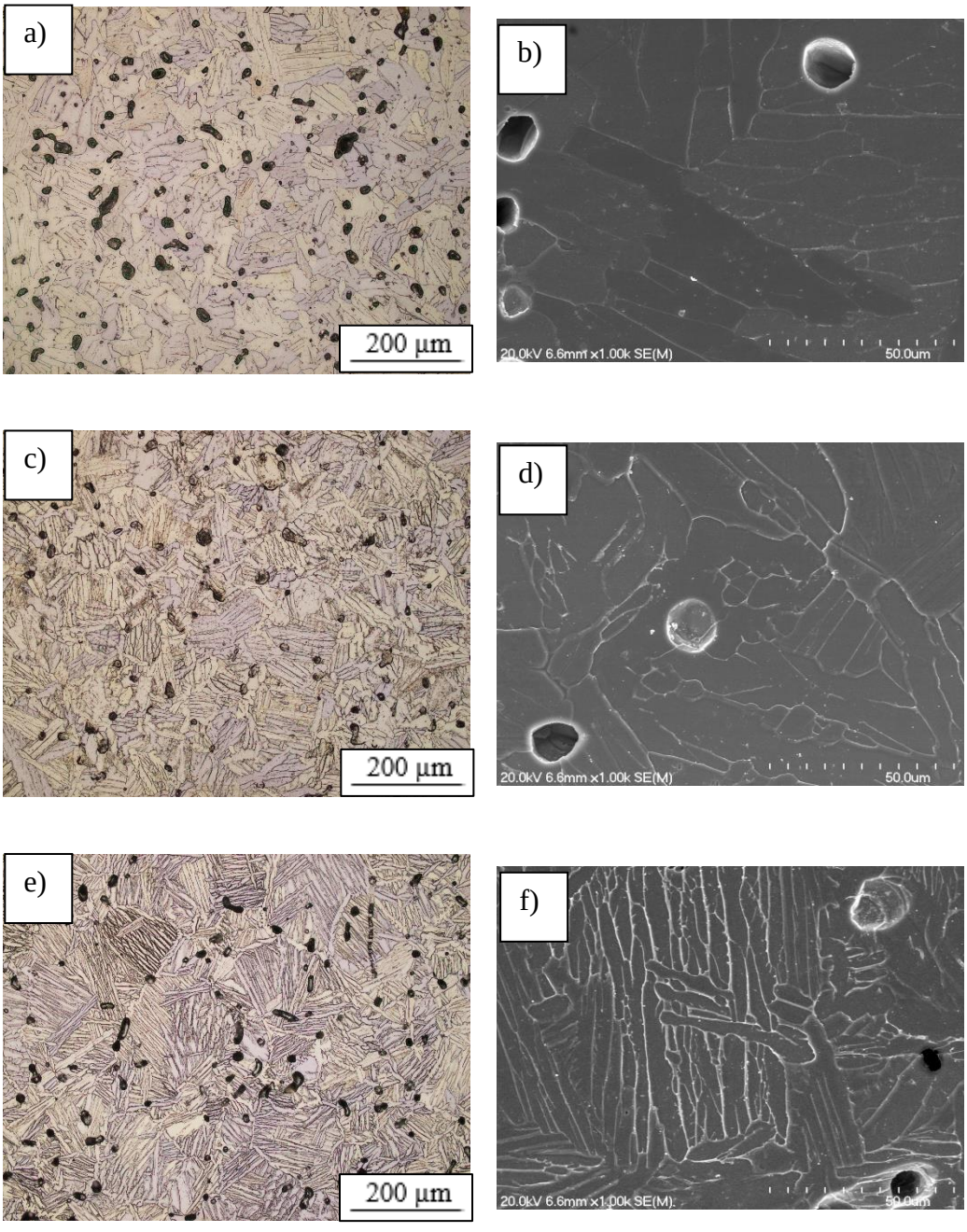

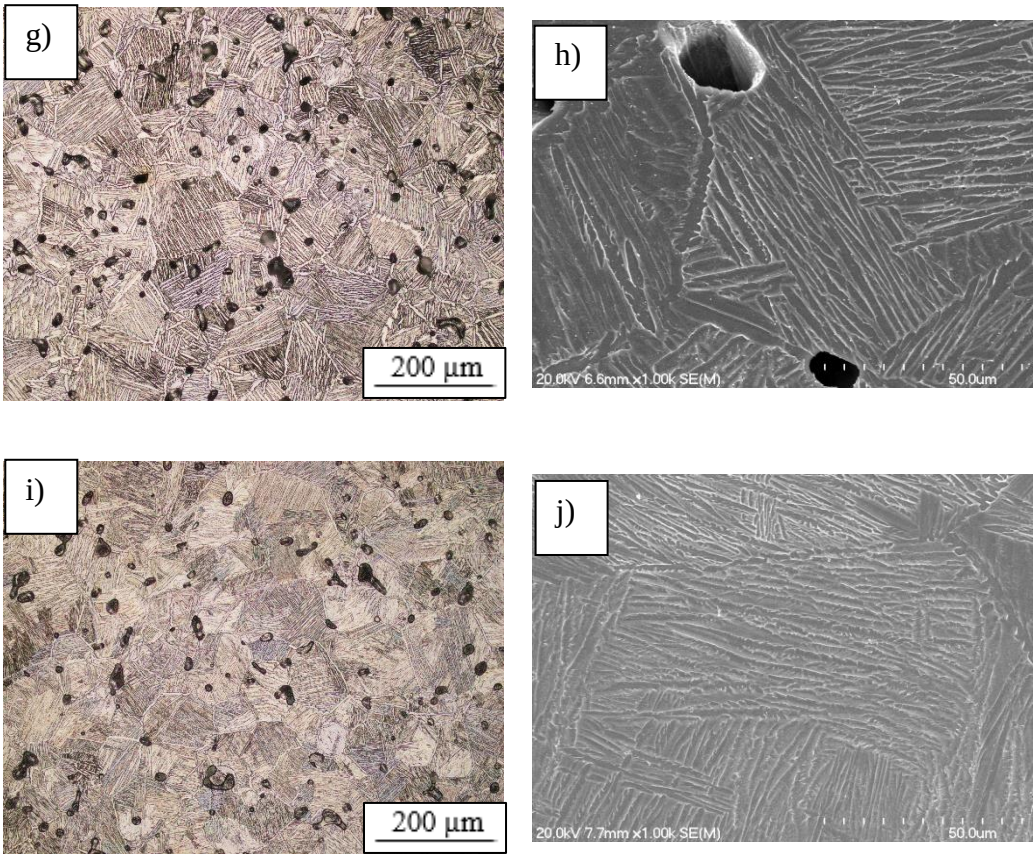

Figure 4-16 Optical and SEM micrographs, respectively, for: (a) and (b) Ti-0.5Fe-0.5Nb, (c) and (d) Ti-1Fe-1Nb, (e) and (f) Ti-2Fe-2Nb, (g) and (h) Ti-3.5Fe-3.5Nb, and (i) and (j) Ti-5Fe-5Nb.

The microstructure of the sintered Ti-Fe-Nb alloys are compared with their predicted MoE and alloy type in Table 3-4. In Table 3-4 it shows that alloys Ti-0.5Fe-0.5Nb, Ti-1Fe-1Nb and Ti-2Fe-2Nb, and Ti-0.5Fe-0.5Nb and Ti-1Fe-1Nb predicted by Eq. 2 and Eq. 1, respectively, agree with the sintered Ti-Fe-Nb alloys. However, alloys Ti-3.5Fe-3.5Nb and Ti-5Fe-5Nb, and Ti-2Fe-2Nb, Ti-3.5Fe-3.5Nb and Ti-5Fe-5Nb predicted by Eq. 2 and Eq. 1, respectively, are not in agreement with the sintered Ti-Mn-Nb alloys. As their microstructure is composed of only α + β lamellae, thus not consisting of near-β and metastable β. Overall Eq. 2 appears to be more accurate than Eq. 1 for predicting the alloy type of sintered Ti-Fe-Nb alloys, as the MoE values are lower than the ones predicted by Eq. 1 (Table 3-4).

Figure 4-17 shows the XRD patterns of the ternary Ti-Fe-Nb alloys. The α-phase was detected in all alloys, whereas the β-phase was only detected in the Ti-2Fe-2Nb, Ti-3.5Fe-3.5Nb and Ti-5Fe-5Nb alloys. The relative intensity of the main β

peak (β (110)) increases as the amount of β-stabilizer (Fe-Nb) increases. Although Fe is a β-eutectoid stabilizer, no TiFe intermetallic phases were detected.

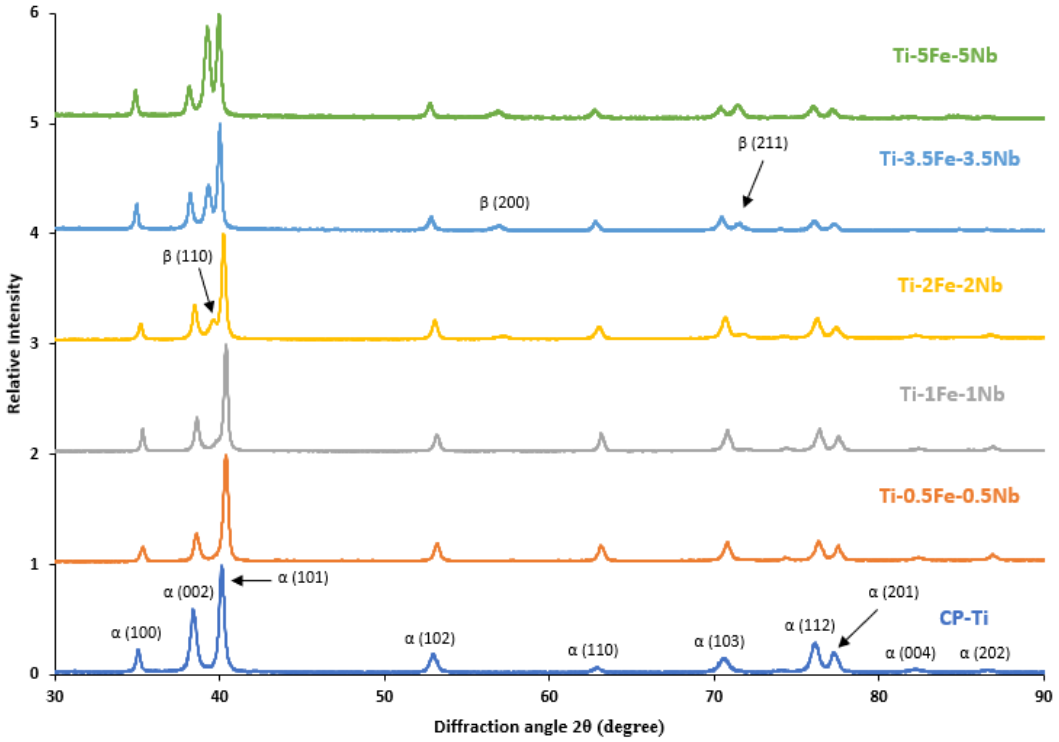

Figure 4-17 XRD patterns of the sintered Ti-Fe-Nb alloys.

4.3.3 Mechanical behaviour

Table 4-3 shows the average mechanical properties of the ternary Ti-Fe-Nb alloys, and Figure 4-18 shows representative stress-strain curves in comparison to CP-Ti.

Table 4-3 Average mechanical properties of the sintered Ti-Fe-Nb alloys.

Material	YS (MPa)	UTS (MPa)	Elongation (%)	Hardness (HRA)
Ti-0.5Fe-0.5Nb	408 ± 17	501 ± 11	10.7 ± 3.0	53 ± 1.3
Ti-1Fe-1Nb	439 ± 7	547 ± 9	11.4 ± 2.0	54 ± 1.3
Ti-2Fe-2Nb	496 ± 6	601 ± 23	6.8 ± 3.0	56 ± 1.2
Ti-3.5Fe-3.5Nb	585 ± 6	700 ± 10	6.0 ± 1.5	59 ± 1.2
Ti-5Fe-5Nb	727 ± 14	800 ± 23	2.3 ± 0.2	62 ± 1.0

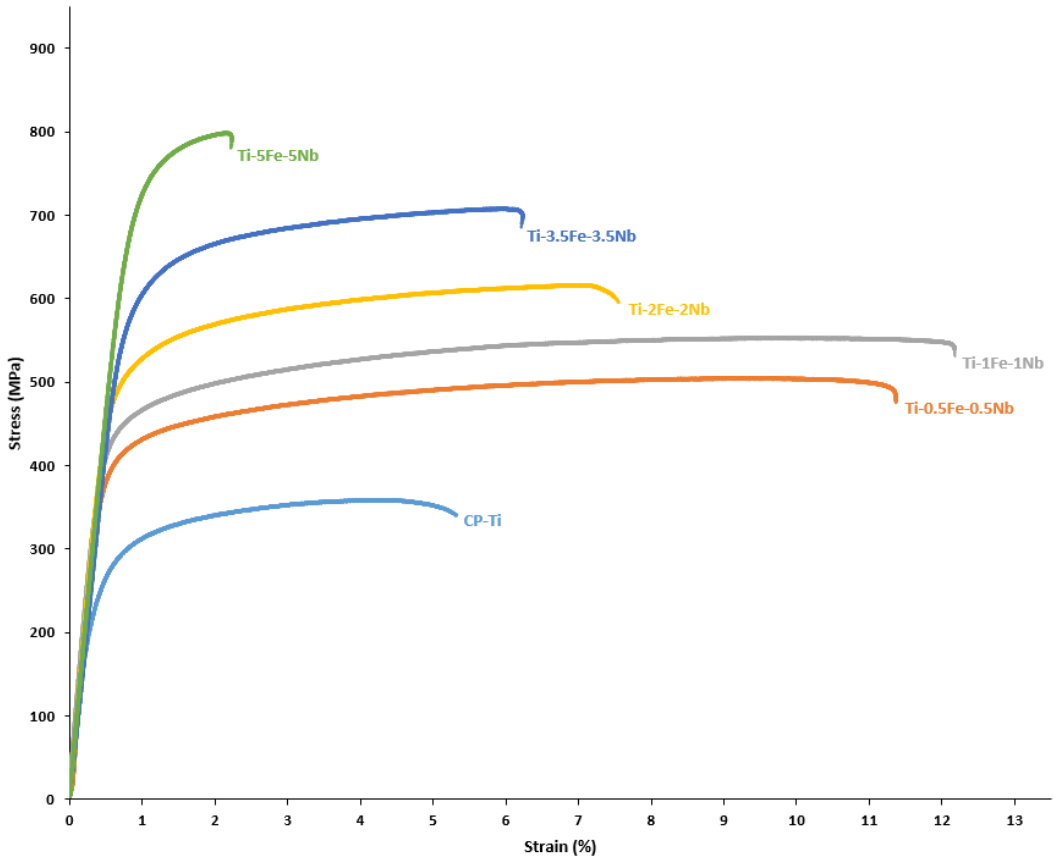

Figure 4-18 Representative stress-strain curves of the sintered Ti-Fe-Nb alloys.

The tensile stress of the alloys increases as the amount of alloying elements (Fe-Nb) increase. The elongation initially increases, reaching the highest value for the Ti-1Fe-1Nb alloy (11.4%), and then decreases. The Ti-Fe-Nb alloys are characterized by a ductile behaviour, showing both an elastic and plastic deformation region in their stress-strain curves. The YS and UTS of the Ti-Fe-Nb alloys increases from 408 MPa to 727 MPa and 501 MPa to 800 MPa, respectively, as the amount of alloying elements increases. The Ti-5Fe-5Nb alloy shows the highest YS and UTS, however the elongation was the lowest (2.3%) in comparison to the other tested samples as shown in Figure 4-18. The hardness of the Ti-Fe-Nb alloys increases linearly (Figure 4-19), from 53 HRA to 62 HRA as the amount of alloying elements increases, and is higher than that of CP-Ti (46 HRA). The addition of Fe and Nb to Ti improves the mechanical properties due to the solid-solution strengthening effect it has in Ti, and the increased volume fraction of the β-Ti phase (as shown in Figure 4-17 (XRD)). The refinement of the lamellar microstructure from Ti-0.5Fe-0.5Nb to Ti-5Fe-5Nb (Figure 4-16), shows the increase in mechanical properties as shown in Figure 4-18.

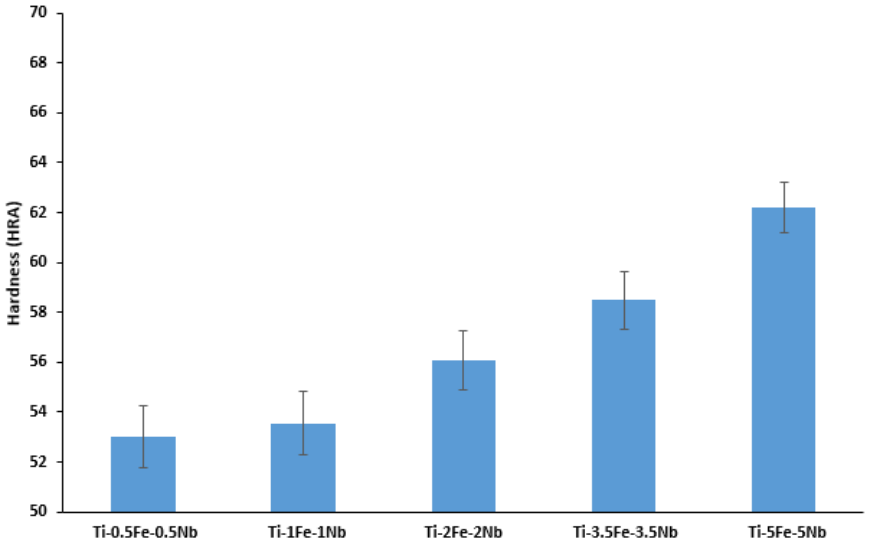

Figure 4-19 Rockwell hardness of the sintered Ti-Fe-Nb alloys.

The mechanical properties (Figure 4-20 (tensile) and Figure 4-21 (hardness)) of the sintered Ti-Fe-Nb alloys are compared with other Fe- and Nb- based Ti alloys, as well as Ti-6Al-4V. The UTS and YS of the sintered Ti-5Fe-5Nb (UTS = 800 MPa and YS = 727 MPa) are higher compared to the cast Ti-5Nb (UTS = 536 MPa and YS = 407 MPa [16]) alloy, however lower than cast Ti-6Al-4V (UTS = 976 MPa and YS = 847 MPa [70]) and sintered Ti-5Fe (UTS = 930 MPa and YS = 843 MPa [51]) alloys, and is comparable with the cast/solution-treated Ti-2Fe-14Nb (UTS = 830 MPa and YS = 685 MPa [61]) alloy. Furthermore, the sintered Ti-5Fe-5Nb (2.3%) alloy shows a lower elongation than cast/solution-treated Ti-2Fe-14Nb (24%), cast Ti-5Nb (11%) as well as cast Ti-6Al-4V (5.1%), and is comparable to sintered Ti-5Fe (2.6%). The high strength of the sintered Ti-5Fe alloy is due to the fine α + β lamellar microstructure and high relative sintered density (98.7%) in comparison to the sintered Ti-5Fe-5Mn alloy (relative sintered density was 92.3%). Processing of the sintered Ti-5Fe alloy was done via warm pressing (at 250 ºC), which obtains high green density values which, in turn results in high relative density values after sintering and increased mechanical properties in comparison to cold pressing [51]. Although both sintered Ti-5Fe and Ti-5Fe-5Nb alloys have an α + β lamellar microstructure, the difference in relative sintered density has an effect on the mechanical properties of the alloy. The cast/solution-treated Ti-2Fe-14Nb alloy is composed of only equiaxed β grains, the solution-treatment has significantly increased the elongation of the alloy (24%) in comparison to the sintered Ti-5Fe-5Nb alloy (2.3%).

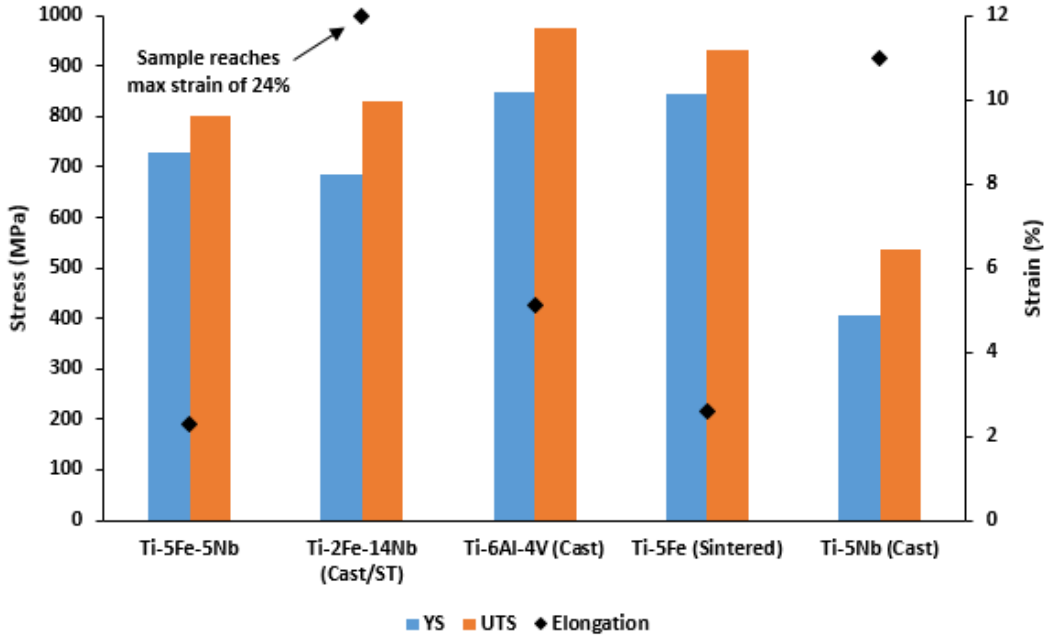

Figure 4-20 Comparison of the tensile properties of the sintered Ti-5Fe-5Nb alloy to other Fe- and Nb- based Ti alloys, as well as Ti-6Al-4V.

In terms of hardness (Figure 4-21), the sintered Ti-5Fe-5Nb (254 HV) alloy shows a higher hardness than cast Ti-5Nb (177 HV), however lower than both cast Ti-6Al-4V (approximately 340 HV) and sintered Ti-5Fe (331 HV) alloys. No hardness was reported for the cast/solution-treated Ti-2Fe-14Nb alloy. Once again, the high hardness of the sintered Ti-5Fe alloy is due to the high relative sintered density in comparison to the sintered Ti-5Fe-5Nb alloy, even though they both have an $\alpha + \beta$ lamellar microstructure.

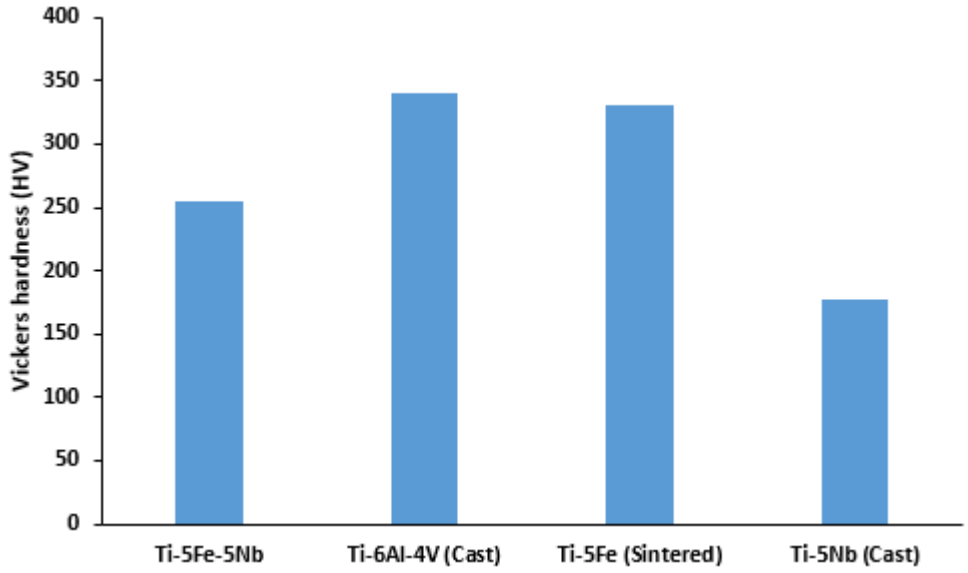

Figure 4-21 Comparison of the hardness of the sintered Ti-5Fe-5Nb alloy to other Fe- and Nb- based Ti alloys, as well as Ti-6Al-4V.

4.4 Sintered Ternary Ti-Fe-Cu Alloys

4.4.1 Density

The physical properties of the ternary Ti-Fe-Cu alloys, including relative green and sintered density, are shown in Figure 4-22.

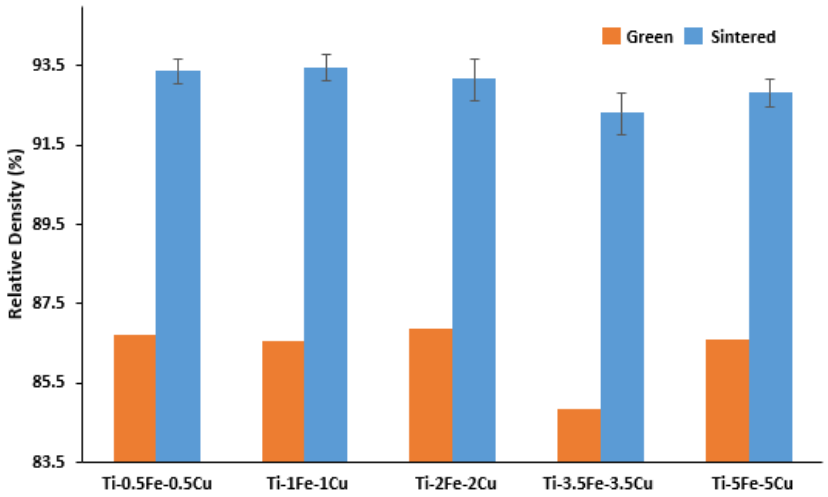

Figure 4-22 Relative densities of the Ti-Fe-Cu alloys.

The relative green and sintered density for the Ti-0.5Fe-0.5Cu, Ti-1Fe-1Cu and Ti-2Fe-2Cu alloys are fairly constant, with the difference being approximately 0.3% in terms of relative sintered density. The relative sintered density for the Ti-3.5Fe-3.5Cu (92.3%) alloy was the lowest, compared to the other ternary Ti-Cu-Fe compositions. Similar relative densities have been reported in literature, as mentioned above in density sections of sintered ternary Ti-Cu-Nb (4.1) and Ti-Fe-Nb (4.3) alloys. The porosity left by the compaction of the powder blends was constant for all the samples (approximately 13%) except Ti-3.5Fe-3.5Cu (approximately 15%), even though the Ti, Fe and Cu powders have different particle sizes (Table 3-1) and morphology (Figure 3-1). After sintering the amount of porosity present in the samples was also constant (approximately 7%).

4.4.2 Microstructure analysis

Figure 4-23 shows the microstructure analysis of the ternary Ti-Fe-Cu alloys. The sintered samples show porosity, where the pores are characterized by a spherical or irregular morphology. The size of the spherical pores is approximately within the range of 5 – 55 μm, and a small amount of irregular/elongated pores are

present. The sintered Ti-Fe-Cu alloys are characterized by an α + β lamellar microstructure. The addition of Fe-Cu (from 0.5 to 5 wt%) to Ti, refines the lamellar microstructure as shown in Figure 4-23. Similar α + β lamellar microstructures have been reported in literature, as mentioned above in microstructure analysis sections of sintered ternary Ti-Cu-Nb (4.1) and Ti-Fe-Nb (4.3) alloys.

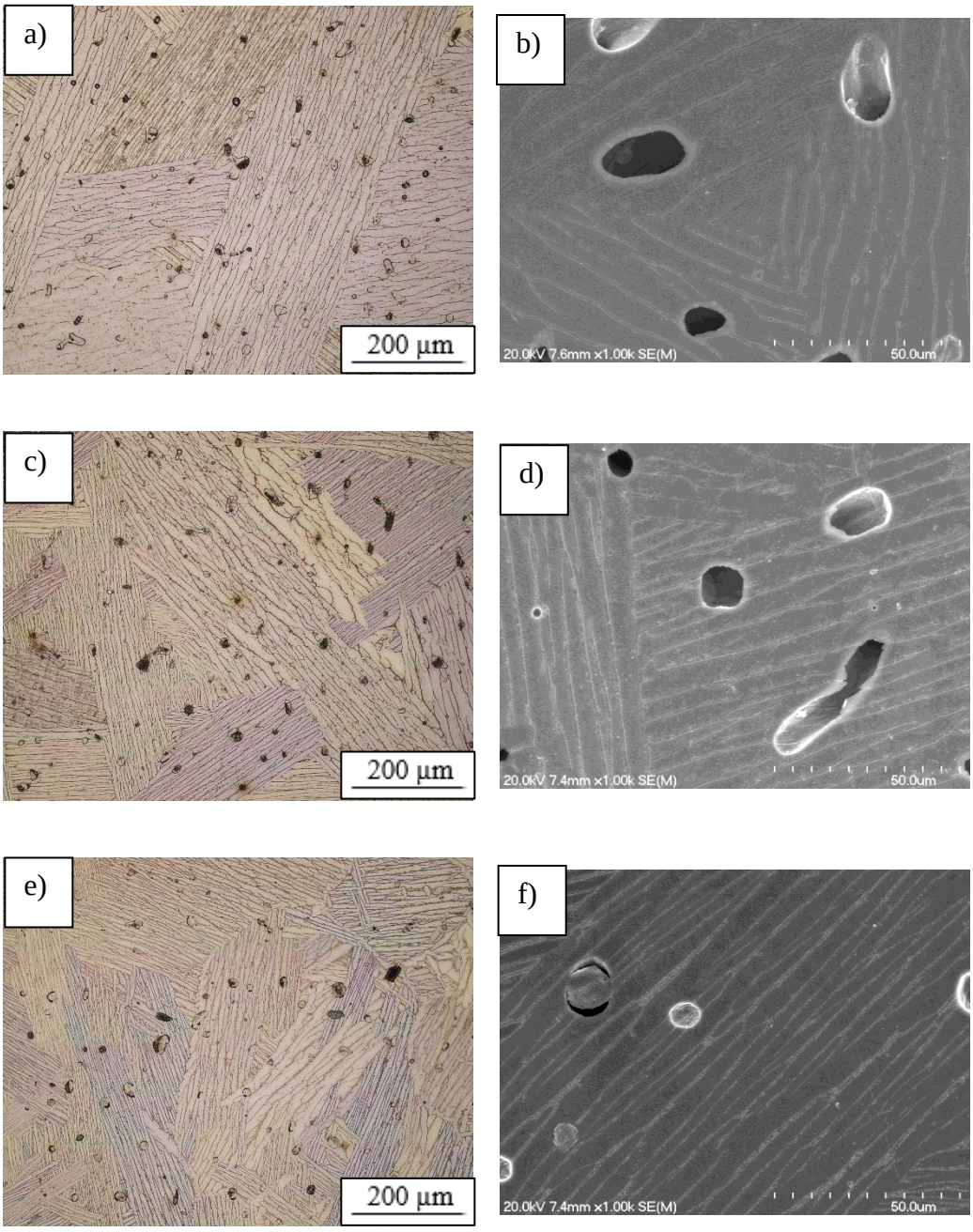

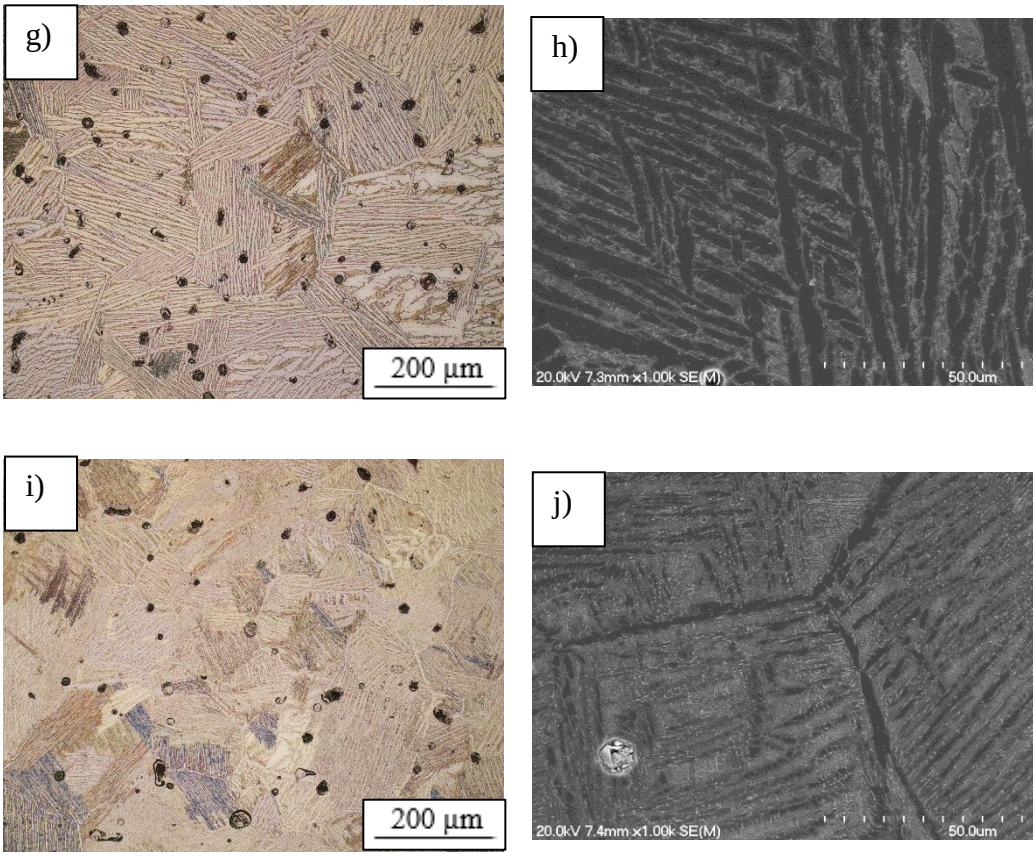

Figure 4-23 Optical and SEM micrographs, respectively, for: (a) and (b) Ti-0.5Fe-0.5Cu, (c) and (d) Ti-1Fe-1Cu, (e) and (f) Ti-2Fe-2Cu, (g) and (h) Ti-3.5Fe-3.5Cu, and (i) and (j) Ti-5Fe-5Cu.

The microstructure of the sintered Ti-Fe-Cu alloys are compared with their predicted MoE and alloy type in Table 3-5. It shows that alloys Ti-0.5Fe-0.5Cu and Ti-1Fe-1Cu predicted by both Eq. 2 and 1 agree with the sintered Ti-Fe-Cu alloys. However, alloys Ti-2Fe-2Cu, Ti-3.5Fe-3.5Cu and Ti-5Fe-5Cu predicted by both equations, are not in agreement with the sintered Ti-Fe-Cu alloys, as their microstructure does not consist of near-β and metastable β. Overall Eq. 2 appears to be more accurate than Eq. 1 for predicting the alloy type of sintered Ti-Fe-Cu alloys, since the MoE values are lower than the ones predicted by Eq. 1 (Table 3-5).

XRD patterns of the ternary Ti-Fe-Cu alloys are shown in Figure 4-24. The α-phase was detected in all alloys, while the β-phase was only detected in the Ti-3.5Fe-3.5Cu and Ti-5Fe-5Cu alloys. The relative intensity of the main β peak (β (110)) increases as the amount of β-stabilizer (Fe-Cu) increases. The Ti_2Cu phase was detected in the Ti-3.5Fe-3.5Cu alloy, and its intensity increases with the addition of Fe-Cu. It has been reported in literature that the Ti_2Cu phase is found at low Cu

concentrations as mentioned above in microstructure analysis section of the sintered ternary Ti-Cu-Nb (4.1) alloys.

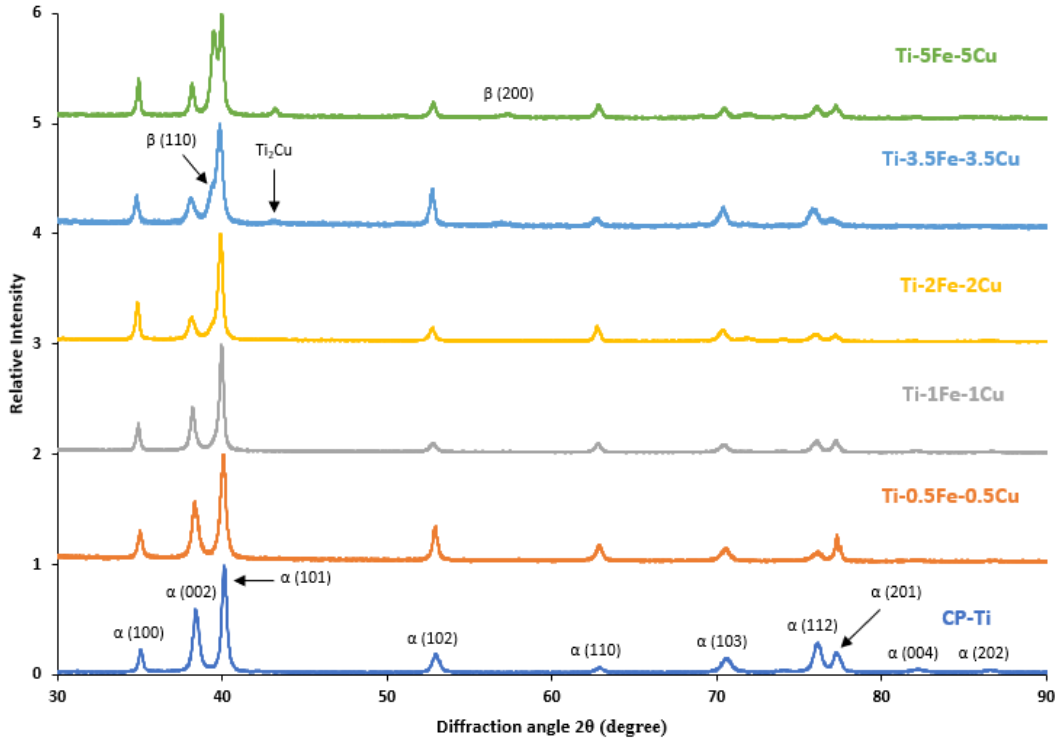

Figure 4-24 XRD patterns of the sintered Ti-Fe-Cu alloys.

4.4.3 Mechanical behaviour

Figure 4-25 shows representative stress-strain curves of the ternary Ti-Fe-Cu alloys in comparison to CP-Ti, and Table 4-4 shows the average mechanical properties. The tensile stress of the alloys increases as the amount of alloying elements (Fe-Cu) increase. The elongation initially increases, reaching the highest value for the Ti-1Fe-1Cu alloy (9.6%), and then decreases. All Ti-Fe-Cu alloys except Ti-5Fe-5Cu (brittle behaviour) are characterized by a ductile behaviour, showing both an elastic and plastic deformation region in their stress-strain curves.

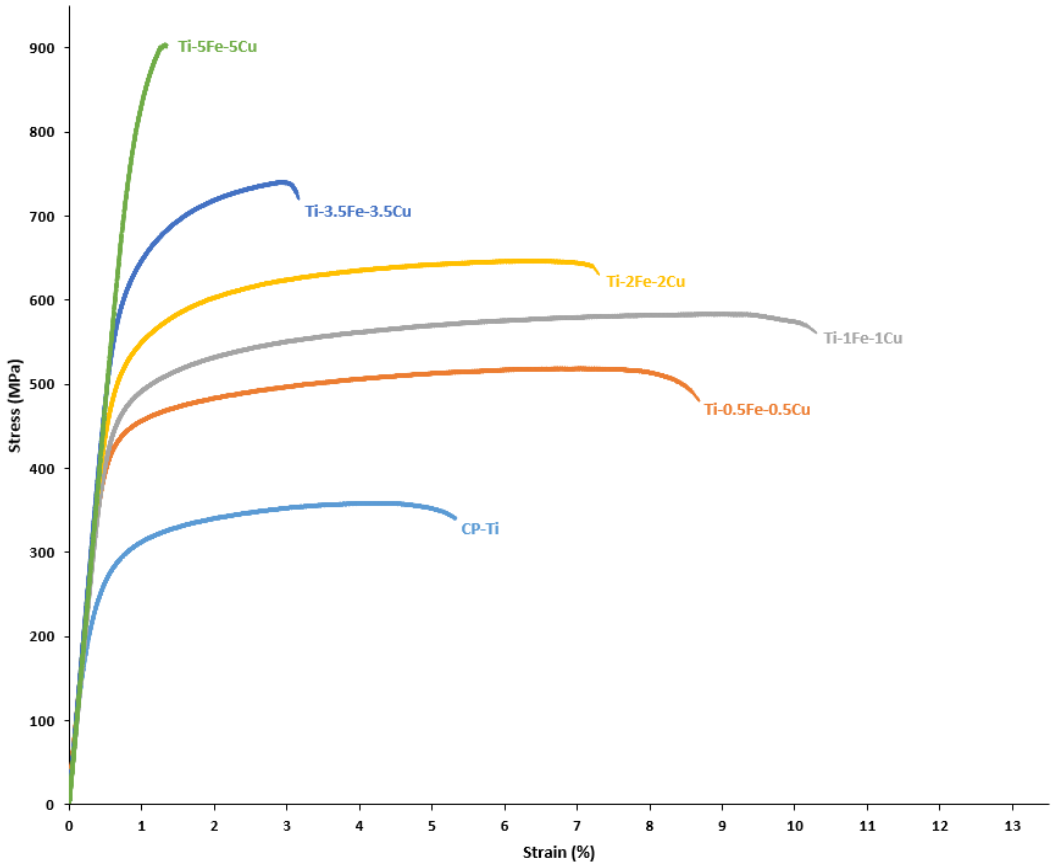

Figure 4-25 Representative stress-strain curves of sintered Ti-Fe-Cu alloys.

Table 4-4 Average mechanical properties of the sintered Ti-Fe-Cu alloys.

Material	YS (MPa)	UTS (MPa)	Elongation (%)	Hardness (HRA)
Ti-0.5Fe-0.5Cu	442 ± 8	526 ± 13	7.6 ± 1.3	54 ± 1.5
Ti-1Fe-1Cu	472 ± 16	581 ± 20	9.6 ± 2.3	53 ± 1.3
Ti-2Fe-2Cu	526 ± 6	653 ± 11	7.6 ± 1.4	58 ± 1.0
Ti-3.5Fe-3.5Cu	630 ± 22	754 ± 34	3.7 ± 0.7	61 ± 0.8
Ti-5Fe-5Cu	864 ± 24	912 ± 29	1.4 ± 0.1	65 ± 1.0

The YS and UTS of the Ti-Fe-Cu alloys increases from 442 MPa to 864 MPa and 526 MPa to 912 MPa, respectively, as the amount of alloying elements increase. The Ti-5Fe-5Cu alloy shows the highest YS and UTS, however the elongation was the lowest (1.4%) in comparison to the other tested samples as shown in Figure 4-25. The hardness of the Ti-Fe-Cu alloys increases linearly (Figure 4-26), from 54 HRA to 65 HRA as the amount of alloying elements increase, and is higher than that of CP-Ti (46 HRA). The addition of Fe and Cu to Ti improves the mechanical properties due to the solid-solution strengthening effect it has in Ti, and the increased volume fraction of the β-Ti phase (as shown in Figure 4-24 (XRD)). A fine lamellar microstructure (Ti-5Fe-5Cu) tends to give higher mechanical

properties, compared to an alloy with a coarse lamellar microstructure such as Ti-0.5Fe-0.5Cu (Figure 4-23 a) and b)). The Ti_2Cu phase is also responsible for improving the mechanical properties, as present in the Ti-3.5Fe-3.5Cu and Ti-5Fe-5Cu alloys.

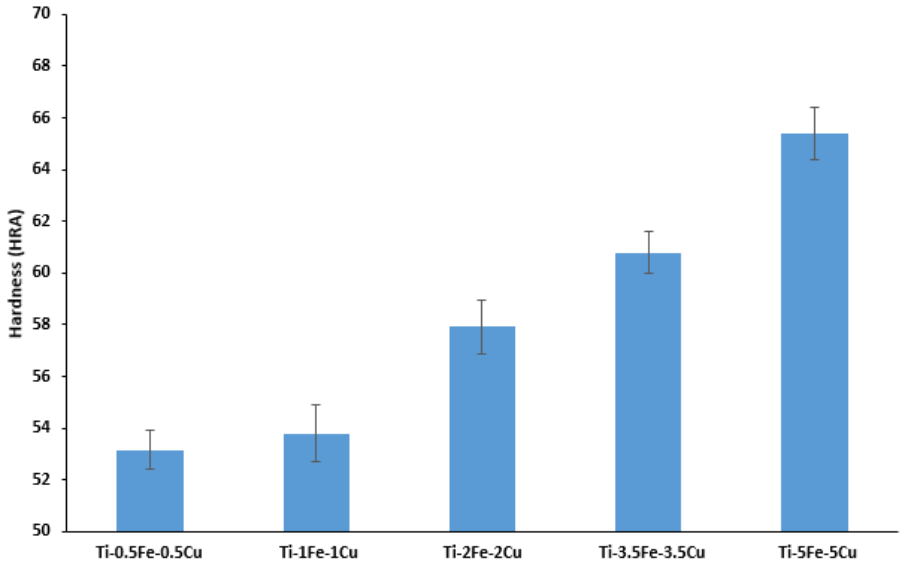

Figure 4-26 Rockwell hardness of the sintered Ti-Fe-Cu alloys.

The mechanical properties (Figure 4-27 (tensile) and Figure 4-28 (hardness)) of the sintered Ti-Fe-Cu alloys are compared with other Fe- and Cu- based Ti alloys, as well as Ti-6Al-4V. From Figure 4-27, the UTS and YS of the sintered Ti-5Fe-5Cu (UTS = 912 MPa and YS = 864 MPa) are higher compared to sintered Ti-5Cu (UTS = 754 MPa and YS = 627 MPa [14]) and cast Ti-5Cu (UTS = approximately 630 MPa and YS = approximately 570 MPa [13]) alloys, however comparable to cast Ti-6Al-4V (UTS = 976 MPa and YS = 847 MPa [70]) and sintered Ti-5Fe (UTS = 930 MPa and YS = 843 MPa [51]) alloys. Furthermore, the elongation of the sintered Ti-5Fe-5Cu (1.4%) alloy is comparable with cast Ti-5Cu (approximately 3.2%) and sintered Ti-5Fe (2.6%) alloys, however is lower than that of sintered Ti-5Cu (9.5%) and cast Ti-6Al-4V (5.1%) alloys. Although the sintered Ti-5Fe-5Cu alloy shows comparable strength with cast Ti-6Al-4V and sintered Ti-5Fe alloys, the full mechanical potential of the alloy is low because of porosity (approximately 7%). If the compaction of the powder blends was done via warm pressing, the strength of the alloy would significantly increase and could potentially be higher than both cast Ti-6Al-4V and sintered Ti-5Fe alloys. The low elongation of the sintered Ti-5Fe-5Cu alloy is due to porosity in the sample. The trends of hardness

(Figure 4-28), are similar to the trends of tensile properties (Figure 4-27). In terms of hardness the sintered Ti-5Fe-5Cu (296 HV) alloy shows a higher hardness than cast Ti-5Cu (230 HV) and sintered Ti-5Cu (227 HV) alloys, however comparable with the cast Ti-6Al-4V (approximately 340 HV) and sintered Ti-5Fe (331 HV) alloys.

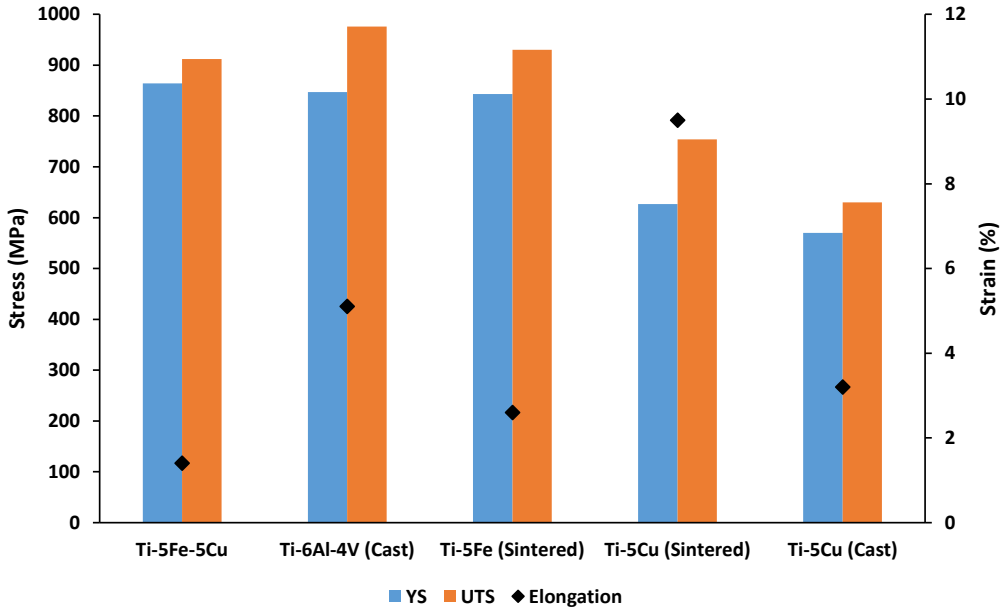

Figure 4-27 Comparison of the tensile properties of the sintered Ti-5Fe-5Cu alloy to other Fe- and Cu- based Ti alloys, as well as Ti-6Al-4V.

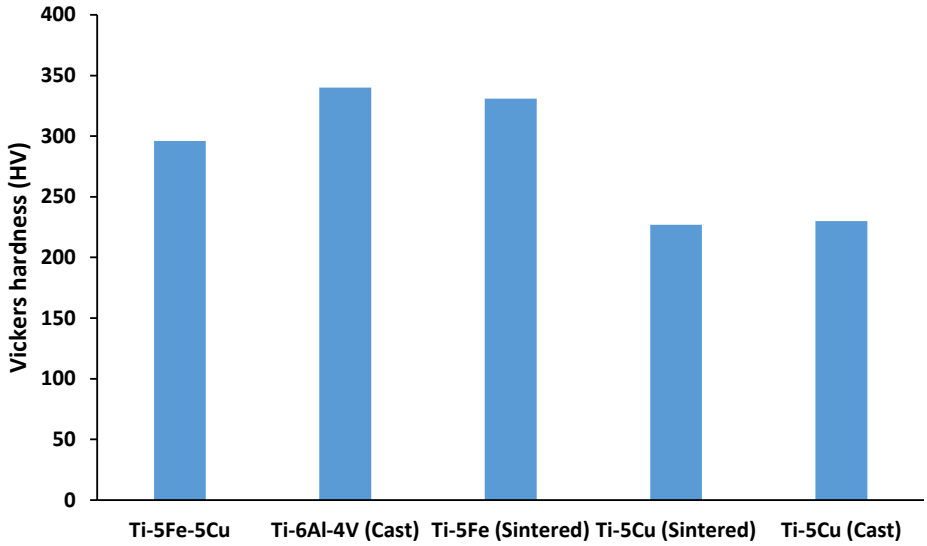

Figure 4-28 Comparison of the hardness of the sintered Ti-5Fe-5Cu alloy to other Fe- and Cu- based Ti alloys, as well as Ti-6Al-4V.

4.5 Sintered Ternary Ti-Fe-Mn Alloys

4.5.1 Density

Figure 4-29 shows the physical properties of the ternary Ti-Fe-Mn alloys, including relative green and sintered density.

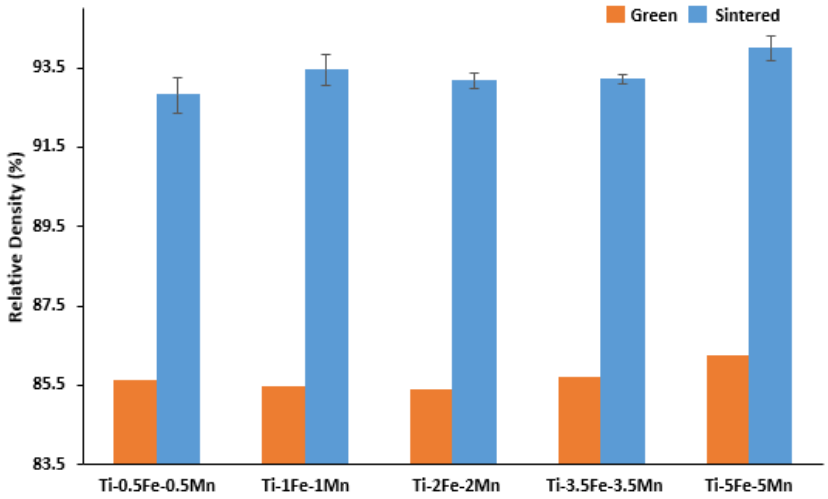

Figure 4-29 Relative densities of the Ti-Fe-Mn alloys.

The relative green density of the ternary Ti-Fe-Mn compositions, except Ti-5Fe-5Mn, were constant with the addition of Fe-Mn, regardless of the different particle sizes (Table 3-1) and morphology (Figure 3-1) of the Ti, Fe and Mn powders. The relative sintered density of the Ti-0.5Fe-0.5Mn, Ti-2Fe-2Mn and Ti-3.5Fe-3.5Mn alloys was fairly constant, with the difference being approximately 0.4% in terms of relative sintered density. Furthermore, the relative sintered density of the Ti-5Fe-5Mn (94%) alloy was the highest, compared to the other ternary Ti-Fe-Mn compositions. Similar relative densities have been reported in literature, as mentioned above in density sections of sintered ternary Ti-Mn-Nb (4.2) and Ti-Fe-Nb (4.3) alloys. The porosity left by the compaction of the powder blends was constant for all the samples (approximately 14%). After sintering the amount of porosity present in the samples was also constant (approximately 7%).

4.5.2 Microstructure analysis

Microstructure analysis of the ternary Ti-Fe-Mn alloys is shown in Figure 4-30. Pores are present in the sintered samples, where they are characterized by a spherical or elongated morphology. The size of the spherical pores is approximately

within the range of 5 – 55 µm, and a small amount of irregular/elongated pores are present. The sintered Ti-Fe-Mn alloys, expect Ti-5Fe-5Mn, are characterized by an α + β lamellar microstructure (Figure 4-30 a) – h)). The microstructure of the Ti-5Mn-5Fe alloy is composed of equiaxed β-phase grains (Figure 4-30 i) and j)), a close up of the β grain boundary is shown in Figure 4-31, which shows a lamellar structure inside of it, suggesting that the alloy is a metastable β alloy. With the addition of 0.5 wt% Fe and Mn to Ti the lamellar microstructure is coarse (Figure 4-30 a) and b)). By increasing the amount of Fe-Mn (from 0.5 to 5 wt%) the lamellar microstructure is refined (Figure 4-30 a) – h)). Similar microstructures have been reported in literature, as mentioned above in microstructure analysis sections of sintered ternary Ti-Mn-Nb (4.2) and Ti-Fe-Nb (4.3) alloys.

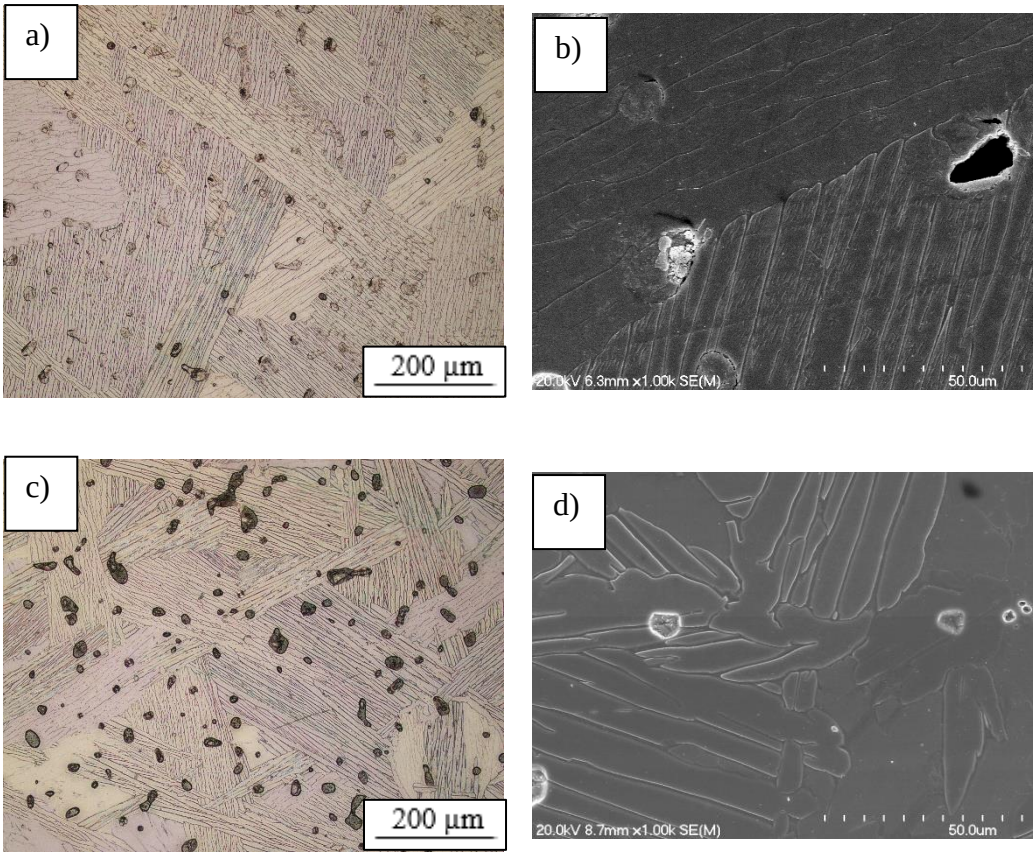

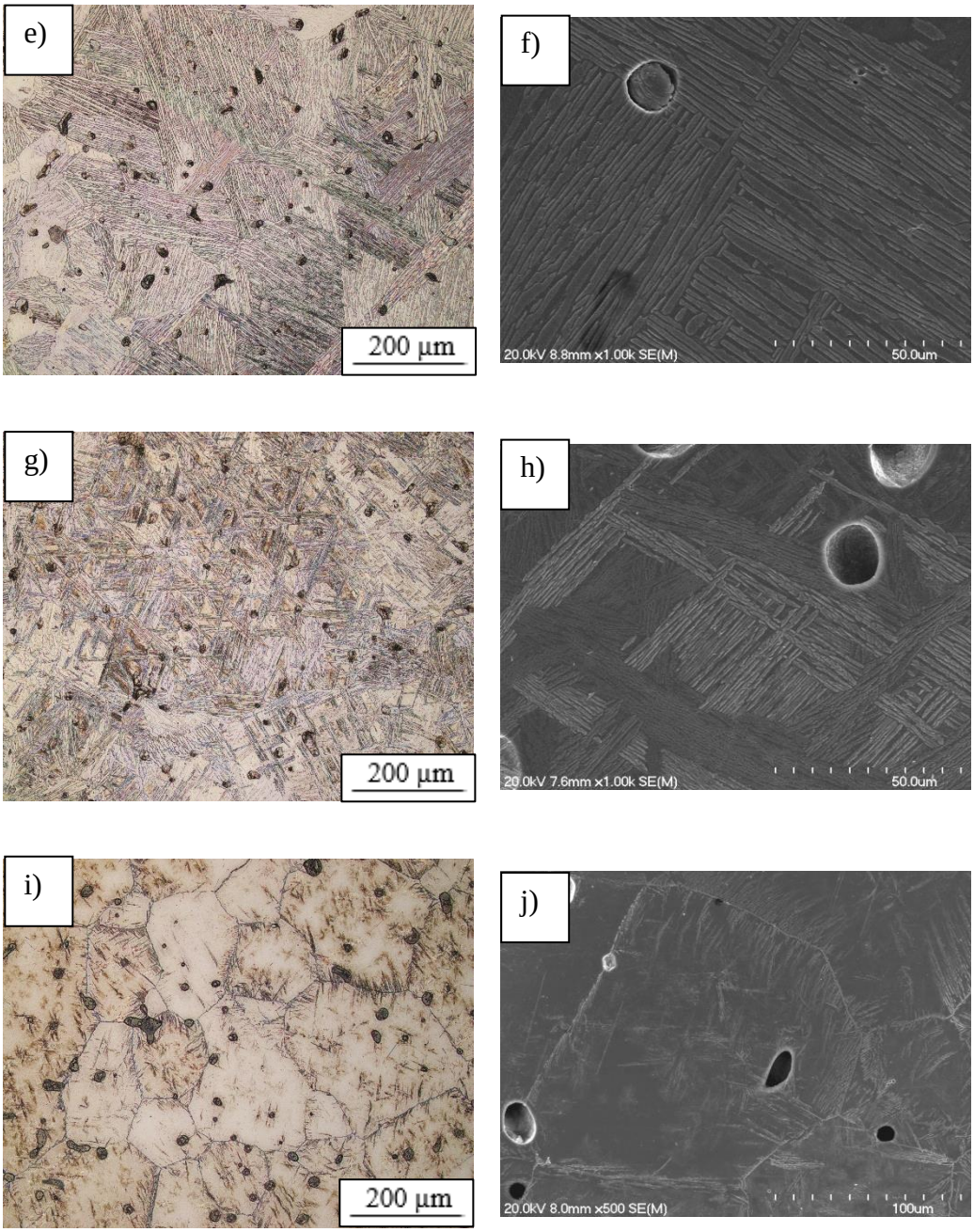

Figure 4-30 Optical and SEM micrographs, respectively, for: (a) and (b) Ti-0.5Fe-0.5Mn, (c) and (d) Ti-1Fe-1Mn, (e) and (f) Ti-2Fe-2Mn, (g) and (h) Ti-3.5Fe-3.5Mn, and (i) and (j) Ti-5Fe-5Mn.

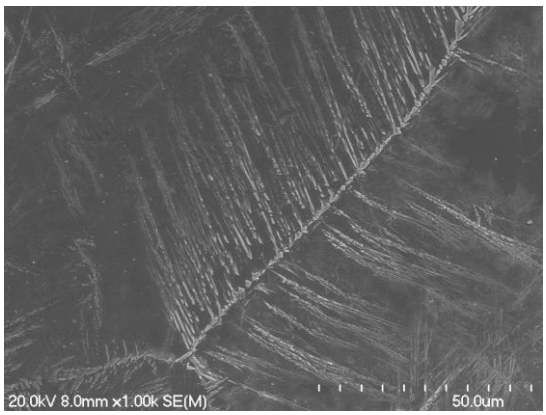

Figure 4-31 SEM micrograph of the Ti-5Fe-5Mn alloy.

The microstructure of the sintered Ti-Fe-Mn alloys are compared with their predicted MoE and alloy type in Table 3-6. It shows that alloys Ti-0.5Fe-0.5Mn and Ti-1Fe-1Mn predicted by both Eq. 2 and 1 agree with the sintered Ti-Fe-Cu alloys, as their microstructure is composed of α + β lamellae. However, alloys Ti-2Fe-2Mn and Ti-3.5Fe-3.5Mn predicted by both equations are not in agreement with the sintered Ti-Fe-Cu alloys, as their microstructure does not consist of near-β and metastable β. The MoE and alloy type predicted by both equations for the Ti-5Fe-5Mn alloy agrees with the sintered Ti-5Fe-5Mn showing a metastable β microstructure composed of equiaxed β-phase grains (Figure 4-30 i) and j)). Both equations predicted the same alloy type for each ternary Ti-Fe-Mn compositions, however both equations were only correct for the Ti-0.5Fe-0.5Mn and Ti-1Fe-1Mn alloys, and not for the Ti-2Fe-2Mn and Ti-3.5Fe-3.5Mn alloys (Table 3-6).

XRD patterns of the ternary Ti-Fe-Mn alloys are shown in Figure 4-32. The α-phase was detected in all alloys, while the β-phase was also detected in all alloys (except Ti-0.5Fe-0.5Mn). The relative intensity of the main β peak (β (110)) increases as the amount of β-stabilizer (Fe-Mn) increases.

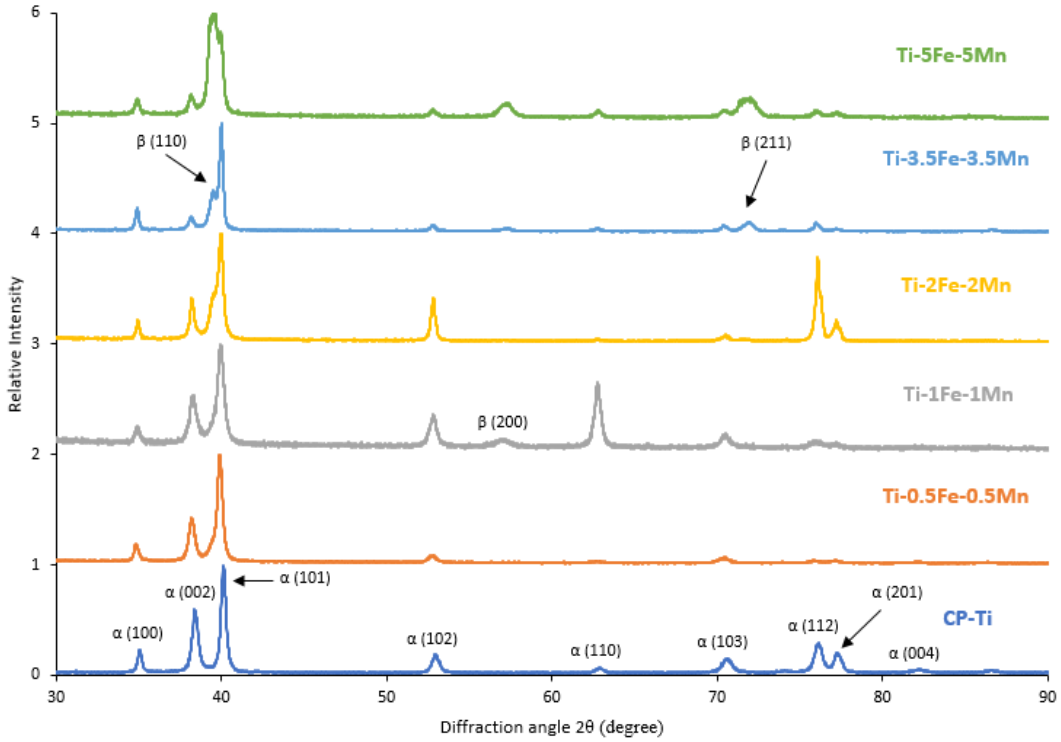

Figure 4-32 XRD patterns of sintered Ti-Fe-Mn alloys.

4.5.3 Mechanical behaviour

Table 4-5 shows the average mechanical properties of the ternary Ti-Fe-Mn alloys, and Figure 4-33 shows representative stress-strain curves in comparison to CP-Ti.

Table 4-5 Average mechanical properties of the sintered Ti-Fe-Mn alloys.

Material	YS (MPa)	UTS (MPa)	Elongation (%)	Hardness (HRA)
Ti-0.5Fe-0.5Mn	433 ± 14	519 ± 17	9.3 ± 2.5	54 ± 0.9
Ti-1Fe-1Mn	475 ± 13	567 ± 6	8.5 ± 0.9	56 ± 1.4
Ti-2Fe-2Mn	609 ± 8	676 ± 17	2.1 ± 0.5	59 ± 1.2
Ti-3.5Fe-3.5Mn	816 ± 8	842 ± 15	1.7 ± 0.3	63 ± 0.8
Ti-5Fe-5Mn	–	607 ± 7	0.6 ± 0.1	70 ± 0.5

The tensile stress of the alloys increases as the amount of alloying elements (Fe-Mn) increase. However, the elongation increases, reaching the highest value for the Ti-0.5Fe-0.5Mn alloy (9.3%), and then decreases. All Ti-Fe-Mn alloys (except Ti-5Fe-5Mn) are characterized by a ductile behaviour. The Ti-5Fe-5Mn alloy showed no plastic deformation, only elastic behaviour was observed (Figure 4-33), thus the alloy is characterized by a brittle behaviour (no YS could be calculated). The YS

and UTS of the alloys increase from 433 MPa to 816 MPa and 519 MPa to 842 MPa, respectively, as the amount of alloying elements increase. The Ti-3.5Fe-3.5Mn alloy shows the highest YS and UTS, however the elongation was the second lowest (1.7%) in comparison to the other tested samples as shown in Figure 4-33.

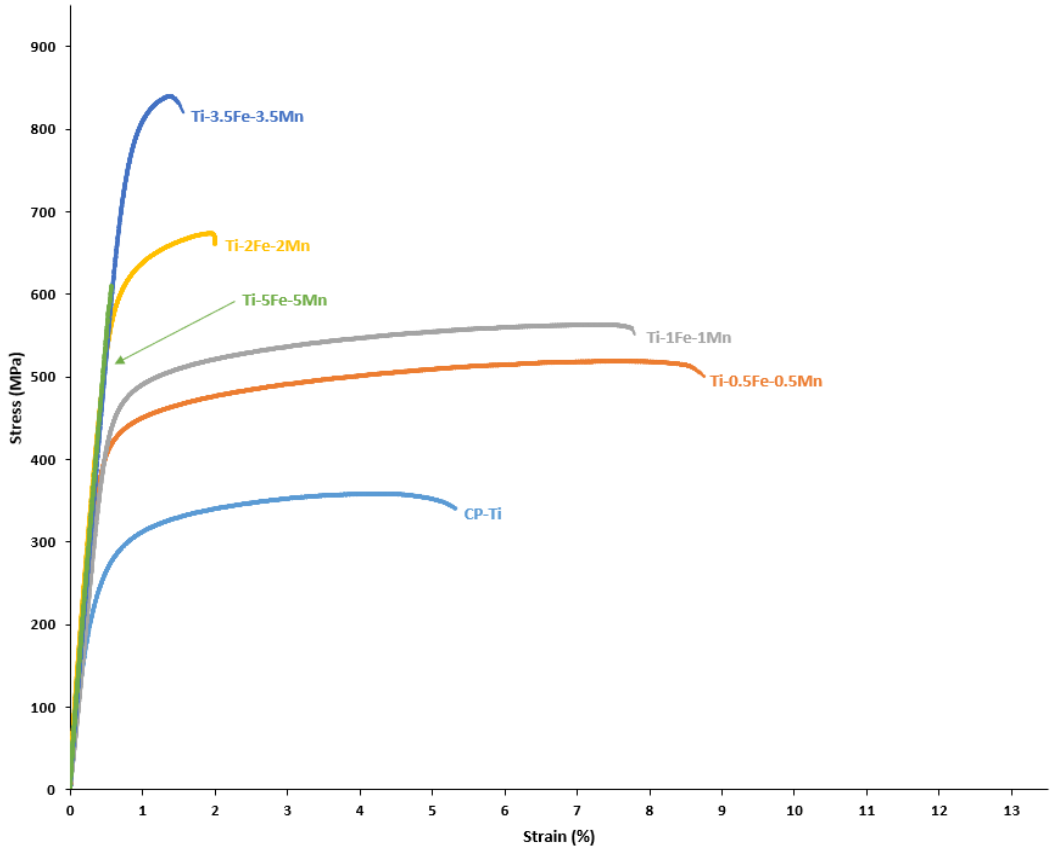

Figure 4-33 Representative stress-strain curves of sintered Ti-Fe-Mn alloys.

The addition of Fe and Mn to Ti improves the mechanical properties. As mentioned before, a fine lamellar microstructure tends to give higher mechanical properties (Ti-3.5Fe-3.5Mn), compared to an alloy with a coarse lamellar microstructure such as Ti-0.5Fe-0.5Mn. The hardness of the Ti-Fe-Mn alloys increases linearly (Figure 4-34), from 54 HRA to 70 HRA as the amount of alloying elements increase, and is higher than that of CP-Ti (46 HRA).

The mechanical properties (Figure 4-35 (tensile) and Figure 4-36 (hardness)) of the sintered Ti-Fe-Mn alloys, are compared with other Fe- and Mn- based Ti alloys, as well as Ti-6Al-4V.

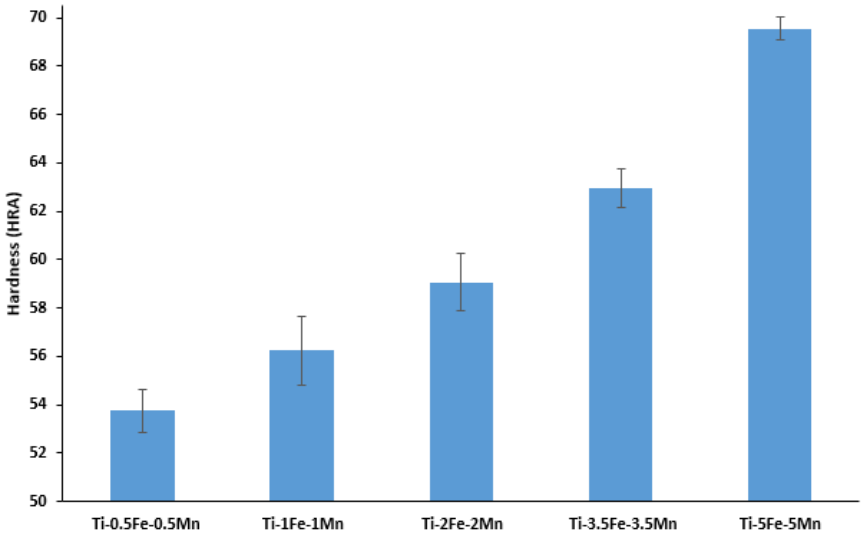

Figure 4-34 Rockwell hardness of the sintered Ti-Fe-Mn alloys.

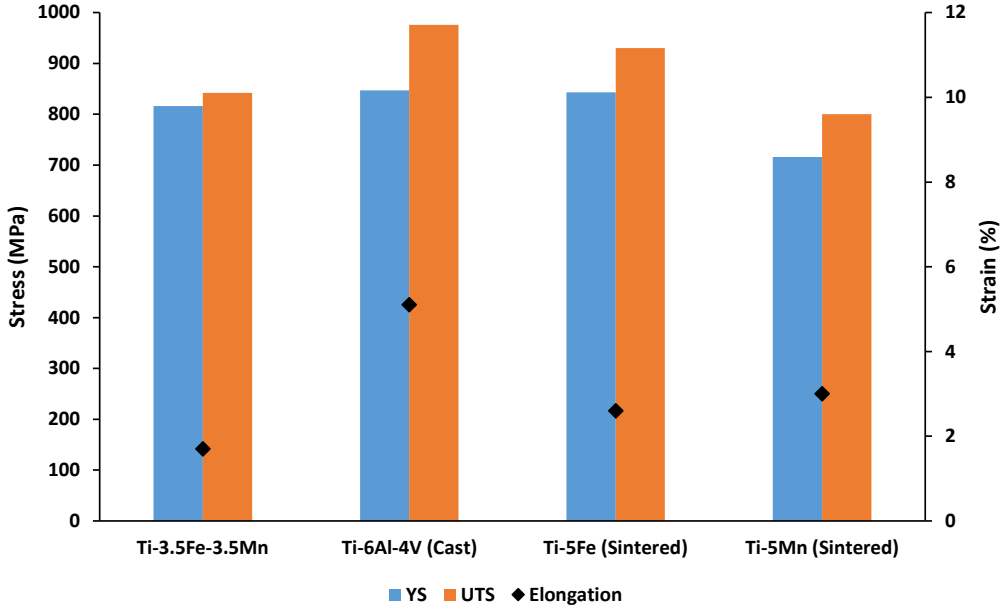

Figure 4-35 Comparison of the tensile properties of the sintered Ti-3.5Fe-3.5Mn alloy to other Fe- and Mn- based Ti alloys, as well as Ti-6Al-4V.

From Figure 4-35, the UTS and YS of the sintered Ti-3.5Fe-3.5Mn (UTS = 842 MPa and YS = 816 MPa) are higher compared to the sintered Ti-5Mn (UTS = 800 MPa and YS = 716 MPa [38]) alloy, however lower than cast Ti-6Al-4V (UTS = 976 MPa and YS = 847 MPa [70]) and sintered Ti-5Fe (UTS = 930 MPa and YS = 843 MPa [51]) alloys. It is worth mentioning that the YS of the sintered Ti-3.5Fe-3.5Mn, cast Ti-6Al-4V and sintered Ti-5Fe alloys are comparable as shown in Figure 4-35. Furthermore, the elongation of the sintered Ti-3.5Fe-3.5Mn (1.7%) alloy is comparable with sintered Ti-5Mn (3%) and sintered Ti-5Fe (2.6%) alloys,

however, is lower than the cast Ti-6Al-4V (5.1%) alloy. The low UTS of the sintered Ti-3.5Fe-3.5Mn alloy in comparison to both cast Ti-6Al-4V and sintered Ti-5Fe alloys, is due to porosity (7%). The sintered Ti-3.5Fe-3.5Mn (268 HV) alloy shows lower hardness than cast Ti-6Al-4V (approximately 340 HV) and sintered Ti-5Fe (331 HV) alloys (as shown in Figure 4-36), however, is comparable with the sintered Ti-5Mn (245 HV) alloy. It is worth mentioning that the sintered Ti-5Fe-5Mn alloy displayed the highest hardness (384 HV) in comparison to the other alloys as shown in Figure 4-36. The high hardness of the sintered Ti-5Fe-5Mn alloy is due to the equiaxed microstructure regardless of the amount of porosity (6%).

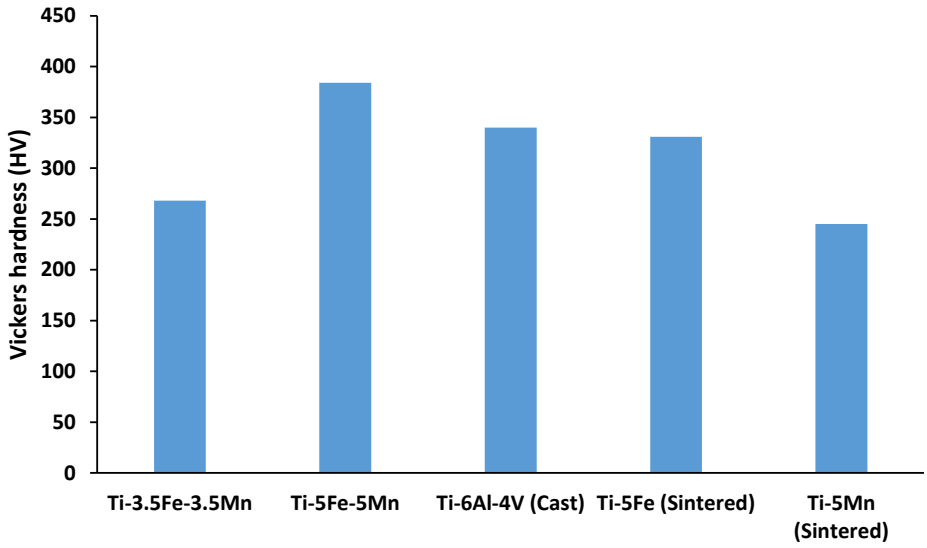

Figure 4-36 Comparison of the hardness of the sintered Ti-3.5Fe-3.5Mn alloy to other Fe- and Mn- based Ti alloys, as well as Ti-6Al-4V.

4.6 Comparison Between the Sintered Ternary Ti Alloys

4.6.1 Ternary Ti-X-Nb alloys (X = Cu, Mn and Fe)

The relative green/sintered density of the ternary Ti-Cu-Nb, Ti-Mn-Nb and Ti-Fe-Nb alloys decreases as more alloying elements are added to Ti. The sintered Ti-5Fe-5Nb (92.3%) alloy showed the highest density compared to the Ti-5Cu-5Nb (91.4%) and Ti-5Mn-5Nb (91.3%) alloys at the same total amount of alloying elements. As mentioned in the literature review (1.2.3.1), Fe has a high diffusivity in Ti, making it favourable for the sinterability, thus having an impact on the relative density of PM Ti alloys.

The effects of the amount and type of alloying elements directly effects the microstructure. The microstructure of the Ti-5Fe-5Nb alloy is significantly finer than Ti-5Cu-5Nb, and is comparable to Ti-5Mn-5Nb at the same total amount of alloying elements. Both Fe and Mn are strong β-stabilizers compared to Cu, thus much finer microstructures are observed with the addition of Fe and Mn as alloying elements to Ti. It is worth mentioning that even at low alloy concentrations of 0.5 wt%, both Ti-0.5Fe-0.5Nb and Ti-0.5Mn-0.5Nb alloys showed a more refined microstructure than Ti-0.5Cu-0.5Nb at the same total amount of alloying elements. As mentioned in the literature review (1.2.2.2), a study by Alqattan *et al.* [32] found that Mn-dominant alloys had a much finer microstructure compared to Cu-dominant alloys at the same concentrations, and is in agreement with the current results. A more refined microstructure tends to give better mechanical properties (tensile and hardness).

Regarding the mechanical behaviour of the ternary Ti-Cu-Nb, Ti-Mn-Nb and Ti-Fe-Nb alloys, the microstructural features of each alloy will have an effect on the mechanical properties of the alloy. The UTS and YS of Ti-5Fe-5Nb (UTS = 800 MPa and YS = 727 MPa) are higher than Ti-5Mn-5Nb (UTS = 726 MPa and YS = 670 MPa) and Ti-5Cu-5Nb (UTS = 655 MPa and YS = 553 MPa) as shown in Figure 4-37.

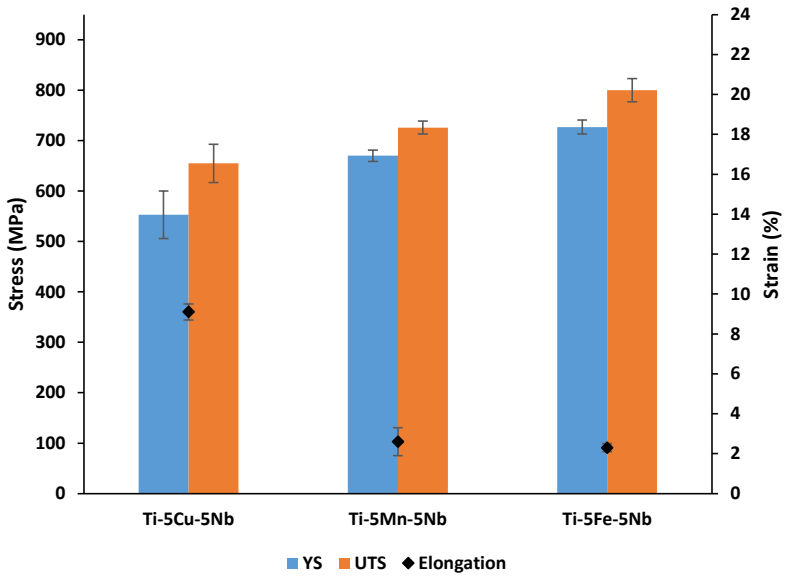

Figure 4-37 Comparison of the highest UTS and YS of Ti-5Cu-5Nb, Ti-5Mn-5Nb and Ti-5Fe-5Nb.

Both Ti-5Fe-5Nb (62 HRA) and Ti-5Mn-5Nb (62 HRA) showed similar hardness, compared to Ti-5Cu-5Nb (58 HRA). The elongation for the Ti-5Cu-5Nb (9.1%) alloy was higher than both Ti-5Mn-5Nb (2.6%) and Ti-5Fe-5Nb (2.3%) alloys. The high strength of the Ti-5Fe-5Nb alloy is due to the refined microstructure as well as Fe having a stronger stabilizing effect on the β-phase of Ti. Mn is also a strong β-stabilizer in Ti, its effects in terms of strength for the Ti-5Mn-5Nb alloy were not observed compared to the Ti-5Fe-5Nb alloy at the same total amount of alloying elements. The relative sintered density of the Ti-5Mn-5Nb alloy was approximately 1% lower than that of Ti-5Fe-5Nb, this implies that the mechanical properties would be low based on a lower relative density (i.e. an alloy with a high relative density results in better mechanical properties, as there are less pores present in the material, thus reducing the stress concentration sites). Even though the Ti_2Cu phase was detected in the Ti-5Cu-5Nb alloy, it did not increase the mechanical properties significantly. However, the elongation was higher with the addition of Cu to Ti-Nb, compared to Mn and Fe alloying elements.

Overall from this group of ternary Ti-Cu-Nb, Ti-Mn-Nb and Ti-Fe-Nb alloy systems, the Ti-Fe-Nb alloy system shows higher mechanical properties (tensile strength and hardness) than both Ti-Mn-Nb and Ti-Cu-Nb alloy systems, at the same total amount of alloying elements.

4.6.2 Ternary Ti-X-Fe alloys (X = Nb, Cu and Mn)

The Ti-5Fe-5Mn (94%) alloy showed the highest relative sintered density compared to the Ti-5Fe-5Cu (92.8%) and Ti-5Fe-5Nb (92.3%) alloys. As mentioned before both Fe and Mn are strong β-stabilizers in Ti, thus having a strong effect on the relative density of PM Ti alloys.

The addition of 5 wt% of both Fe and Mn to Ti caused significant refinement of the microstructure, achieving a β type microstructure composed of equiaxed β-phase grains. Both Ti-5Fe-5Nb and Ti-5Fe-5Cu alloys showed similar microstructures, however the Ti-5Fe-5Cu alloy showed a much more refined microstructure compared to Ti-5Fe-5Nb at the same total amount of alloying elements. As a result, a Ti alloy consisting of a β type microstructure tends have better mechanical properties as the β-Ti phase is highly stabilized. As mentioned before the β-Ti phase has high strength/hardness and low ductility, compared to the α-Ti phase.

The UTS and YS of Ti-5Fe-5Cu (UTS = 912 MPa and YS = 864 MPa) are higher compared to Ti-3.5Fe-3.5Mn (UTS = 842 MPa and YS = 816 MPa) and Ti-5Fe-5Nb (UTS = 800 MPa and YS = 727 MPa) as shown in Figure 4-38.

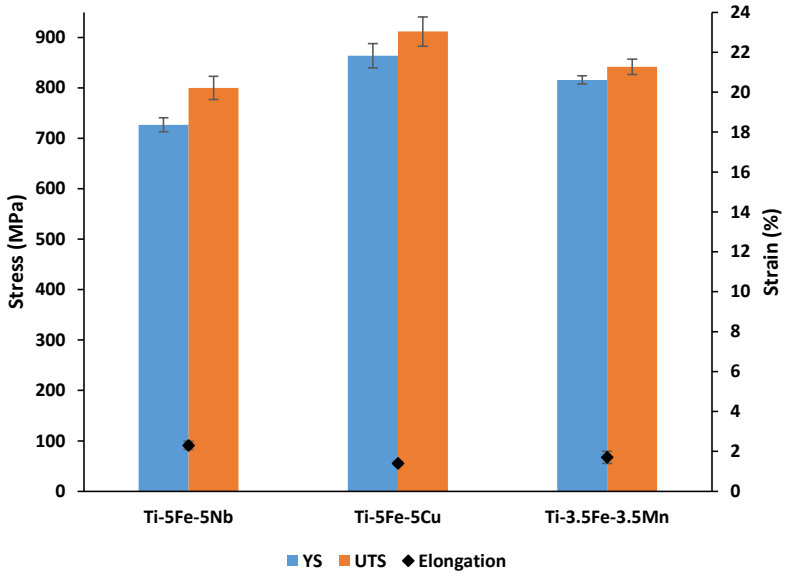

Figure 4-38 Comparison of the highest UTS and YS of Ti-5Fe-5Nb, Ti-5Fe-5Cu and Ti-3.5Fe-3.5Mn.

The Ti-5Fe-5Mn alloy showed only brittle behaviour (no YS could be measured), and therefore it is best to look at the mechanical behaviour of the Ti-3.5Fe-3.5Mn

alloy as both UTS and YS are found. Hardness of the Ti-5Fe-5Mn (70 HRA) alloy was the highest compared to both Ti 5Fe-5Cu (65 HRA) and Ti-5Fe-5Nb (62 HRA) alloys at the same total amount of alloying elements. It is worth mentioning that the hardness of the Ti-3.5Fe-3.5Mn (63 HRA) alloy, was higher than that of the Ti-5Fe-5Nb alloy with a lower amount of alloying elements. The elongation of the Ti-5Fe-5Nb (2.3%) alloys is higher than both Ti-3.5Fe-3.5Mn (1.7%) and Ti-5Fe-5Cu (1.4%) alloys. Once again, the high tensile properties of the Ti-5Fe-5Cu alloy are due to the refined microstructure as well as Fe having a stronger stabilizing effect on the β-phase of Ti. The presence of the Ti_2Cu phase (detected in XRD) in Ti-5Fe-5Cu is also responsible for the high tensile properties, as it leads to precipitation strengthening, thus increasing the strength and reducing the ductility (Ti_2Cu phase is brittle) of the alloy [32]. The Ti-3.5Fe-3.5Mn alloy showed higher tensile properties compared to the Ti-5Fe-5Nb alloy, with a lower amount of alloying elements, thus being cost effective. Hardness of the Ti-5Fe-5Mn alloy was the highest, as mentioned before both Fe and Mn are strong β-stabilizers in Ti, thus providing strong solid-solution strengthening effect.

Overall from this group of ternary Ti-Fe-Nb, Ti-Fe-Cu and Ti-Fe-Mn alloy systems, the Ti-Fe-Cu alloy system shows greater tensile properties than the Ti-Fe-Nb alloy system, and is comparable with the Ti-Fe-Mn alloy systems. However, hardness of the Ti-Fe-Mn alloy system is better than both Ti-Fe-Nb and Ti-Fe-Cu alloy systems.

4.6.3 Comparison of the mechanical properties of the sintered ternary Ti alloys

The UTS and YS of Ti-5Fe-5Cu (UTS = 912 MPa and YS = 864 MPa) are higher than Ti-3.5Fe-3.5Mn (UTS = 842 MPa and YS = 816 MPa), Ti-5Fe-5Nb (UTS = 800 MPa and YS = 727 MPa), Ti-5Mn-5Nb (UTS = 726 MPa and YS = 670 MPa) and Ti-5Cu-5Nb (UTS = 655 MPa and YS = 553 MPa) as shown in Figure 4-39. All ternary Ti alloys except Ti-5Cu-5Nb showed comparable elongations (Figure 4-39), at the highest UTS and YS of each alloy system.

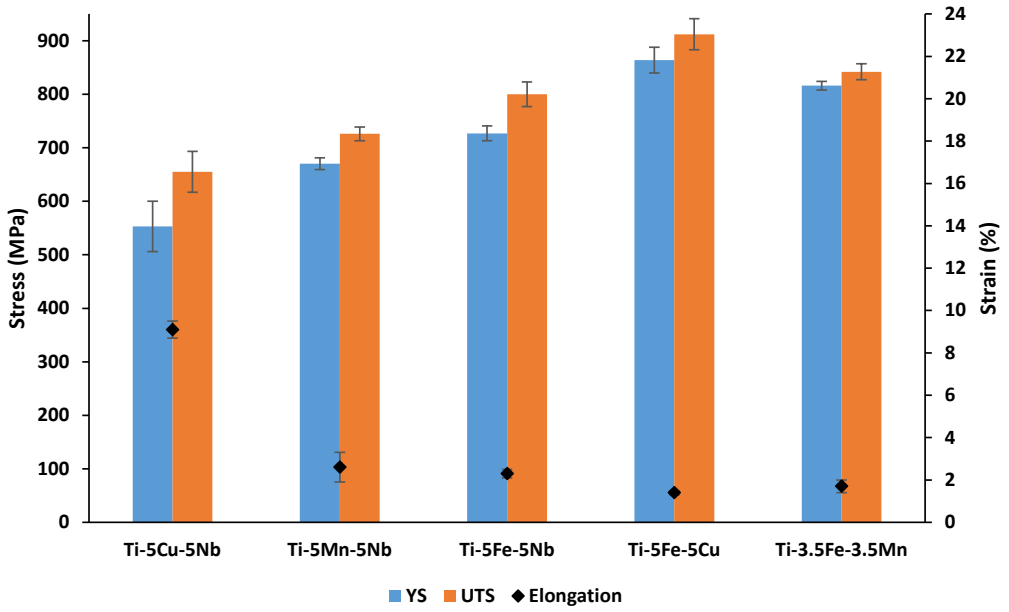

Figure 4-39 Comparing the highest UTS and YS of each alloy system.

It is worth mentioning that the Ti-3.5Fe-3.5Mn alloy has higher UTS and YS than Ti-3.5Fe-3.5Cu (UTS = 754 MPa and YS = 630 MPa) at the same total amount of alloying elements, indicating that Mn is a stronger β-stabilizer than Cu, therefore having better tensile properties (UTS and YS) compared to Cu at the same total amount of alloying elements when alloyed to Ti-Fe. However, the elongation of the Ti-3.5Fe-3.5Cu (3.7%) alloy is twice that of Ti-3.5Fe-3.5Mn (1.7%), thus showing that Cu is more ductile than Mn at the same total amount of alloying elements.

The elongation of Ti-1Cu-1Nb (23%) was higher than alloys at the highest elongation of each alloy system as shown in Figure 4-40. The Ti-0.5Fe-0.5Mn (9.3%) alloy showed the lowest elongation compared to both Ti-1Mn-1Nb (13.2%) and Ti-1Fe-1Nb (11.4%) alloys, however comparable with the Ti-1Fe-1Cu (9.6%) alloy. From Figure 4-40, all ternary Ti alloys of each alloy system showed similar UTS and YS at the same total amount of alloying elements, this had no effect on the elongation of the alloys. It is worth mentioning that the all Ti-xCu-xNb alloys showed very high elongations, when compared to the other alloy systems at the same total amount of alloying elements. It can be concluded that Cu and Nb as alloying elements added to Ti show high elongations compared to Fe and Mn. Generally, Mn and Fe are more ductile at lower additions as mentioned in the literature review.

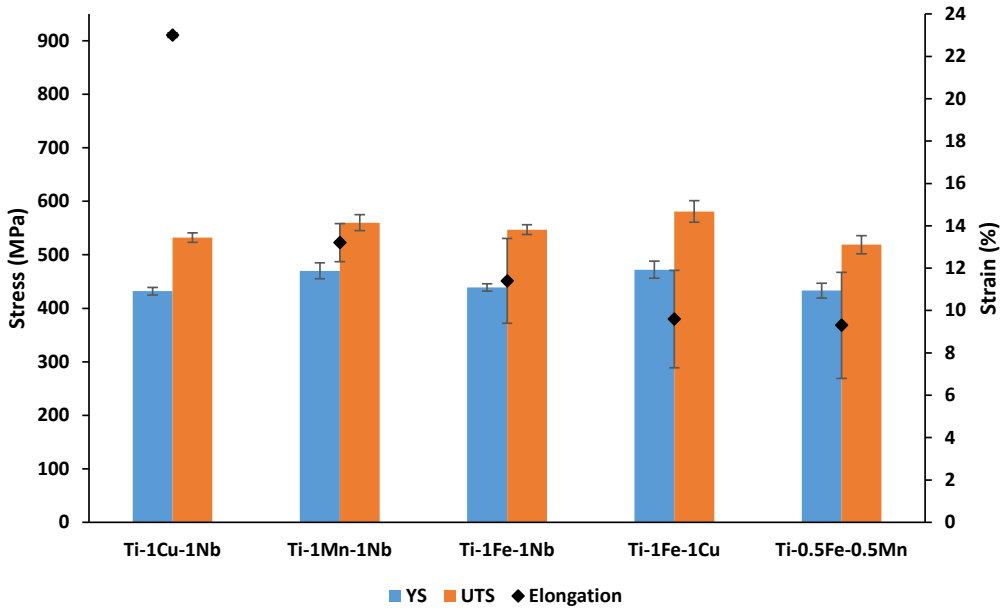

Figure 4-40 Comparison of the highest elongation of each alloy system.

The hardness of the Ti-5Fe-5Mn (70 HRA) was significantly higher than all alloys at the highest hardness of each alloy system as shown in Figure 4-41. As mentioned before both Fe and Mn (Mn being more than Fe) are strong β-stabilizers because they have a stronger stabilizing effect on the β-Ti phase, as well as having high diffusivity in Ti. It is worth mentioning that Nb has a poor diffusivity in Ti, thus the effects are observed in the mechanical properties of the sintered ternary Ti alloys.

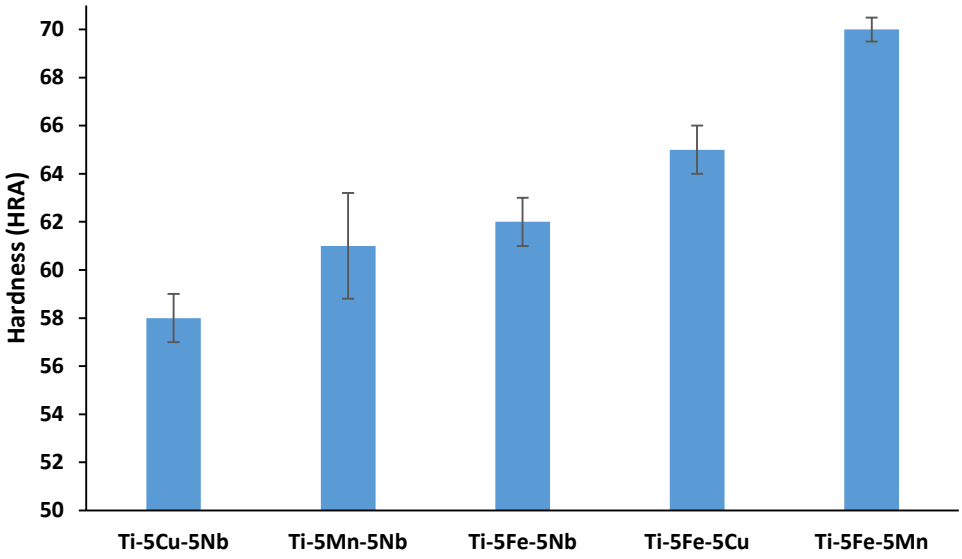

Figure 4-41 Comparison of the highest hardness of each alloy system.

Chapter 5
Conclusion and Recommendation

Concluding, novel ternary Ti-xCu-xNb, Ti-xMn-xNb, Ti-xFe-xNb, Ti-xFe-xCu, Ti-xFe-xMn alloys were successfully fabricated via cost effective PM route (i.e. cold press and vacuum sintering), and characterized. The addition of alloying elements (Cu, Nb, Mn and Fe) to Ti caused significant changes in the microstructures as well as increasing the mechanical properties compared to CP-Ti.

The progressive increment of the alloying elements decreases the density of the alloys, especially for the Ti-xCu-xNb, Ti-xMn-xNb and Ti-xFe-xNb alloys, but was fairly constant for the Ti-xFe-xCu and Ti-xFe-xMn alloys. With the addition of 0.5 wt% of alloying elements (Cu, Nb, Mn and Fe) to Ti, the microstructure changes from an equiaxed structure (CP-Ti) into a $\alpha + \beta$ lamellar structure (the increment of the alloying elements from 0.5 to 5 wt% caused significant refinement of the $\alpha + \beta$ lamellar microstructure), this was exhibited for all the sintered ternary Ti alloy systems. Ti-5Fe-5Mn was the only alloy to show an equiaxed microstructure (agreed with the MoE). As result of the microstructural changes, the strength and hardness of the ternary Ti alloys increases, nevertheless, the ductility decreases. High tensile properties were observed for the Ti-5Fe-5Cu alloy (due to the formation of the Ti_2Cu phase as well as the strong β-stabilizer effects of Fe), in comparison to all the sintered ternary Ti alloys. Ti-5Fe-5Mn showed the highest hardness compared to all the sintered ternary Ti alloys, owing to the strong β-stabilizer effects of Fe and Mn (strong solid-solution strengthening effect). Cu and Nb as alloying elements added to Ti show high elongations compared to Fe and Mn, because of that the Ti-xCu-xNb alloy system showed higher elongations than the other alloy systems at the same total amount of alloying elements. The sintered novel ternary Ti alloys exhibit mechanical properties comparable to Ti based alloys used on engineering applications, thus could have potential use in industrial applications. It is worth mentioning that Ti-5Fe-5Cu was the only alloy to show comparable UTS and YS with Ti-6Al-4V, and Ti-5Fe-5Mn showed higher hardness compared to Ti-6Al-4V.

Future work such as antibacterial activity and corrosion behaviour should be investigated on the novel ternary Ti alloys, as the alloying elements Cu, Nb and Mn have excellent biocompatibility when alloyed to Ti. Hot working treatments could also be investigated, as they tend to improve the physical and mechanical properties as well as change the microstructure of the alloy.

References

[1] Peters, M., Hemptenmacher, J., Kumpfert, J., & Leyens, C. (2003). Structure and properties of titanium and titanium alloys. In *Titanium and Titanium Alloys, Fundamentals and Applications* (pp. 1-36). Wiley-VCH Verlag GmbH & Co. KGaA, Weinheim.

[2] Donachie, M. J. (2000). *Titanium: A Technical Guide*. Materials Park: ASM International.

[3] Polmear, I., St. John, D. D., & Ravi, V. (2005). Titanium alloys. In *Light Alloys: From Traditional Alloys To Nanocrystals* (4th ed., pp. 299-365). Oxford, United Kingdom: Elsevier Science & Technology.

[4] Weiss, I., & Semiatin, S. L. (1998). Thermomechanical processing of beta titanium alloys - an overview. *Materials Science and Engineering A, 243*(1-2), 46-65.

[5] Kolli, R. P., & Devaraj, A. (2018). A review of metastable beta titanium alloys. *Metals, 8*(7), art. no. 506.

[6] Callister, W. D., & Rethwisch, D. G. (2001). *Materials Science and Engineering: An Introduction*. (9th ed.). Somerset: Wiley.

[7] Yan, M. (2015). Microstructural characterization of as-sintered titanium and titanium alloys. In *Titanium Powder Metallurgy; Science, Technology and Application* (pp. 555-578). Elsevier Inc.

[8] Froes, F. H. (2015). A historical perspective of titanium powder metallurgy. In *Titanium Powder Metallurgy; Science, Technology and Applications* (pp. 1-19). Elsevier Inc.

[9] Froes, F. H. (2013). Powder metallurgy of titanium alloys. In *Advances in Powder Metallurgy : Properties, Processing and Applications* (pp. 202-240). Cambridge, United Kingdom: Elsevier Science & Technology.

[10] Yolton, C. F., & Froes, F. H. (2015). Conventional titanium powder production. In *Titanium Powder Metallurgy; Science, Technology and Applications* (pp. 21-32). Elsevier Inc.

[11] Engineering Study Materials (Compiler) (2018, May 14). *Powder metallurgy manufacturing process, applications, advantages*. Youtube https://www.youtube.com/watch?v=Y0EXdgjC9PA.

[12] Fang, Z. Z., Paramore, J. D., Sun, P., Chandran, K. S. R., Zhang, Y., Xia, Y., Cao, F., Koopman, M., & Free, M. (2018). Powder metallurgy of titanium–past, present, and future. *International Materials Reviews, 63*(7), 407-459.

[13] Kikuchi, M., Takada, Y., Kiyosue, S., Yoda, M., Woldu, M., Cai, Z., Okuno, O., & Okabe, T. (2003). Mechanical properties and microstructures of cast Ti-Cu alloys. *Dental Materials, 19*(3), 174-181.

[14] Alshammari, Y., Yang, F., & Bolzoni, L. (2019). Low-cost powder metallurgy Ti-Cu alloys as a potential antibacterial material. *Journal of the Mechanical Behavior of Biomedical Materials, 95*, 232-239.

[15] Lee, C. M., Ju, C. P., & Chern Lin, J. H. (2002). Structure-property relationship of cast Ti-Nb alloys. *Journal of Oral Rehabilitation, 29*(4), 314-322.

[16] Zhang, Y., Sun, D., Cheng, J., Tsoi, J. K. H., & Chen, J. (2020). Mechanical and biological properties of Ti–(0–25 wt%)Nb alloys for biomedical implants application. *Regenerative Biomaterials, 7*(1), 119-127.

[17] Yi, C., Ke, Z., Zhang, L., Tan, J., Jiang, Y., & He, Z. (2020). Antibacterial Ti-Cu alloy with enhanced mechanical properties as implant applications. *Materials Research Express, 7*(10), art. no. 105404.

[18] Xu, Y., Jiang, J., Yang, Z., Zhao, Q., Chen, Y., & Zhao, Y. (2020). The Effect of Copper Content on the Mechanical and Tribological Properties of Hypo-, Hyper- and Eutectoid Ti-Cu Alloys. *Materials, 13*(15), 1-12.

[19] Machio, C., Mathabathe, M. N., & Bolokang, A. S. (2020). A comparison of the microstructures, thermal and mechanical properties of pressed and sintered Ti–Cu, Ti–Ni and Ti–Cu–Ni alloys intended for dental applications. *Journal of Alloys and Compounds, 848*, art. no. 156494.

[20] Wang, J., Zhang, S., Sun, Z., Wang, H., Ren, L., & Yang, K. (2019). Optimization of mechanical property, antibacterial property and corrosion resistance of Ti-Cu alloy for dental implant. *Journal of Materials Science and Technology, 35*(10), 2336-2344.

[21] Zhang, E., Wang, X., Chen, M., & Hou, B. (2016). Effect of the existing form of Cu element on the mechanical properties, bio-corrosion and antibacterial properties of Ti-Cu alloys for biomedical application. *Materials Science and Engineering C, 69*, 1210-1221.

[22] Zhang, E., Ren, J., Li, S., Yang, L., & Qin, G. (2016). Optimization of mechanical properties, biocorrosion properties and antibacterial properties of as-cast Ti-Cu alloys. *Biomedical Materials (Bristol), 11*(6).

[23] Zhang, E., Li, S., Ren, J., Zhang, L., & Han, Y. (2016). Effect of extrusion processing on the microstructure, mechanical properties, biocorrosion properties and antibacterial properties of Ti-Cu sintered alloys. *Materials Science and Engineering C, 69*, 760-768.

[24] Liu, J., Li, F., Liu, C., Wang, H., Ren, B., Yang, K., & Zhang, E. (2014). Effect of Cu content on the antibacterial activity of titanium-copper sintered alloys. *Materials Science and Engineering C, 35*(1), 392-400.

[25] Kikuchi, M., Takahashi, M., & Okuno, O. (2003). Mechanical properties and grindability of dental cast Ti-Nb alloys. *Dental Materials Journal, 22*(3), 328-342.

[26] Xu, L. J., Xiao, S. L., Tian, J., Chen, Y. Y., & Huang, Y. D. (2009). Microstructure and dry wear properties of Ti-Nb alloys for dental prostheses. *Transactions of Nonferrous Metals Society of China (English Edition), 19*(SUPPL. 3), s639-s644.

[27] Han, M. K., Kim, J. Y., Hwang, M. J., Song, H. J., & Park, Y. J. (2015). Effect of Nb on the microstructure, mechanical properties, corrosion behavior, and cytotoxicity of Ti-Nb alloys. *Materials, 8*(9), 5986-6003.

[28] Zhao, D., Chang, K., Ebel, T., Qian, M., Willumeit, R., Yan, M., & Pyczak, F. (2013). Microstructure and mechanical behavior of metal injection molded Ti-Nb binary alloys as biomedical material. *Journal of the Mechanical Behavior of Biomedical Materials, 28*, 171-182.

[29] Yılmaz, E., Gökçe, A., Findik, F., & Gulsoy, H. O. (2018). Metallurgical properties and biomimetic HA deposition performance of Ti-Nb PIM alloys. *Journal of Alloys and Compounds, 746*, 301-313.

[30] Kalita, D., Rogal, Ł., Czeppe, T., Wójcik, A., Kolano-Burian, A., Zackiewicz, P., Kania, B., & Dutkiewicz, J. (2020). Microstructure and mechanical properties of Ti-Nb alloys prepared by mechanical alloying and spark plasma sintering. *Journal of Materials Engineering and Performance, 29*(3), 1445-1452.

[31] Takahashi, M., Kikuchi, M., & Takada, Y. (2016). Mechanical properties and microstructures of dental cast Ti-6Nb-4Cu, Ti-18Nb-2Cu, and Ti-24Nb-1Cu alloys. *Dental Materials Journal, 35*(4), 564-570.

[32] Alqattan, M., Peters, L., Yang, F., & Bolzoni, L. (2021). Microstructure, mechanical behaviour and antibacterial activity of biomedical Ti-xMn-yCu alloys. *Journal of Alloys and Compounds, 856*, art. no. 158165.

[33] Sato, K., Takahashi, M., & Takada, Y. (2020). Construction of Ti-Nb-Ti_2Cu pseudo-ternary phase diagram. *Dental Materials Journal, 39*(3), 422-428.

[34] Mutlu, I. (2021). Single-step sinter-aging heat treatment of metastable-beta type Ti–Nb–Cu alloy. *Powder Metallurgy, 64*(1), 43-53.

[35] Mutlu, I., Yeniyol, S., & Oktay, E. (2016). Characterisation of corrosion properties of Ti-Nb-Cu alloy foam by electrochemical impedance spectroscopy method. *Corrosion Engineering Science and Technology, 51*(2), 110-117.

[36] Mutlu, I., Yeniyol, S., & Oktay, E. (2017). Corrosion behaviour of alkali treated highly porous Ti-Nb-Cu alloy. In *EUROCORR 2017 - The Annual Congress of the European Federation of Corrosion, 20th International Corrosion Congress and Process Safety Congress 2017*.

[37] Mutlu, I., & Oktay, E. (2015). Localised corrosion behaviour of biomedical implant materials using electrochemical potentiokinetic reactivation and critical pitting potential methods. *Corrosion Engineering Science and Technology*, *50*(1), 72-79.

[38] Alshammari, Y., Yang, F., & Bolzoni, L. (2019). Mechanical properties and microstructure of Ti-Mn alloys produced via powder metallurgy for biomedical applications. *Journal of the Mechanical Behavior of Biomedical Materials, 91*, 391-397.

[39] Santos, P. F., Niinomi, M., Cho, K., Liu, H., Nakai, M., Narushima, T., Ueda, K., & Itoh, Y. (2017). Effects of Mo addition on the mechanical properties and microstructures of Ti-Mn alloys fabricated by metal injection molding for biomedical applications. *Materials Transactions, 58*(2), 271-279.

[40] Gouda, M. K., Gepreel, M. A. H., & El Moniem, A. A. (2013). A study on phases change of Ti-Mn alloys produced by metal injection molding. In *AIP Conference Proceedings* (Vol. 1569, pp. 203-207).

[41] Santos, P. F., Niinomi, M., Liu, H., Cho, K., Nakai, M., Trenggono, A., Champagne, S., Hermawan, H., & Narushima, T. (2016). Improvement of microstructure, mechanical and corrosion properties of biomedical Ti-Mn alloys by Mo addition. *Materials and Design, 110*, 414-424.

[42] Kim, J. W., Hwang, M. J., Han, M. K., Kim, Y. G., Song, H. J., & Park, Y. J. (2016). Effect of manganese on the microstructure, mechanical properties and corrosion behavior of titanium alloys. *Materials Chemistry and Physics, 180*, 341-348.

[43] Chen, Z., Liu, Y., Jiang, H., Liu, M., Wang, C. H., & Cao, G. H. (2017). Microstructures and mechanical properties of Mn modified, Ti-Nb-based alloys. *Journal of Alloys and Compounds, 723*, 1091-1097.

[44] Ehtemam, H. S., Attar, H., Dargusch, M. S., & Kent, D. (2019). Microstructure, phase composition and mechanical properties of new, low cost Ti-Mn-Nb alloys for biomedical applications. *Journal of Alloys and Compounds, 787*, 570-577.

[45] Chicardi, E., Aguilar, C., Sayagués, M. J., & García-Garrido, C. (2018). Influence of the Mn content on the TiNbxMn alloys with a novel fcc structure. *Journal of Alloys and Compounds, 746*, 601-610.

[46] Chen, B. Y., Hwang, K. S., & Ng, K. L. (2011). Effect of cooling process on the α phase formation and mechanical properties of sintered Ti-Fe alloys. *Materials Science and Engineering A, 528*(13-14), 4556-4563.

[47] Bolzoni, L., Ruiz-Navas, E. M., & Gordo, E. (2016). Understanding the properties of low-cost iron-containing powder metallurgy titanium alloys. *Materials and Design, 110*, 317-323.

[48] Raynova, S., Yang, F., & Bolzoni, L. (2021). The effect of thermomechanical treatments on the properties of powder metallurgy Ti–5Fe alloy. *Materials Science and Engineering A, 801*, art. no. 140389.

[49] Raynova, S., Yang, F., & Bolzoni, L. (2021). Mechanical behaviour of induction sintered blended elemental powder metallurgy Ti alloys. *Materials Science and Engineering A, 799*, art. no. 140157.

[50] Romero, C., Yang, F., Wei, S., & Bolzoni, L. (2020). Thermomechanical processing of cost-affordable powder metallurgy Ti-5Fe alloys from the blended elemental approach: Microstructure, tensile deformation behavior, and failure. *Metals, 10*(11), 1-16.

[51] Alshammari, Y., Raynova, S., Yang, F., & Bolzoni, L. (2020). Effect of particle size and manufacturing technique on the properties of the PM Ti-5Fe alloy. *International Journal of Refractory Metals and Hard Materials, 90*, art. no. 105246.

[52] Romero, C., Raynova, S., Yang, F., & Bolzoni, L. (2018). Ultrafine microstructures in eutectoid element bearing low-cost Ti-Fe alloys enabled by slow bainite formation. *Journal of Alloys and Compounds, 769*, 226-232.

[53] Alshammari, Y., Manogar, B., Raynova, S., Yang, F., & Bolzoni, L. (2020). Behaviour of novel low-cost blended elemental Ti–5Fe-xAl alloys fabricated via powder metallurgy. *Journal of the Mechanical Behavior of Biomedical Materials, 110*, art. no. 103865.

[54] Contieri, R. J., Lopes, E. S. N., Taquire De La Cruz, M., Costa, A. M., Afonso, C. R. M., & Caram, R. (2011). Microstructure of directionally solidified Ti-Fe eutectic alloy with low interstitial and high mechanical strength. *Journal of Crystal Growth, 333*(1), 40-47.

[55] Niu, J., Guo, Y., Li, K., Liu, W., Dan, Z., Sun, Z., Chang, H., & Zhou, L. (2021). Improved mechanical, bio-corrosion properties and in vitro cell responses of Ti-Fe alloys as candidate dental implants. *Materials Science and Engineering C, 122*, art. no. 111917.

[56] Hsu, H. C., Hsu, S. K., Wu, S. C., Lee, C. J., & Ho, W. F. (2010). Structure and mechanical properties of as-cast Ti-5Nb-xFe alloys. *Materials Characterization, 61*(9), 851-858.

[57] Ehtemam-Haghighi, S., Liu, Y., Cao, G., & Zhang, L. C. (2016). Phase transition, microstructural evolution and mechanical properties of Ti-Nb-Fe alloys induced by Fe addition. *Materials and Design, 97*, 279-286.

[58] Ehtemam-Haghighi, S., Liu, Y., Cao, G., & Zhang, L. C. (2016). Influence of Nb on the $\beta \rightarrow \alpha''$ martensitic phase transformation and properties of the newly designed Ti-Fe-Nb alloys. *Materials Science and Engineering C, 60*, 503-510.

[59] Ehtemam-Haghighi, S., Prashanth, K. G., Attar, H., Chaubey, A. K., Cao, G. H., & Zhang, L. C. (2016). Evaluation of mechanical and wear properties of Ti-xNb-7Fe alloys designed for biomedical applications. *Materials and Design, 111*, 592-599.

[60] Afonso, C. R. M., Chaves, J. M., & Florêncio, O. (2017). Effect of Rapid Solidification on Microstructure and Elastic Modulus of β Ti–xNb–3Fe

Alloys for Implant Applications. *Advanced Engineering Materials*, *19*(6), art. no. e201600370.

[61] Li, Q., Miao, P., Li, J., He, M., Nakai, M., Niinomi, M., Chiba, A., Nakano, T., Liu, X., Zhou, K., & Pan, D. (2019). Effect of Nb content on microstructures and mechanical properties of Ti-xNb-2Fe alloys. *Journal of Materials Engineering and Performance*, *28*(9), 5501-5508.

[62] Chirico, C., Tsipas, S. A., Wilczynski, P., & Gordo, E. (2020). Beta titanium alloys produced from titanium hydride: Effect of alloying elements on titanium hydride decomposition. *Metals*, *10*(5), art. no. 682.

[63] Cho, K., Niinomi, M., Nakai, M., Hieda, J., & Kawasaki, Y. (2013). Development of high modulus TiFeCu alloys for biomedical applications. *Materials Transactions*, *54*(4), 574-581.

[64] Ikeda, M., Ueda, M., Kinoshita, T., Ogawa, M., & Niinomi, M. (2012). Influence of Fe content of Ti-Mn-Fe alloys on phase constitution and heat treatment behavior. *Materials Science Forum*, *706-709*, 1893-1898.

[65] Tang, B., Chu, Y., Zhang, M., Meng, C., Fan, J., Kou, H., & Li, J. (2020). The ω phase transformation during the low temperature aging and low rate heating process of metastable β titanium alloys. *Materials Chemistry and Physics*, *239*, art. no. 122125.

[66] Bania, P. J. (1994). Beta titanium alloys and their role in the titanium industry. *JOM*, *46*(7), 16-19.

[67] Wang, Q., Dong, C., & Liaw, P. K. (2015). Structural stabilities of β-Ti alloys studied using a new Mo Equivalent derived from [β/(α + β)] phase-boundary slopes. *Metallurgical and Materials Transactions A: Physical Metallurgy and Materials Science*, *46*(8), 3440-3447.

[68] Edge, E. (2017, March 30). *Densities of metals and elements table*. Retrieved May 6, 2021, from https://www.engineersedge.com/materials/densities_of_metals_and_elements_table_13976.htm

[69] Bolzoni, L., Alqattan, M., Peters, L., Alshammari, Y., & Yang, F. (2020). Ternary Ti alloys functionalised with antibacterial activity. *Scientific Reports*, *10*(1), art. no. 22201.

[70] Niinomi, M. (1998). Mechanical properties of biomedical titanium alloys. *Materials Science and Engineering A*, *243*(1-2), 231-236.